POLITECNICO DI MILANO

School of Industrial and Information Engineering

Master Degree in Biomedical Engineering

EFFECT OF REPEATED ETHYLENE OXIDE STERILIZATION ON POLYDIMETHYLSILOXANE RUBBER

Master Degree Thesis

Advisor: Dr. Maria Cristina Tanzi
Co-advisors: Dr. Jan Van Humbeeck
Dr. Peter Van Puyvelde

Author:
Gregorio Cattignoli
Student ID: 801551

Academic Year: 2013-2014

The present thesis represents a work in collaboration among Politecnico di Milano, Katholieke Universiteit Leuven and Cochlear Industry in Mechelen.

Acknowledgments

The present thesis has been performed and completed at KU Leuven University in Belgium, therefore I want to thank this university for this important experience.
I would like to express my gratitude to professor Jan Van Humbeeck and Peter Van Puyvelde for their guidance and assistance during the course of this research, both in terms of council and assistance with the manuscript. I also wish to thank Daniel Smyth for his support and help in particular with statistical interpretation of data and Cochlear Industry in Mechelen for this opportunity. Similarly I would like to thank professor Maria Cristina Tanzi and Silvia Farè for the continuous feedback and their advice in test choice and result analysis. In addition I wish to express my gratitude towards MTM and Chemical Engineering departments at KU Leuven and all the staff who help me: Rob Van Hooghten for his help with the interpretation of wettability data, Danny Winant for the training and advice about thermal analyses, Dominiek Demaerel and Johannes Van Deursen for the preparation of DMA samples, Dirk Dom for the assistance with ATR-FTIR, Diego Nieves for taking the photos related to uniaxial tensile test. Finally I would like to thank professor Alberto Cesare Redaelli, Rita Vanroelen and Pascale Conard for the constant help provided with bureaucratic issues.
Last, but not least, I truly would like to thank my family for the trust and comprehension in such a long period abroad to complete the present work, for their support even in the moments carrying more difficulties and problems.

Contents

List of Figures

List of Tables

1 Sommario

Introduzione

Il Polidimetilsilossano (PDMS) è un materiale ampiamente impiegato in molti campi industriali. Il termine "silicone" si riferisce ad un polimero sintetico che presenta una catena principale di Si-O-Si con ai suoi lati diversi gruppi organici. Questi composti si dividono in varie tipologie e mostrano proprietà diverse a seconda soprattutto del grado di crosslinking e della lunghezza delle catene. Il PDMS, la cui struttura con due gruppi metilici ai lati di ciascun Si è riassunta come CH_3 $[Si(CH_3)_2O]_n$ $Si(CH_3)_3$, rappresenta l'esempio più noto di questa categoria di materiali. Esso viene sintetizzato partendo dalla silice (SiO_2) dalla quale si ottengono oligomeri ciclici e lineari che vanno poi polimerizzati per ottenere lunghe catene di prodotto finale.

Il successo del PDMS in campo industriale è dovuto alle sue numerose proprietà vantaggiose: il materiale è infatti non tossico, chimicamente inerte, idrofobico e altamente insolubile in acqua, oltre che estremamente flessibile. Sebbene rigonfi in maniera minima in acqua e solventi polari, è invece particolarmente permeabile ai gas. La trasparenza, l'adesività a certi substrati, la stabilità termica e le proprietà di isolante elettrico lo rendono un materiale indicato per vari scopi tra cui quello di incapsulamento e di isolante sia termico che elettrico. Per incapsulare dei prodotti, gli elastomeri in silicone sono spesso usati per via della loro bassa Tg ($\approx -125°$ C) che garantisce grande flessibilità e recupero delle deformazioni. Il materiale viene creato attraverso un processo di *curing* che induce la formazione di legami (*hard segments*) tra le singole catene (*soft segments*). Tra i processi disponibili per questa finalità quello catalizzato attraverso l'azione del platino (*Pt-curing*) è ritenuto uno dei migliori nelle applicazioni biomediche. La polimerizzazione del PDMS avviene attraverso i gruppi vinilici alla fine delle catene di silossano ed i gruppi Si-H degli agenti crosslinkanti con la formazione di ponti $Si\text{-}CH_2\text{-}CH_2\text{-}Si$ (nessun sottoprodotto viene generato).

Come già detto il PDMS e i siliconi possono essere usati in un'ampia gamma di settori, tuttavia è in campo biomedico che questo materiale riveste un ruolo cruciale vista la sua flessibilità e compatibilità con sangue e tessuti biologici. Cateteri, drenaggi, protesi estetiche e ricostruttive, membrane di scambio sono solo alcuni tra gli esempi più noti. L'impianto nel corpo umano di dispositivi contenti elementi elettronici (neurostimolatori,

impianti cocleari e pacemaker per esempio) richiede un sistema di incapsulamento per proteggere da correnti e corrosione. Uno strato sottile e ben adeso di PDMS generalmente garantisce una protezione efficace per 12 anni almeno.

Prima di essere impiantato qualsiasi dispositivo deve essere sterilizzato, in particolare per il PDMS una delle procedure più impiegate è l'Ossido di Etilene (Etox). Per i polimeri le sterilizzazioni legate a trattamenti termici o radiazioni sono infatti generalmente da evitarsi. Questa procedura permette di inserire direttamente il prodotto confezionato nella camera di processo dove l'Etox viene rilasciato in forma pura o diluita. L'umidità, la temperatura, il tempo di esposizione e la quantità di Etox impiegata sono i principali parametri di processo. Dopo questo trattamento il prodotto deve essere aerato in maniera sufficiente ad evitare che nessun residuo di Etox rimanga al suo interno.

L'Ossido di Etilene è gassoso a pressione atmosferica e dispone di un notevole potere mutageno e cariogeno. La sua struttura chimica C_2H_4O consiste in una struttura instabile ad anello che in presenza di gruppi solfidrilici, idrossilici, amminici e carbossilici si apre avviando una reazione di alchilazione. Batteri e virus dispongono di questi gruppi all'interno dei loro componenti cellulari e vengono dunque impossibilitati a riprodursi e condurre il normale metabolismo. Generalmente i prodotti medicali non presentano i gruppi citati, perciò teoricamente il materiale non dovrebbe essere alterato da questo agente sterilizzante. Nonostante i dibattiti riguardo la sicurezza nell'impianto di materiali trattati con questo gas siano ancora attuali, l'Etox è considerato sicuro se il processo che lo impiega rispetta precise normative di sicurezza. Tuttavia il timore verso questa tecnologia non è solo riferito al rischio d'intrappolamento di Ossido di Etilene all'interno del materiale, ma anche ad alcuni dei suoi derivati.

Scopo della Tesi

La presente tesi riguarda la sterilizzazione di PDMS mediante Etox. L'industria Cochlear presso Mechelen (Belgio) si serve di questa combinazione per il materiale di incapsulamento dei propri impianti cocleari. Tuttavia nonostante questa combinazione sia estremamente diffusa in campo biomedicale, la letteratura al riguardo è piuttosto limitata, con numerosi casi di discordanze nei risultati e carenza di dettagli nei materiali impiegati. Oltre a ciò quasi tutte le fonti si focalizzano su cicli di sterilizzazione singoli, non

prendendo in considerazione la possibilità di sterilizzare dispositivi impiantabili più di una volta. In questo modo le industrie sono obbligate a disfarsi di materiale che richiederebbe una seconda sterilizzazione (ad esempio per processi di controllo o aggiunta/modifica post-sterilizzazione).

Questa tesi vuole quindi indagare le proprietà di questo materiale per esposizione a cicli multipli di Etox. Una vasta gamma di esperimenti è proposta al fine di analizzare varie proprietà del materiale sotto esame. L'analisi statistica indica se i campioni esposti ad un numero diverso di sterilizzazioni possano essere considerati simili. Qualora alcuni cambiamenti vengano rilevati nel materiale, si dovrebbe ricercare una possibile interpretazione dell'effetto dell'Ossido di Etilene.

Materiali e Metodi

I test sono eseguiti su campioni in MED-4860P, un silicone Pt-cured le cui caratteristiche sono sotto riportate (Tab.I).

Properties	Average Result	Standard
Uncured:		
Appearance	Translucent	ASTM D2090
Specific Gravity	1.15	ASTM D792
Durometer, Type A	60	ASTM D2240
Tensile Strength	1350 psi (9.3 MPa)	ASTM D412
Elongation	530%	ASTM D412
Tear Strength	255 ppi (45.0 kN/m)	ASTM D624
Stress @ 200% Strain	600 psi (4.1 MPa)	ASTM D412, D882
Tissue Culture (Cytotoxicity Testing)	Pass	USP <87> ISO 10993-5
Elemental Analysis of Trace Metals	Pass	ASTM E305

Tabella I:Datasheet del materiale su cui sono eseguiti gli esperimenti (MED-4860P).

Esso viene ottenuto mediante il mescolamento di due parti: PMDS lineari con estremità funzionalizzate da gruppi vinilici, silice amorfa (come riempitivo) e copolimeri di Dimetil,MetilIdrogeno Silossano (come agente crosslinkante) vengono quindi combinati nella struttura finale.

I campioni e i test sono selezionati in base alla letteratura e agli standard sperimentali. I campioni commissionati ad un'industria di stampaggio non sono stati prodotti e ricevuti in tempo, per questo motivo sono impiegati dei campioni già disponibili. Ciò risulta

inevitabilmente in esperimenti meno precisi e nell'ignorare talvolta i requisiti specificati dagli standard, con risultati potenzialmente diversi da quelli indicati in letteratura o nei datasheet. Ad ogni ciclo i campioni sono sterilizzati per 16 ore con una temperatura media di 52° C, umidità che varia dal 40% al 90% con 50 Pa di pressione e 10,6 g di gas rilasciati. L'aerazione dura almeno 50 ore con temperatura variabile da 23° C a 53° C.
In base a quanto riportato in letteratura, gli esperimenti sono condotti confrontando campioni sterilizzati una, quattro e dieci volte (C1, C4 and C10). Campioni non sterilizzati (C0) non vengono generalmente impiegati dal momento che solo campioni sterilizzati possono essere impiantati, tuttavia la compatibilità tra C0 e C1 viene controllata nel corso dell'esperimento di trazione uniassiale.

L'esperimento di **trazione uniassiale** viene eseguito con un Instron 5985 seguendo l'ASTM D412 e impiegando due velocità (500 e 100 mm/min). Campioni a clessidra sono utilizzati anche se la lunghezza del tratto centrale è più lunga di quella richiesta per questo tipo di materiale.
Mediamente 8 campioni per caso sono utilizzati e per ciascuno viene creato un file Excel i cui dati sono usati per calcolare l'UTS, Ultimate Elongation, E_lin and E_200. E_lin indica il coefficiente angolare nel grafico sforzo-deformazione fino ad una deformazione del 30%, E_200 invece rappresenta il modulo secante per una deformazione del 200%. I valori medi, le deviazioni standard e le mediane per le due velocità di deformazione sono riportate separatamente. Al fine di ottenere valori di Ultimate Elongation, E_lin ed E_200 più precisi possibili, viene calcolato un fattore di conversione da estensione a deformazione pari a 0,02. Tale calcolo viene eseguito attraverso il software Sketchup e numerose fotografie del campione in estensione (ogni 10 mm). Una stima dello slittamento delle estremità del campione dalle ganasce viene riportata, impiegando allo stesso modo Sketchup e le foto di alcune prove a trazione.

Alcuni test di **DMA** mediante un DMA Q800 con *shear sandwich clamp* sono impiegati per misurare lo Storage Modulus (E') e il Loss Modulus (E'') anche se i campioni sono fissati nelle morse mediante un serraggio manuale. Oscillazioni di 50 μm con frequenze di 1, 50 e 100 Hz sono ripetute mentre la temperatura all'interno della camera di test sale da -

50° C a 100° C. Parallelepipedi tagliati da barre sterilizzate (15 campioni per tipologia) vengono impiegati come campioni.

Un durometro di tipo Shore A viene impiegato per la misura della **durezza superficiale** seguendo l'ASTM D2240. La procedura è effettuata manualmente, registrando il valore riportato dallo strumento dopo 1 secondo dalla pressione sulla superficie. I campioni a disposizione non sono larghi e spessi a sufficienza per potervi adagiare completamente la base dello strumento, per questo motivo 6 parallelepipedi vengono sequenzialmente combinati in modo da creare un parallelepipedo più grande da campionare fino a 18 volte.

Diverse prove di **DSC** sono eseguite mediante un DSC Q2000 con un campione di zaffiro impiegato come materiale di confronto, in ogni prova vengono utilizzati 23 mg di campione. Due tipi di test vengono eseguiti: un primo test impiega un raffreddamento lento (*equilibration*) registrando solo la curva di riscaldamento mentre il secondo ne impiega uno veloce (30°C/min) registrando le curve sia di raffreddamento che di riscaldamento. La Tg (temperatura di transizione vetrosa), le temperature e le entalpie associate ai picchi di fusione e cristallizzazione sono calcolate attraverso il software Analysis 2000.

L'analisi mediante **ATR-FTIR** viene condotta mediante un Agilent Cary 620 FTIR microscope con un ATR slide-on, Ge-crystal (128 scans) al fine di determinare variazioni nella superficie (più precisamente nelle vibrazioni dei suoi legami chimici). L'esperimento prevede l'analisi di un campione per tipologia, acquisendo il segnale di background e poi sottraendolo dagli spettri successivamente registrati (in modo da limitare il disturbo relativo alla CO_2 e H_2O). Gli spettri sono acquisiti tra 4000 e 400 cm^{-1}.

Variazioni nell'idrofobicità superficiale tipica del PDMS vengono ricercate mediante **test di bagnabilità.** 5 fotografie acquisite a distanza di 30 secondi tra loro permettono di calcolare l'evoluzione temporale degli angoli di contatto di una goccia. Essa viene creata sulla punta di una siringa, fatta poi delicatamente appoggiare al substrato di PDMS e liberata quando la siringa viene velocemente rimossa. Numerose prove vengono eseguite su dei campioni di forma discoidale.

Nonostante il PDMS assorba quantità estremamente ridotte di acqua, si esegue un **test di swelling** in acqua parzialmente demineralizzata (6,25 < pH < 7) mediante almeno 5 campioni per tipologia. I campioni sono pesati prima e dopo determinati tempi d'immersione (1, 2 e 9 settimane) e questi pesi sono usati per calcolare le *swelling ratio* (rapporti di rigonfiamento). I campioni impiegati tuttavia possono differire tra loro dal momento che alcune facce sono state esposte direttamente all'Ossido di Etilene, mentre altre sono state create dal taglio di campioni più grandi (e quindi non esposte direttamente all'agente sterilizzante).

Infine la ricerca è arricchita da dei **test *in vitro* di citotossicità indiretta** al fine di valutare il rilascio di sostanze tossiche per le cellule (di tipo *L929 murine fibroblasts cell line*) in base allo standard ISO-10993. L'esperimento richiede l'analisi di un peso pari a due dischi di PDMS (0,2 g in totale) per tipo di campione e tempo d'incubazione. I campioni sono immersi in DMEM con un 10% di FBS e 1% di penicillina/streptomicina, mantenendo un rapporto tra materiale e medium di 0.2 g/ml. Dopo 3 ore, 1 e 3 giorni di incubazione, una parte del medium è estratto e messo in coltura con le cellule indicate per 24 ore. La loro morfologia è quindi studiata attraverso il microscopio ottico. Campioni di controllo per confrontare i risultati consistono in DMEM completo incubato con le stesse tempistiche senza il PDMS sterilizzato e poi coltivato per 24 ore.

I risultati ottenuti sono integrati con **analisi statistiche** in modo da poter valutare se campioni che hanno ricevuto esposizioni diverse all'Ossido di Etilene possono essere considerati simili. A seconda del numero di campioni e del numero di gruppi da confrontare contemporaneamente, la scelta ricade su 3 tipi di test statistici. Per ciascuno di essi il p value risultante e la *statistical power* associata sono calcolati mediante il software Minitab. Per i test si sceglie un intervallo di confidenza del 95% (p value < 0,05 comporta il rifiuto dell'ipotesi nulla) con una *statistical power* di almeno 0,8.
Il **t-test a 2 code** viene scelto quando dataset con almeno 10 campioni vengono confrontati a coppie (ipotesi nulla: $\mu_1 = \mu_2$), il **test di Mann-Whitney** (metodo non parametrico) viene impiegato invece quando meno di 10 campioni sono disponibili. Per poter applicare efficacemente il primo test le distribuzioni dovrebbero essere Gaussiane (test di Anderson-Darling per dataset numerosi, di Shapiro-Wilk altrimenti), mentre sia l'indipendenza che

l'equivalenza tra le varianze dei due gruppi (mediante F-test) dovrebbero essere soddisfatte. Qualora ciò non avvenga, i metodi non parametrici sono da preferirsi. La terza tipologia di test statistico permette di confrontare C1, C4 e C10 tra loro. L'**ANOVA test** risulta abbastanza affidabile anche per ridotta normalità e omogeneità di varianza nelle distribuzioni, tuttavia alcune condizioni nei residui devono essere rispettate affinché il risultato sia considerato attendibile. Infatti i dataset dei residui nei tre gruppi devono avere varianza costante, media nulla, essere normali e indipendenti.

Risultati

I valori dell'**UTS** sia per 500 mm/min che per 100 mm/min non consentono il rifiuto dell'ipotesi nulla a causa del ridotto numero di campioni (≤ 10) e della notevole variabilità dei risultati che comportano grandi deviazioni standard. Per sopperire a ciò, viene accertata la compatibilità tra i dati per velocità di deformazione diverse e quindi i dataset per lo stesso materiale (ma con velocità diverse) vengono uniti. In questo caso, confrontando C4 e C10, l'ipotesi nulla viene rifiutata. A questi valori vengono aggiunti anche quelli di C0 come riportato nella tabella sotto. Anche se l'analisi statistica complessiva manca di rilevanza statistica, l'UTS potrebbe essere sospettato di diminuire leggermente dopo l'esposizione all'Ossido di Etilene (Fig.I).

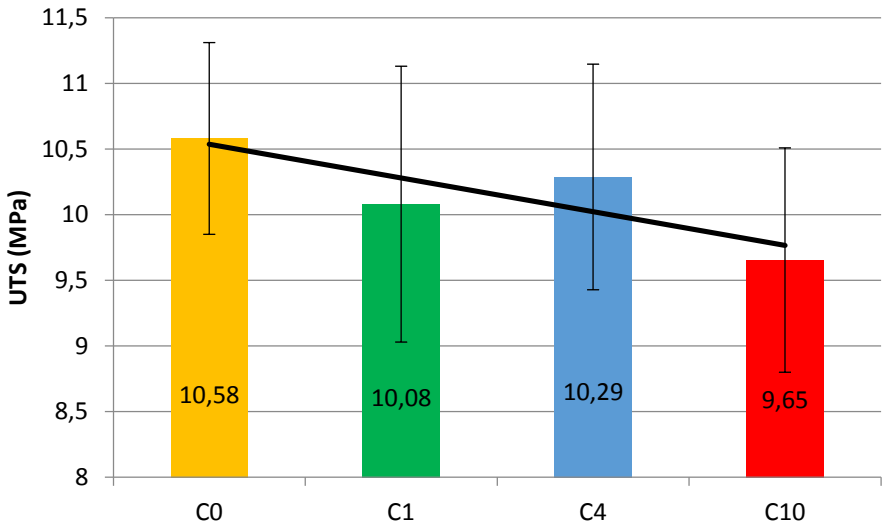

Figura I: Risultati per UTS dopo che i gruppi relativi alle due velocità sono stati uniti.

Quanto descritto per il precedente parametro vale anche per l'**Ultimate Elongation** con l'ipotesi nulla accettata per entrambe le velocità di deformazione e C10 leggermente inferiore agli altri due gruppi. In questo caso però i dataset non possono essere uniti come nel precedente caso poiché i valori sono diversi a seconda della velocità scelta. Anche i moduli elastici (**E_lin** e **E_200**) appaiono simili tra i tre gruppi.
Lo slittamento del campione viene stimato rappresentare fino al 5,5% della deformazione totale. La compatibilità tra C0 e C1 (assunta poi anche per gli altri test) potrebbe essere assunta per il parametro di Ultimate Elongation anche se non in maniera netta, mentre per quanto riguarda i moduli elastici i valori di C0 e C1 sono praticamente identici.

E' e **E''** sono valutati solo per le temperature di 0° C e 37° C. Tutte le 12 possibili combinazioni (tra i 2 parametri, le 2 temperature e le 3 frequenze) mostrano simili andamenti con C1 leggermente inferiore a C4 e C10 che invece sono abbastanza simili. L'ipotesi nulla negli ANOVA test non viene mai rifiutata come suggerisce il grafico sotto (Fig.II) che mostra il confronto con il p value più basso (0,193), simile è il risultato statistico impiegando dei test non parametrici anziché l'ANOVA test.

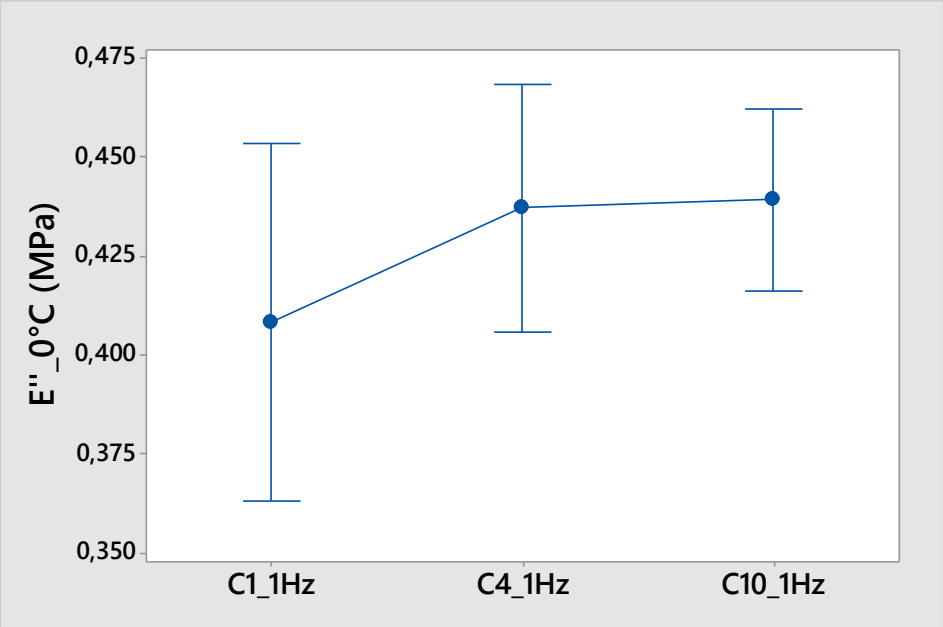

Figura II: Loss Modulus a 0° C con frequenza di 1 Hz nel test di DMA in base al numero di sterilizzazioni.

Al contrario la **Durezza** aumenta sensibilmente dopo l'esposizione all'Ossido di Etilene (meno di 1 unità Shore A dopo 10 cicli) come suggerito in Fig.III.

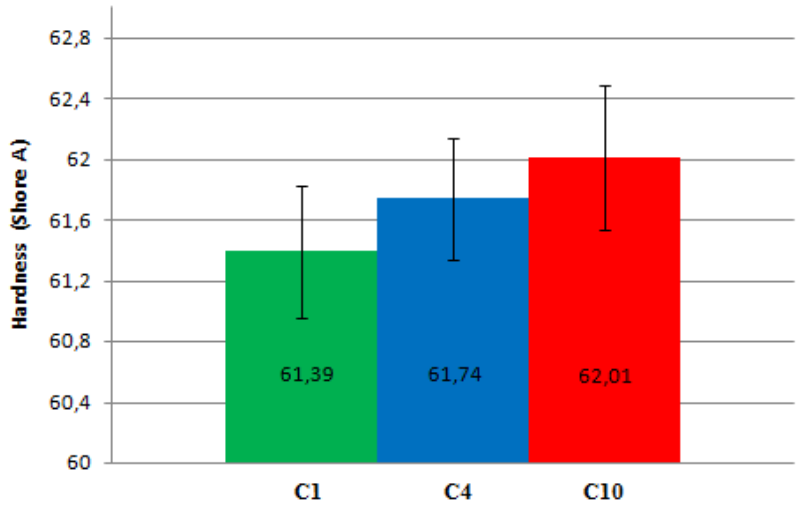

Figura III: All'aumentare dell'esposizione del materiale all'Etox, la durezza aumenta leggermente.

Nonostante le differenze nei valori medi siano ridotte, il gran numero di dati (18) garantisce il rifiuto dell'ipotesi nulla: per l'ANOVA test il p value è 0 con una *statistical power* di 0,97, per il t-test il gruppo C1 differisce dagli altri, mentre C4 e C10 hanno un p value vicino al treshold, ma insufficiente a rifiutare l'ipotesi nulla.

Nella **DSC** con raffreddamento lento solo il picco di fusione (Tm) è riconoscibile. Sia la Tm (-44° C circa) che l'entalpia associata a questo picco non permettono il rifiuto dell'ipotesi nulla (tramite ANOVA test). La Tg, che di solito si presenta come un gradino tra due tratti orizzontali della curva, non è qui visibile mentre lo è nei termogrammi relativi al raffreddamento veloce (intorno a -134° C). Questa differenza è dovuta appunto alla velocità di raffreddamento che, se elevata, non permette alla struttura vetrosa che si va formando di organizzarsi in maniera ordinata, risultando in una notevole componente amorfa anziché cristallina (raggiunta invece con un raffreddamento lento). Anche per Tg tuttavia nessuna differenza risulta esistere tra i tre dataset. Per quanto riguarda i due picchi rimanenti per il secondo tipo di test, essi spesso presentano diversi outlier (o almeno potenziali outlier). Riguardo al picco di fusione a -44° C, l'entalpia associata ad esso non è dimostrabile essere diversa nei tre casi anche se i p value sono abbastanza piccoli e 2

outlier sono sospettati. Per quanto riguarda invece la temperatura Tm anche in questo caso un potenziale outlier è presente. L'analisi è condotta prima escludendo questo valore e poi considerandolo. Sia l'ANOVA test che il test di Mann-Whitney non restituiscono un p value < 0,05 anche se in certi casi i p value sono molto vicini a questo valore. Per quanto riguarda il picco di cristallizzazione nella curva di raffreddamento (intorno a -82° C), i risultati sia per la Tc che per l'entalpia del picco differiscono. Se per il primo parametro il risultato non è chiaro (C4 è maggiore degli altri due gruppi), per l'entalpia invece sembra che questo parametro incrementi (anche se la differenza nelle varianze suggerisce di usare cautela nell'interpretare questo risultato) come suggerito in Fig.IV. Sia il p value dell'ANOVA test (0,044) che quello del t-test tra C4 e C10 (0,019) comportano il rifiuto dell'ipotesi nulla.

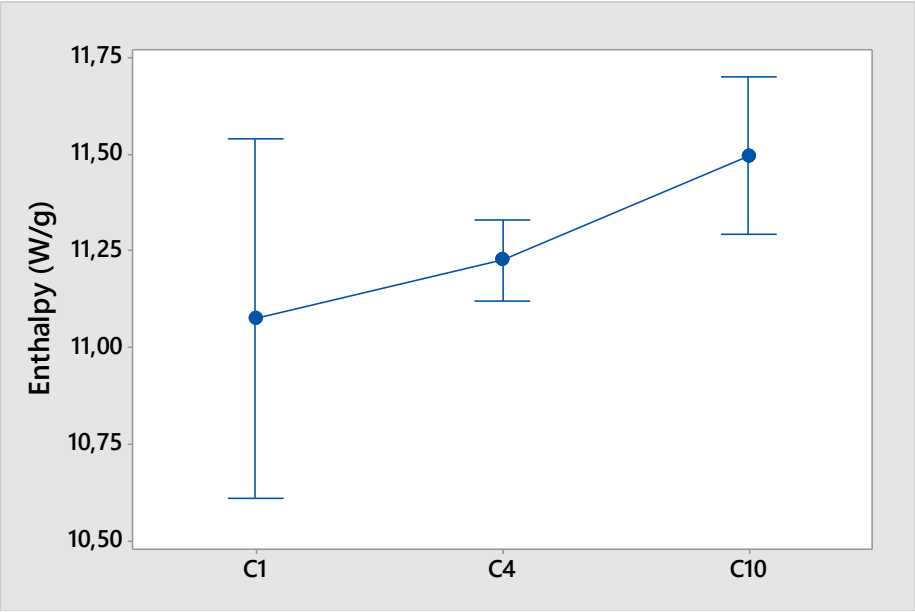

Figura IV: L'entalpia per il picco di cristallizzazione per un DSC con raffreddamento veloce mostra un incremento statisticamente rilevante.

Gli spettri registrati mediante **ATR-FTIR** sono riportati in Fig.V e mostrano come essi si sovrappongano molto bene lungo tutto l'intervallo investigato, in particolare per i tre picchi principali. Lo spettro combacia con la struttura chimica riportata per il materiale in esame. Infatti le seguenti interpretazioni dello spettro sono proposte: stretching asimmetrico in CH_3 (2962 cm^{-1}), stretching in Si-O-Si (1010 cm^{-1}), stretching in Si-O-C (1110-1050 cm^{-1}), flessione fuori dal piano in CH_2 (1125 cm^{-1}) e la presenza di Si-CH_3

(1259 cm^{-1} e 790 cm^{-1}), di $Si(CH_3)_2O$ (864 cm^{-1}) e di R-Si-O-Si-R (1080-1040 cm^{-1}). Le zone di tremolio nello spettro sono associate alla CO_2 e H_2O che la procedura di acquisizione del background non è riuscita comunque ad eliminare completamente. L'unico dubbio riguardo i picchi rimane per quello a 701 cm^{-1}, per il quale l'ipotesi più plausibile rimane la flessione fuori dal piano del CH nel legame C=C tipico degli alcheni. Questo sarebbe spiegato assumendo che alcune estremità funzionalizzate delle catene di silossano rimangano tali anche dopo il processo di curing (le catene rimangono con un'estremità libera o completamente scollegate dal reticolo che si è formato).

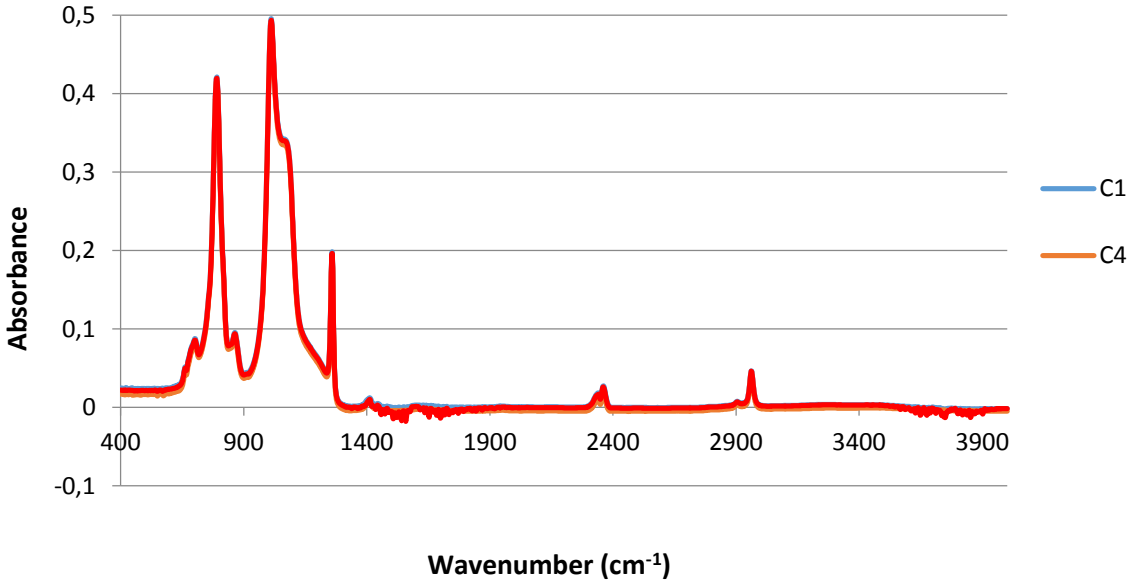

Figura V: Gli spettri ATR-FTIR per i 3 materiali non dimostrano differenze evidenti in corrispondenza dei picchi principali.

A parte l'assenza di differenze macroscopiche nello spettro, queste vengono ricercate anche su scala più ridotta. Vista la costante differenza rilevata tra le baseline dei 3 campioni, un metodo di shift tra gli spettri a livello locale (come se le baseline venissero fatte sovrapporre) rivela che le differenze tra i 3 spettri in corrispondenza dei picchi non supererebbe l'1%.

Gli angoli di contatto nel **test di bagnabilità** rivelano un decremento nell'idrofobicità superficiale come mostrato in Fig.VI, anche se questa differenza diventa rilevante dal punto di vista statistico solo per C10. I p value infatti sono sempre inferiori a 0,05 e le

statistical power > 0,95 se il t-test include C10. Invece C1 e C4 appaiono leggermente diversi, ma nei test statistici le ipotesi nulle non sono rifiutate.

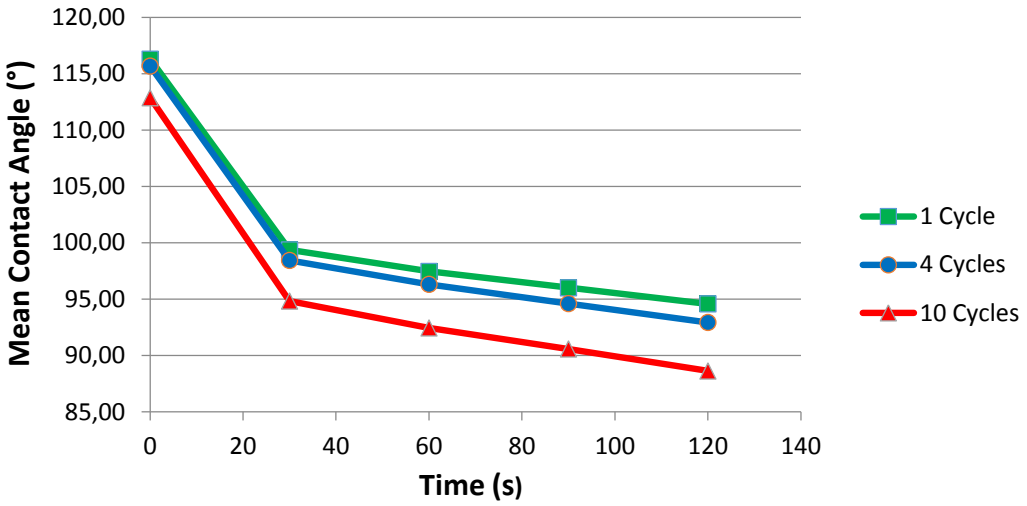

Figura VI: Gli angoli di contatto nel test di bagnabilità appaiono inferiori (il materiale è quindi meno idrofobico) per il PDMS sterilizzato per più volte (C10).

Com'è possibile osservare in Fig.VII, nel **test di swelling** le *swelling ratio* aumentano all'aumentare del numero di cicli di sterilizzazione in base ai valori osservati per 1 e 2 settimane. Nel primo caso tuttavia le differenze non sono statisticamente rilevanti, mentre nel secondo caso C1 risulta diverso da C4 e C10. I valori diminuiscono dalla prima settimana in poi, mostrando che il campione lascia che gli elementi a basso peso molecolare rimasti intrappolati nel reticolo senza però legarvisi possano diffondere all'esterno dello stesso. Tuttavia per la nona settimana il valore di C10 è inferiore a C4 e comparabile a C1, da ciò i test statistici suggeriscono il rifiuto dell'ipotesi nulla anche per questo tempo d'immersione. Visto il tipo di solvente, le ridotte swelling ratio e la preparazione dei campioni, i risultati di questo test non dovrebbero essere considerati comunque totalmente attendibili.

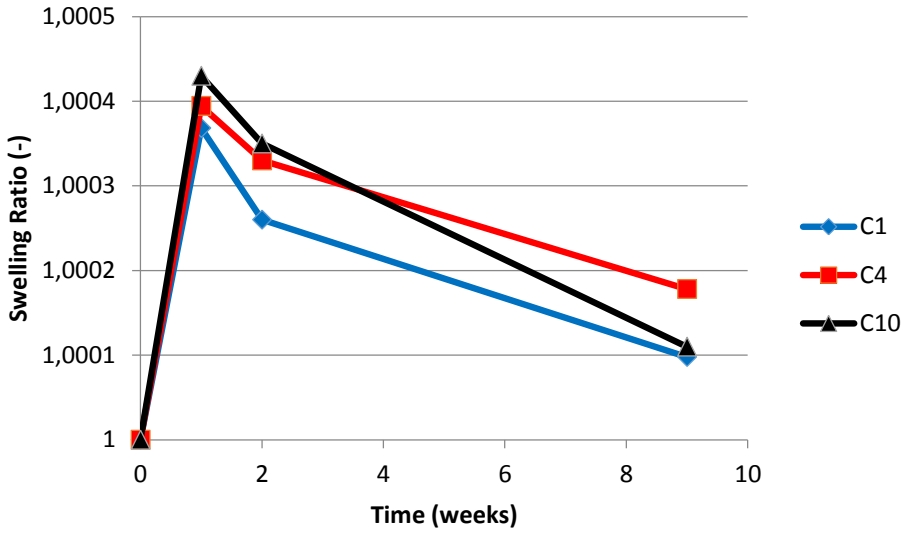

Figura VII:Il PDMS assorbe una quantità estremamente limitata di acqua, suggerendo tuttavia l'esistenza di alcune differenze tra le tre classi di materiali.

Le immagini acquisite durante il **test di citotossicità indiretta** dimostrano che il PDMS sterilizzato più volte con Ossido di Etilene non è citotossico. Nessuna differenza tra i campioni sembra esistere e le cellule mostrano inoltre una buona adesione cellulare con l'assenza di cellule morte (anche se quest'analisi è puramente qualitativa mentre una di tipo quantitativo sarebbe preferibile).

Discussione

La prima indicazione ottenuta dai test riguarda la grande variabilità nei risultati ottenuti (in particolare per il test di trazione uniassiale) che risulta in larghe deviazioni standard e in risultati statistici spesso con ridotta *statistical power*. Da ciò si evince che un numero di campioni molto più elevato sarebbe raccomandabile e che i risultati talvolta contrastanti in letteratura non devono quindi stupire.

Per quanto riguarda i **test meccanici**, l'UTS e l'Ultimate Elongation sono sospettati di diminuire leggermente ma non vi è sufficiente rilevanza statistica, mentre i moduli elastici dovrebbero rimanere costanti. La durezza invece cresce sensibilmente, all'incirca di 0,06 Shore A/ciclo. Gli esperimenti andrebbero comunque ripetuti con i campioni corretti per risultati più attendibili.

L'**analisi termica** mediante DMA suggerisce che E' ed E'' potrebbero leggermente aumentare (anche se l'analisi soffre di un numero limitato di campioni), mentre la DSC rivela che il picco di fusione e la Tg non dovrebbero cambiare (perciò non dovrebbe verificarsi ulteriore crosslinkining post-curing). Se i Tc calcolati mostrano un andamento non chiaro, l'entalpia di questo picco suggerisce un aumento quando il numero dei cicli di Ossido di Etilene aumenta. Tuttavia la diffusa presenza di potenziali outlier non permette di concludere generalmente nulla di particolarmente preciso per i vari parametri. Per tutti i dati finora elencati i trend sospettati sono generalmente in accordo con la maggior parte delle fonti.

L'**interazione con solventi** (acqua in questo caso) rivela una diminuzione dell'idrofobicità superficiale che probabilmente si riflette sull'aumento di liquido assorbito da parte del campione immerso. Meno chiaro è il valore di *swelling ratio* di C10 dopo 9 settimane.

L'utilizzo di altri solventi in grado di garantire maggior assorbimento potrebbe restituire risultati più affidabili ed evidenti. L'**analisi spettrografica** infine non rivela alcun cambiamento nelle vibrazioni molecolari dei legami di superficie e anche l'**analisi citotossica indiretta**, seppur solo qualitativa, non evidenzia differenze tra i vari campioni. Certamente un'analisi quantitativa anziché puramente qualitativa sarebbe migliore, ma andrebbe eseguito anche un test che studi l'adesione, il movimento e la differenziazione delle cellule in contatto diretto con il substrato (visti i potenziali cambiamenti della superficie).

Poiché i test di bagnabilità e di durezza dimostrano dei cambiamenti nel materiale nonostante l'analisi ATR-FTIR non faccia altrettanto, si potrebbe sospettare come responsabile una **variazione della rugosità superficiale**. Tale parametro infatti è risaputo accrescere l'idrofobicità/idrofilicità di un materiale idrofobico/idrofilico quando essa aumenta, mentre esso influenza il calcolo della durezza poiché il calcolo della stessa si basa su una superficie assunta perfettamente piatta.

Assumendo che la sterilizzazione tramite Ossido di Etilene diminuisca la rugosità mediante l'abbassamento dei picchi la superficie diventerebbe meno idrofobica e il durometro misurerebbe una durezza maggiore perché la penetrazione registrata diminuirebbe. L'indentatore raggiungerebbe la linea rossa in Fig.VIII qua sotto partendo da due altezze

diverse, sicché la differenza C viene convertita in differenza di durezza registrata. Analisi mediante SEM o AFM potrebbero confermare questa ipotesi.

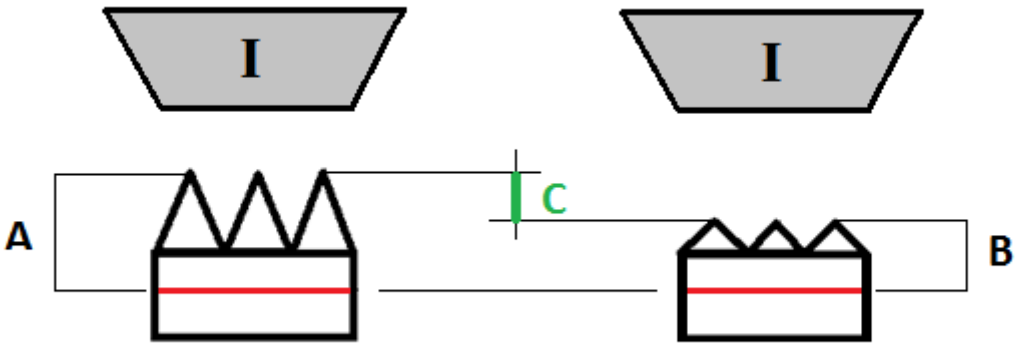

Figura VIII: Ipotesi che spiegherebbe l'influenza di una variazione nella rugosità superficiale sulla registrazione di una diversa durezza. Assumendo stessa profondità di penetrazione nel secondo strato (linea rossa), l'indentatore comincia a registrare la penetrazione ad altezze diverse (differenza pari a C): questa differenza di penetrazione spiegherebbe quella di durezza.

Il valore medio di ***swelling ratio*** alla nona settimana appare sospetto e la semplice ipotesi che esso sia frutto di qualche errore casuale, magari legato alle differenze nei campioni, rimane discutibile. Un'altra interpretazione potrebbe riguardare un diverso rilascio di oligomeri a basso peso molecolare nei tre casi, il cui posto viene preso dalle molecole di acqua (con densità inferiore). Oltre al fenomeno di assorbimento e diffusione anche il fenomeno di depredazione/idrolisi potrebbe influire sull'esperimento. Alcuni studi riferiscono che le perdite di peso in questi esperimenti sono legati alla quantità di *filler* interni alla struttura che sono maggiori per materiali con durezza maggiore. Ciò potrebbe far pensare ad una liberazione di *filler* addizionali originatisi da processi non ben identificati legati presumibilmente all'idrolisi o, meno probabile, all'Etox.

Scissioni di piccola entità potrebbero verificarsi alle estremità libere delle catene legate al reticolo solo per una estremità (le estremità reattive si piegherebbero su se stesse accorciando la catena risultante e generando degli elementi ciclici). Un'altra interpretazione potrebbe riguardare l'erosione meccanica effettuata involontariamente nell'asciugare i campioni prima di pesarli (legati potenzialmente ad una superficie diversa e quindi con resistenza differente all'erosione).

Infine il fatto che la **Tg** non dimostri un cambiamento evidente non dovrebbe di fatto escludere piccoli cambiamenti interni al materiale. Questo parametro infatti cambia in base

al grado di crosslinking, tuttavia similmente è influenzato da tanti altri fattori, tra cui cristallinità, peso molecolare, velocità di test, presenza di elasticizzanti ecc. Con ciò si vuole indicare che piccoli cambiamenti risultanti in contributi opposti alla Tg (shift del parametro in direzioni opposte) potrebbero comunque far risultare il parametro alterato a livello complessivo.

Conclusioni

Il materiale MED-4860P esposto a sterilizzazione mediante Ossido di Etilene mostra cambiamenti statisticamente rilevanti a livello superficiale come dimostrato dai test di bagnabilità e durezza (e parzialmente da quello di swelling). Per le altre proprietà si possono formulare alcune ipotesi ma niente di sicuro può essere dimostrato. Ciò permette di concludere che questo agente sterilizzante sembra alterare maggiormente le *surface properties* e scarsamente le *bulk properties.*

La seconda conclusione della presente tesi è che i campioni sterilizzati più di quattro volte non andrebbero impiegati dal momento che i campioni C10 sono quelli che generalmente, al di là della rilevanza statistica, mostrano valori diversi dagli altri gruppi. Invece i campioni sterilizzati poche volte dovrebbero essere comunque ancora compatibili con quelli sterilizzati una singola volta anche se la rilevanza statistica spesso limitata richiederebbe ulteriori indagini per poter asserire ciò. L'aggiunta di test cellulari quantitativi e di contatto diretto permetterebbe inoltre di interpretare meglio la compatibilità all'impianto di questi materiali sterilizzati più volte.

Abstract

Sterilization by Ethylene Oxide (Etox) represents the most employed sterilization procedure for medical and health care devices. Despite its ubiquitous use in the medical device industry, little data have been published on the effect of this sterilization on the mechanical properties of polydimethylsiloxane (PDMS) silicone rubber. The alkylating reaction guarantees the high sterilizing efficiency of this procedure even though certain functional groups in some polymers are known to react as well. Polydimethilsiloxane sterilized by this technique is known to be safe, however the present work aims at determining whether no alterations occur in material properties when this material is exposed to several sterilization cycles instead of a single one. In fact biomedical industries get rid of those materials which a second sterilization cycle is required for.
For this purpose samples sterilized one, four and ten times are investigated by different tests in order to detect eventual changes. Experiments deal with both surface and bulk property investigation, in addition indirect cytotoxicity tests are performed as well since the material is intended to implantation in the human body. Statistical analysis is performed aiming at checking whether samples which undergo different Etox exposures can be considered similar (t-test, Mann-Whitney and ANOVA tests are employed).
Test outcomes suggest bulk properties are slightly affected by Etox exposure even for massively repeated cycles. Differences in mean values can be seen for UTS, Ultimate Elongation, Storage and Loss Moduli, however these results lack statistical relevance. On the contrary surface properties appear altered since hardness, wettability and swelling tests return statistically significant changes. In fact as Etox exposure increases, surface hydrophobicity decreases (6° difference after 2 minutes) and hardness slightly increases (approximately 1 Shore A difference). Surface inspection by ATR-FTIR fails in recognizing any difference among spectra, so that changes in surface properties cannot be ascribed to alterations in molecular vibrations in material surface. An alternative hypothesis explaining both hardness and hydrophobicity changes is proposed: surface roughness is hypothesized to decrease when the material undergoes sterilization, explaining both hardness and wettability outcomes. Interpretations of swelling results are proposed as well, hypothesizing little hydrolysis or surface erosion while drying the samples. As Tg results not to change when Etox exposure increases, a short reflection about the variation of this parameter is presented.
This work demonstrates samples sterilized more than four times should not be employed, whereas for fewer cycles further analyses should be carried out as obtained results often lack complete trustworthiness (because of small sample groups and the questionable method accuracy in certain cases). However the employment of samples sterilized for few times after the first cycle seems reasonable as there is no proof of significant induced changes. Further analyses of surface properties and leaching behavior would enrich the present work and may support the proposed hypotheses.

Abstract (Italiano)

La sterilizzazione mediante Ossido di Etilene rappresenta la procedura di sterilizzazione più usata per strumenti medici. Nonostante il diffusissimo utilizzo nel campo dell'industria biomedicale, è relativamente scarsa la quantità di informazioni pubblicate riguardo gli effetti di questa sterilizzazione sulle proprietà meccanica degli elastomeri in Polidimetilsilossano (PDMS). La reazione di alchilazione garantisce l'alta efficienza del processo anche se certi gruppi funzionali in alcuni polimeri sono noti reagire similmente. Il Polidimetilsilossano sterilizzato mediante questa procedura è considerato sicuro, tuttavia l'attuale tesi vuole determinare se allo stesso modo non avviene alcuna alterazione il materiale è sottoposto a diversi cicli anziché ad un unico. Infatti le industrie biomedicali si disfano dei materiali e prodotti per cui sarebbe richiesta una seconda sterilizzazione.
A tal proposito alcuni campioni sterilizzati una, quattro e dieci volte sono studiati attraverso differenti esperimenti in modo da riconoscere eventuali cambiamenti. Le prove riguardano sia lo studio delle *surface properties* che delle *bulk properties,* inoltre dei test di citotossicità indiretta sono eseguiti poiché il materiale è destinato all'impianto nel corpo umano. L'analisi statistica riportata verifica se campioni esposti a quantità diverse di Etox possano essere considerate simili (sono impiegati t-test, Mann-Whitney e ANOVA).
I risultati dei test suggeriscono che le *bulk properties* siano leggermente alterate dopo una notevole esposizione all'Etox. Differenze nei valori medi possono essere viste per UTS, Ultimate Elongation, Storage e Loss Modulus, tuttavia questi risultati mancano di rilevanza statistica. Al contrario le *surface properties* appaino alterate dal momento che i test di durezza, di bagnabilità e di swelling mostrano risultati statisticamente rilevanti. Infatti all'aumentare dell'esposizione all'Etox, l'idrofobicità superficiale cala (6° di differenza dopo 2 minuti) mentre la durezza aumenta sensibilmente (approssimativamente 1 Shore A di differenza). L'ispezione superficiale mediante ATR-FTIR non riconosce alcuna differenza tra gli spettri, perciò i cambiamenti superficiali negli altri esperimenti non possono essere imputati ad alterazioni nelle vibrazioni molecolari del materiale in superficie. Un'ipotesi alternativa che spiega sia i cambiamenti nella durezza e nell'idrofobicità è quindi proposta: la rugosità superficiale è ipotizzata diminuire quando il materiale viene sterilizzata, spiegando i risultati sia del test di durezza che di bagnabilità. Interpretazioni dei risultati della prova di swelling sono proposte similmente, ipotizzando una leggera idrolisi o l'erosione della superficie mentre il campione viene asciugato. Una maggiore esposizione all'Etox non altera la Tg, tuttavia una breve riflessione riguardo la Tg è presentata.
Questa tesi dimostra che i campioni sterilizzati più di quattro volte non dovrebbero essere impiegati, mentre per meno cicli ulteriori analisi dovrebbero essere condotte poiché i risultati ottenuti spesso difettano di completa attendibilità (a causa del limitato numero di campioni e della discutibile accuratezza della procedura usata in alcuni casi). Tuttavia l'impiego di campioni sterilizzati poche volte dopo la prima pare ragionevole poiché non c'è prova di cambiamenti indotti significativi. Ulteriore analisi delle proprietà superficiali e lisciviazione arricchirebbero il lavoro presente a potrebbero confermare le ipotesi proposte.

List of Abbreviations and Symbols

C1	sample group which undergoes 1 Etox sterilization cycle
C4	sample group which undergoes 4 Etox sterilization cycles
C10	sample group which undergoes 10 Etox sterilization cycles
C0	unsterilized samples
N	number of samples
C1-C4	comparison between C1 and C4
MW	Mann-Whitney test
t-t	t-test
Mean (μ)	mean value
StDev	standard deviation
PV	p value
SP	statistical power
UTS	Ultimate Tensile Strength
UE	Ultimate Elongation
E_lin	tangent modulus
E_200	secant modulus (stress at 200% strain)
Tg	Glass Transition temperature
Tc	Cold Crystallization temperature
Tm_1	First Melting Transition temperature
Tm_2	Second Melting Transition temperature
Tm	Melting Transition temperature
E’	Storage Modulus
E’’	Loss Modulus
tanδ	ratio between E’’ and E’ (ratio of viscous to elastic response in viscoelastic material)
SR	swelling ratio

1 Introduction

1.1 PDMS

1.1.1 PDMS structure and Properties

Polydimethylsiloxane, commonly referred to as PDMS or silicone rubber, is a largely used material in several industrial fields.

Silicones are entirely synthetic polymers presenting a Si-O-Si backbone with organic groups attached to Si. Friedel and Crafts firstly synthesized Si-O bond in 1863 [1] whereas the term "silicones" was assigned by Kipping in 1904 based on their similarity with ketones. In fact Kipping described the new compound with the brutal formula R_2SiO which recalls the one ketones are referred to [2]. In the following years more specific nomenclature was developed while these materials and their applications were flourishing.

Combination of the organic groups linked to an inorganic backbone, chain length and degree of crosslinking are the most influent factors in silicone classification. Depending on them they can be divided into fluids, compounds, lubricants, resins and rubbers, showing combination of distinctive properties and application fields. Some examples of these groups are phenyl, vinyl and trifluoro-propyl groups. Nevertheless PDMS represents the main example of this kind of material, with 2 methyl groups as organic groups for each Si molecule along the backbone [1,2]. Chemical composition of PDMS and its chemical formula are reported below (Fig.1).

$$CH_3\,[Si(CH_3)_2O]_n\,Si(CH_3)_3$$

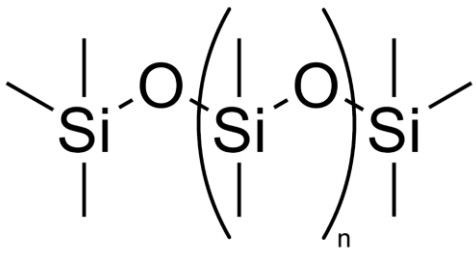

Figure 1. Two different ways to represent PDMS: its chemical formula (up) and its structural formula (down). The higher n, the greater chain length and molecular weight are.

This chemical product can be synthesized mainly by the following process: silica (SiO_2) is reduced to silicon, which is used in combination with 2 chloromethane molecules (CH_3Cl) to obtain dimethyldichlorosilane (Me_2SiCl_2). This product undergoes hydrolysis which leads to a mixture of linear and cyclic oligomers (Fig.2A). Then, if even longer chains are requested (as most cases do), the cyclic oligomers can be polymerized with the help of a strong acid or base (Fig.2B) whereas the linear ones can condense to extend the chain by connecting their extremities [2,3].

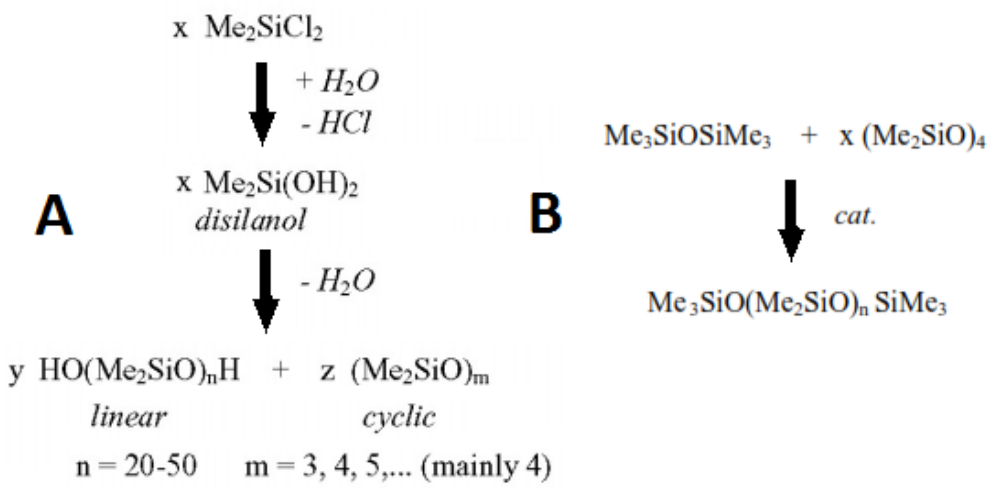

Figure 2. Dimethyldichlorosilane reacts with water releasing hydrogen chloride and producing linear and cyclic polymer (A). Cyclic oligomers can open and undergo polymerization in order to get longer chains (B).

However during the first passage hydrogen chloride (HCl) is produced, making this reaction not recommended for medical purposes. A different reaction is suitable for biomedical applications: the chlorine atoms in the silane precursor can be switched with acetate groups, producing acetic acid instead of hydrogen chloride. Even if the curing process requires more time, this choice has the advantage of a lower chemical aggressiveness by $C_2H_4O_2$ with respect to HCl [4].

In addition to the contribution to different properties, the presence of functional groups allows also other specific treatments, including crosslinking processes (necessary to create an elastomer) which will be discussed in the next pages.

Knowledge about PDMS properties and technologies has reached a fairly high level nowadays. PDMS benefits of an essentially non-toxic nature, viscoelasticity, chemical

inertness, hydrophobicity and a unique flexibility (shear modulus G may vary between 100 KPa and 3 MPa) given by the flexibility of Si-O-Si backbone and the very low cohesive energy existing among methyl groups. In fact these pendant groups show the weakest intermolecular interactions known: the London dispersion forces (sometimes called "instantaneous dipole–induced dipole forces"). The low surface tension, which is a direct manifestation of low intermolecular forces, confirms that the interactions between two PDMS chains occur only through their methyl groups [2].

This material is also highly insoluble in water, in fact hydrophobicity results in the beading of polar solvents on the surface with difficulties to soak the material. On the other hand it can absorb water vapor and hydrophobic contaminants contained in the water, releasing not crosslinked components into the liquid [5]. PDMS is also greatly permeable to gas because of its flexibility in the Si-O chains: in fact they provide "openings" which form and disappear with chain movement permitting gas diffusion.

Other properties are transparency at optical frequencies, low autofluorescence, surface tension, chemical reactivity (except of at extreme pH) and damping, high compressibility and dielectric strength (~ 14 V/μm), making this material suitable as electric insulator. Its low chemical reactivity turns into a good resistance to oxygen, ozone and UV light. Nevertheless plasma treatment can oxide the surface of PDMS producing silanol terminations (SiOH) and making PDMS hydrophilic and resistant to hydrophobic and negatively-charged molecules adsorption for some minutes [5]. Treatment by plasma is commonly used to seal microfluidic PDMS structures to glass. Silicone rubber can stick efficiently to glass and other substrates (e.g. ceramic, alumina, titanium, tin and chromium), however its adhesive properties depend on the substrate nature so that it gets quickly detached with certain surfaces (e.g. gold and platinum) [6,7].

Furthermore it is characterized by a low glass transition temperature (Tg ≈ −125°C), low thermal conductivity, applicability over a broad range of temperatures (at least from −100 °C up to +100 °C) and small temperature variations of the physical constants (except for the thermal expansion) [2,8]. The last 3 properties explain PDMS success in all the fields requiring large heat resistance and heat stability in a reasonable temperature range.

On the other hand polydimethylsiloxane has some drawbacks with respect to other polymers used in biomedical applications, such as polyurethanes. As PDMS, these materials show a certain variability in their properties according to the way they are

prepared. Nevertheless PDMS generally exhibits lower UTS, hardness and elastic modulus with respect to polyurethanes, even if it is characterized by higher deformations and degradation resistance [9]. According to that, polyurethanes should be chosen instead of silicone rubbers in certain applications (such as those requiring great mechanical and load-bearing properties).
A good compromise between the two cases is represented by the incorporation of PDMS into the soft segments of polyurethanes, obtaining materials with mechanical properties similar to polyurethanes but with higher resistance to oxidation and ESC (environmental stress cracking) [10].

As reported at the beginning of this paragraph, PMDS can be divided into fluids, compounds, lubricants, resins and rubbers (or elastomers).
For encapsulation purposes, the last type is used. Just to mention some other elastomers as examples in addition to the silicon rubber described in the present work, also Polyacrylic rubber, Styrene-butadiene rubber, Polybutadiene and Butyl rubber belong to this material category. Elastomers according to IUPAC definition are polymers displaying rubber-like elasticity. They are characterized by weak inter-molecular forces, low elastic modulus and huge strain-resistance before fracture. Their good flexibility is due to their Tg, which is much lower than common temperature ranges. The final material is created by curing which makes the long polymer chains crosslink. Fig.3 shows their typical stress-strain relation, whereas the chain structure in elastomers is displayed in Fig.4. When a stress is applied, the long polymeric chains (soft segments) sharing common parts (cross-linkages, hard segments or entanglements) are allowed to get extended up to a certain limit by chain reconfiguration. Stress removal results in the recovery of the original shape thanks to crosslinking sites/hard segments [11,12]. The lower the temperature and the higher the crosslink density (or ratio between hard and soft segments), the brittler the material behaves.
Crosslink density indicates how highly crosslinked a silicone is. Swelling tests of the material in appropriate solvents allow the estimation of this parameter. Obviously hard polymers show greater difficulty in swelling with respect to the softer ones. In fact a lower crosslinking density, resulting in a lower hardness, permits a better solvent absorption [13].

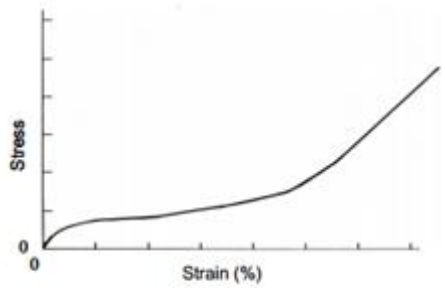

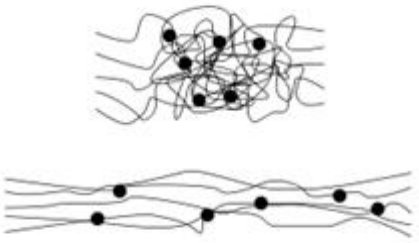

Figure 3. Typical stress-strain relation in elastomeric materials. The curve is monotone and characterized by low stress and high strain values.

Figure 4. Representation of the elastomeric components with and without applied stress (black dots represent the hard segments).

Silicone can be crosslinked and cured into solids by using different cure systems. Platinum-catalyzed cure system, condensation cure system, peroxide cure system and oxime cure system are the most known typologies dealing with this process. The curing process makes PDMS a thermosetting material, explaining its resistance to high temperature [3].

In health care applications addition (platinum is generally employed) and free radical (peroxide) curing systems are the most famous ones, in particular the first one can be accelerated by adding heat or pressure. An addition cure system consists in an organometallic crosslinking reaction, where platinum or another metal complex catalyst is exploited in order to launch the polymerization among vinyl and Si-H groups. Siloxane base oligomers contain vinyl groups as terminal parts, whereas the crosslinking oligomers (a common example is represented by Polymethylhydrosiloxane) contain at least 3 silicon hydride bonds each. The two groups form Si-CH_2-CH_2-Si linkages through an addition reaction and multiple reaction sites on each component generate a 3D crosslinking. Furthermore more crosslinked and harder elastomers can be created simply increasing the ratio between curing agent and base (oligomers). No by-products (even no water) are generated by this reaction (addition) whereas 5-15 ppm of Pt can be considered an effective value for catalysis action [14,15]. Since platinum is used as a catalyst it does not

join the reaction but only promotes it; if necessary the reaction can be accelerated by heating the reaction environment [15].

Fig.5 shows the polymerization process occurring between the 2 parts when a catalyst is present. However the main drawback of this technique resides in catalyst costs that are reflected on the price of finished products.

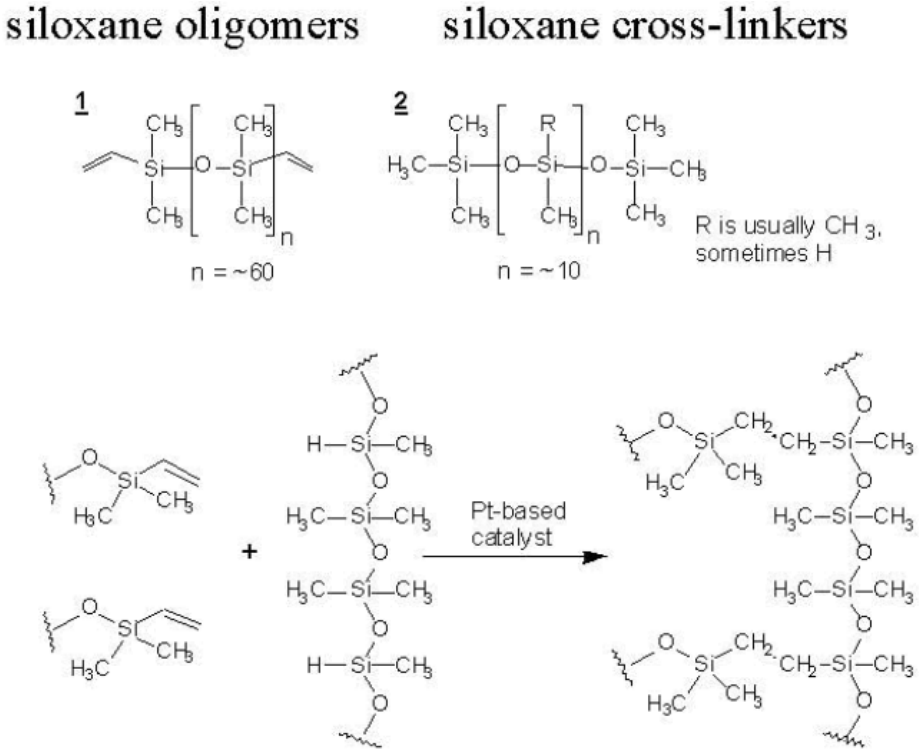

Figure 5. The addition cure system takes advantage of platinum in order to launch the crosslinking between the two displayed components. The vinyl and Si-H groups form Si-CH_2-CH_2-Si linkages through addition reaction. This reaction is repeated along different sites of different chains.

With respect to addition curing, free radical curing has the advantage of a relatively cheap process even if high temperatures are required. In fact it uses free radicals generated by organic peroxides (1% relative composition) which decompose at elevated temperatures, launching a crosslinking reaction. The main flaw is represented by those peroxides and radicals that are not consumed during the reaction: that means by-products are generated

with this curing process representing a product contamination. Volatile organic acids generally remain entrapped inside the final product, even if a post-cure treatment (high temperature exposure for a long period) can overcome this problem by removing them [14]. Techniques as leaching analysis (e.g. GC-MS) can extract these by-products from the silicone matrix. According to J. Heiner [16] cumyl alcohol and acetophenone can be extracted from the peroxide-cured elastomer using GC-MS due to dicumyl peroxide which breaks down into acetophenone and cumyl alcohol. The formation of cumyl alcohol is most likely to occur in an acid environment, whereas in an alkaline environment the formation of acetophenone through a cumyloxy radical is more likely. These substances (both harmful and irritant) can induce a crosslinking reaction in the material during a sterilization procedure. In addition to these drawbacks, E. Gautriaud [17] reports how Pt-curing guarantees smaller variation and higher stability in mechanical parameters (hardness, tensile modulus and tensile strength in particular) than peroxide-curing when γ or e-beam radiations are employed. However this difference between the two curing techniques is not that evident if Etox sterilization is applied: in fact in this case some parameters of Pt-cured material show smaller alteration whereas peroxide-cured ones are higher and vice versa.

1.1.2 PDMS applications, Medical devices in PDMS and Cochlear Implants

As already mentioned the term "silicone" does not refer to a unique type of material, since the presence of different side groups results in materials with different properties, nevertheless this term generally refers to PDMS in industrial field.

Applications of PDMS spread onto a very wide range of fields. It can be used as surfactant [18] and antifoaming agent [19] due to its hydrophobicity and antifoaming properties, for the same reason it can be employed in water-repellent coatings. Other industrial applications are in plastic industry, textile field (fiber production, softening action on tissues, water resistant coatings etc.), heat resistant and antifouling paintings and cleaning products [2]. In automotive industry fluid silicone is used in automotive viscous limited slip differentials and couplings, whereas silicone external gaskets and external trim owe their success to the resistance to ozone, oxygen and UV light [2]. The same properties

allow this material to be largely used in construction industry (e.g. coating and glazing seals). Soft lithography is another field where PDMS finds massive applications: elastic stamps are created enabling the transfer of a certain pattern (with few nm resolution) onto silicon, glass and polymer substrates. Photolithography and plasma lithography are generally employed to prepare the pattern fashion on the stamp [20]. Soft lithography enables also the creation of microfluidic structures, optic telecommunication systems and Bio-MEMS [5,20]. These last elements are a particular application of soft lithography where a silicon substrate is used as negative pattern which PDMS is shed over. Once PDMS is cured, it is removed and treated to get the desired surface behavior, finally it is sealed (generally with a glass layer) to create a close channel. PDMS coatings with controlled thickness can also be created (during the crosslinking) over a substrate by spincoating and multilayers PDMS devices can be prepared by plasma treatment and metal deposition [5]. Research in flexible electronics found PDMS to be particularly useful because of its flexibility and optical transparency, in addition to its ease in fabrication and cheapness. In fact burning due to moisture condensation on engines represents a problem which a simple PDMS sealing encapsulation can overcome (this technique will be resumed later dealing with medical implants) [2]. In food and beverage industry PDMS is extremely diffused according to its water insolubility, thermal stability and chemical inertness, furthermore it can be sprayed onto plant leaves. FDA (Food and Drug Administration) accepted its use because PDMS of sufficient molecular weight does not penetrate through biological membranes, not being metabolized but excreted unchanged. In domestic use PDMS is well known as rubbery caulks, adhesives, heat resistant tiles, shower or aquarium sealants (it can form watertight seals), grease agent, damping and heat transfer fluids, cosmetics (as dimethicone) and hair conditioners [2].

As described in this paragraph PDMS has many applications, nevertheless a crucial employment of this material resides in the biomedical field. Also in this case its application is very spread depending on the material properties. Aside from medical devices polydimethylsiloxanes can be mixed with silicon dioxide to get activated dimethicone, often used in over-the-counter drugs as an antifoaming agent and carminative. Simethicone for example is used to reduce bloating, discomfort or pain due to excessive gas amount in stomach or intestines [21]. Products with PDMS are employed in

the treatment of head lice and skin-moisturizing lotions [22] whereas silicone rubber is commonly used also in baby bottle nipples.

In general silicone rubber can be considered ideal for those application requiring flexibility, long term stability and hemo/bio-compatibility once they are inserted into the body and get in contact with blood. PDMS can be used both in a solid state both in fluid/gel form. Examples of the second type are bandages, implant fillers and silicone oil during vitrectomy surgery [3].

Medical devices in PDMS can be divided into those which will be implanted and those whose application is temporary (sometimes they are not necessarily introduced inside the body). In the first category can be listed soft contact lenses, scar treatment sheets, catheters (Fig.6A), shunts (Fig.6B), drains (the device can be either entirely in silicone or silicone-coated on the surface to lower host reaction to foreign material contact) and extra corporal machine components [3,12]. Blood oxygenator, kidney dialysis system and CPB (cardiopulmonary bypass) machine use external networks for blood circulation consisting in silicone tubes connected each other or to other hemocompatible components. Hemocompatibility of PDMS is not the unique reason of its success in such applications, high gas permeability plays a fundamental role as well in oxygenation membranes and devices requiring high aeration [3].

About implanted PDMS some examples are represented by filler fluid in breast implants [12], flexible tubes used as voice prostheses (placed in the throat after laryngectomy), bile duct repair and urethra replacement [3] and encapsulation systems [6]. Ophthalmological field largely uses this material for many purposes: silicone vitreous fluid replacement and elastomer IOL after retinal reattachment or cataract surgery are just a couple of examples. Also aesthetic and reconstructive plastic surgery takes advantage of this material for the replacement of breast, testicles (Fig.6D), chin, nose and buttocks [12]. Finally in orthopedic applications hand and foot joint implants (Fig.6C) and cement restrictors (used in joint replacement surgery involving cement) are generally made of silicone rubber [13].

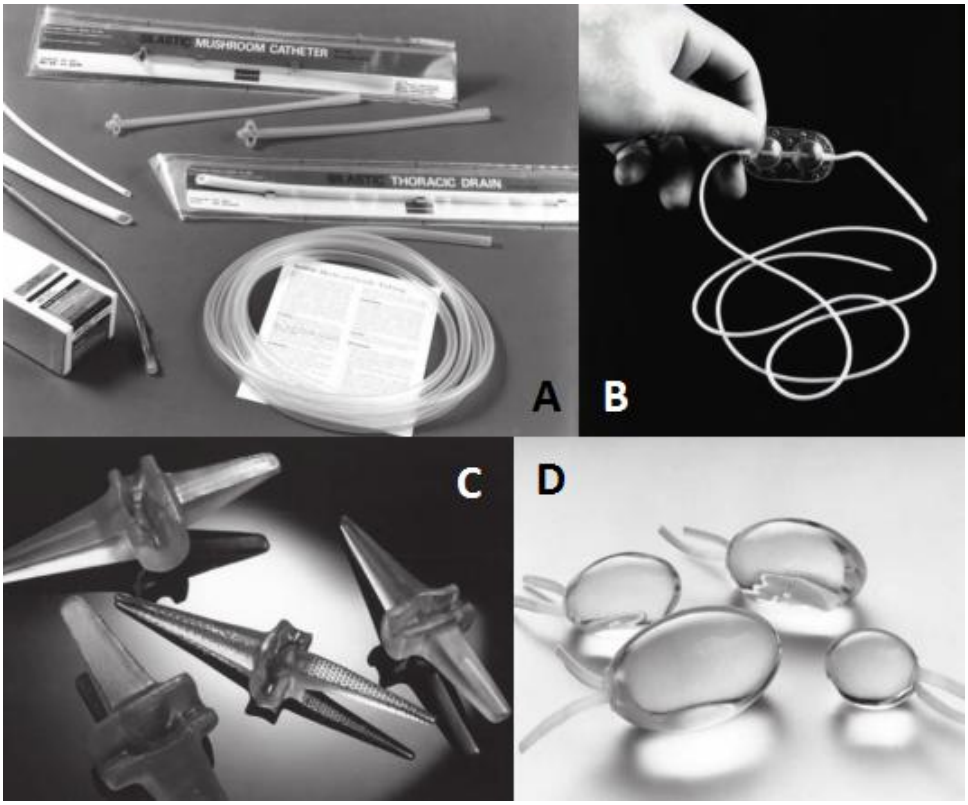

Figure 6. Examples of PDMS use in biomedical devices: tubes and catheters (A), shunts (B), hand joint implants (C) and testicle prostheses (D).

Encapsulation systems have been mentioned above as common biomedical application for this material. The importance of these protections grew exponentially with a more and more common use of the "active implantable medical devices" (AIMD). This term refers to any medical device relying for its functioning on a source of electrical energy (or any source of power other than that directly generated by the human body or gravity) and which is intended to be totally or partially introduced into the human body [23].

Encapsulation aims at protecting and insulating electrical components, circuits and all those parts which are particularly sensitive to moisture and fluid contact. They supply a double protection: the prevention of leakage currents due to device voltages and the protection against corrosion [24]. Neurostimulators, pacemakers and cochlear implants require such a protection in order to be implanted in a safe way. Due to its excellent dielectric properties, a protective PDMS layer allows their encapsulation. The combination

of all the properties listed in the previous paragraphs, hydrophobicity and high dielectric breakdown (avoiding signal loss) in particular, allow these devices to resist in harsh and aggressive environments [2]. Nevertheless in order to get an effective insulation, the encapsulant polymer must be bonded to the substrate to prevent ionic currents from flowing and water from filling the gap (between polymer and device). If there are no gaps at the interface, water vapor permeating the silicon rubber cannot condense on the substrate, so that no ionic conduction occurs [24]. These types of implants have been shown to be resistant at 37° C for 12 years at least if the encapsulation process is performed correctly and the interface bond is perfectly developed [6,7].

Fig.7 shows the failure process in a substrate with conductive metal components. At the beginning no voids are exhibited (Fig.7A), however the interface bond can deaden with time till a gap is created (Fig.7B). Water vapor can now condense on the substrate and the resulting water can launch a corrosion process (Fig.7C). Generally the implant function continues but the risk can also be associated to the corrosion products which can permeate the insulating membrane and diffuse in the surrounding tissues. An even more dangerous case is represented by the encapsulation bursting because of the inflation of gases created by electrolysis if a highly conductive electrolyte forms [24].

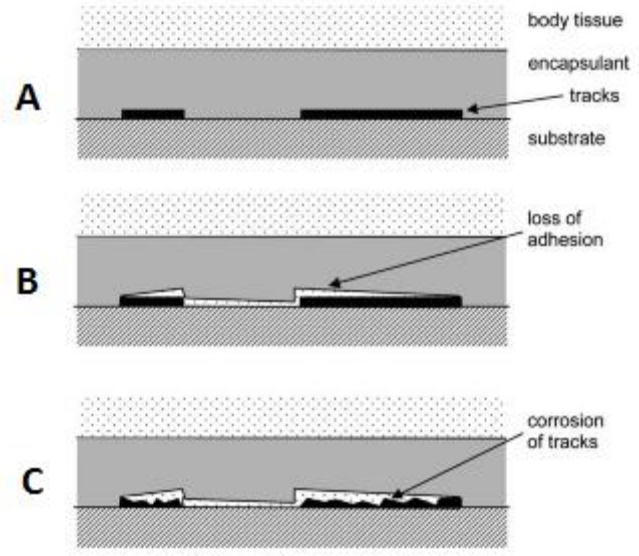

Figure 7. Stages of implant failure: manufacture and then implantation of the encapsulated device (A), adhesion failure and following condensation of water vapor (B), corrosion of metallic components due to water in the void.

Cochlear implants represent an example of devices requiring this protection. Cochlear Ltd, the world leading manufacturer of implantable hearing solutions, encapsulates their cochlear implants in polydimethylsiloxane (Fig.8). PDMS is used to provide an ionic moisture barrier and infer biocompatibility to the hermetic electronic package of the implant.

A cochlear implant is a surgically implanted electronic device, composed of two components (only one is implanted), which helps speech and environmental sound recognition by patients with severe and profound sensorineural hearing loss. This device replaces the pathological cochlea in its function of transmitting the collected sounds to the acoustic nerve. In addition to signal transmission, it conducts filtering and elaboration processes. An external microphone transforms the received sounds into electrical signals and through a speech processor the information are transmitted to the internal component. This second part consists of a ceramic or titanium housing (containing a microchip), a coil antenna for transcutaneous transmission of power and data and an intracochlear electrode array. The microchip decodes the signals coming from the external component, transmitting the analyzed information to the intracochlear electrodes.
In December 2012 approximately 324,000 people worldwide have received cochlear implants; in the U.S. children with CI represent 39,5 % of implant recipients [25].

In addition to the already mentioned main aims of PDMS encapsulation, some extra features are important for this type of implant and explain the choice of PDMS. Firstly this material sticks efficiently to both titanium and ceramic (materials the housing is made of) [7]. Cochlear implants are implanted and anchored to the squama temporalis so that a certain stability within a reasonable temperature range is needed due to skin proximity. It asks also for a certain flexibility and shape-recovery because the implant may be exposed to sudden deformation (impacts) or long-lasting deformation (sleeping with that side of the head leaning on the pillow). Obviously biocompatibility, inertness, stability and resistance are other properties which the PDMS has been chosen for as encapsulation system for cochlear implants. Finally this material is generally sterilized with ethylene oxide which is the preferred technology for these polymers (PDMS is stable to high temperature as well, whereas several polymers are hugely heat sensitive and strictly require Etox treatment).

Figure 8. Implanted component in a cochlear implant device. The transparency of the material allows to see the encapsulated elements.

1.2 ETOX

1.2.1 The role of sterilization in medical field

Sterilization is a crucial step in biomedical implants because eventual pathogens introduced inside the body can induce infection: it results in the removal of the device (new surgery), drug therapy to kill the pathogens, huge institutional costs related to nosocomial infections and mortality/morbidity concerns. The reported issues justify why a proper sterilization of biomaterials used in implants is a critical prerequisite for their successful clinical application [3,26]. Many sterilization technologies are available nowadays: the most widely used are gamma or electron beam irradiation, steam and ethylene oxide (generally shorted as EO, EtO or Etox).

Gamma or electron beam irradiation are quite common in medical applications but their limit consists in the induced scissions and crosslinking due to free radical propagation in polymers [27]. Steam sterilization has definitely the advantage of being extremely cheap and it is really common to quickly sterilize metal objects and instrumentation in laboratories. On the other hand polymers and those materials suffering for high temperature and high moisture exposure cannot be sterilized with this technology.

All these sterilization methods could therefore prevent the expected behavior and performance of the material by causing degradation and changes in properties [26].

Raw material designation	Radiation	EtO	Moist Heat	Dry Heat	Hydrogen Peroxide	Ozone
Cellulose ester	2	4	1-2	1-3	1	1-3
Cellulose, paper, cardboard	2-3	4	1-2	1-2	1	1-3
EPDM	3-4	4	3-4	2-3	2-3	2
Perfluoro alkoxy (PFA)	1	4	4	4	4	4
Polyamides (eg. Nylon)	2-3	4	1-4	1-4	3	3
Polycarbonates (PC)	3-4	4	1-3	2	4	4
Polyethylene (PE)	3-4	4	1-3	1-2	4	4
Polypropylene (PP) stabilised	2-3	4	2-3	1-3	4	4
Polytetrafluoroethylene (PTFE)	1	4	4	4	4	4
Polyvinylchloride (PVC)	3	4	1-2	1-2	4	4
Silicone adhesives	2-3	4	1-3	2-4	2	3
	1 = Do not use	=>	4 = Completely compatible			

Table 1. The impact of the most common sterilization techniques on some materials generally used in medical application. Higher numbers represent lower impact of a specific sterilant on a certain material. Thus the value "4" suggests the combination of silicone and Etox to represent a good choice.

1.2.2 Ethylene Oxide properties and sterilization process

In order to avoid these drawbacks, Etox often replaced the previous techniques, getting more and more relevance and spread application in medical field. Its importance grew together with the disposable MD (medical device) market with the purpose of cost saving in health management. Today, Etox sterilization is described as the most cost-effective, low-temperature sterilization process available, leading the industrial terminal sterilization market for approximately 50% [3]. Sterilization by Etox consists in inserting packaged and sealed devices into an ethylene oxide chamber, exposing them to a sterilization cycle through pure or diluted Etox. Humidity, temperature and time can influence this process as well. Employed packaging must let Etox and water vapor enter and exit. Post-sterilization aeration process follows the gas exposure, letting the residues leave the device. Strict monitoring of the process, including often biologic indicator test, is required [3].

Etox appears as a colorless gas at atmosphere pressure and room-temperature with high mutagenic and carcinogenic potential, miscible with water and extremely flammable and explosive. Its main properties are listed in the Tab.2.

This substance is industrially produced by direct oxidation of ethylene in the presence of silver catalyst; commonly it is handled and shipped as a refrigerated liquid due to the hazards related to its flammability and explosivity [3,26].

Name	Ethylene Oxide
Abbreviations	EO, EtO, Etox
CAS number	75-21-8
Molecular formula	C_2H_4O
Appearance	Colorless Gas
Molar Mass	44.05 g/mol
Density	0.882 g/mL
Melting Point	-111.3 °C
Boiling Point	10.7 ° C

Table 2. Main properties of Ethylene Oxide

Ethylene oxide has emerged as the sterilization method of choice for medical devices because of its undeniable advantages compared with other technologies. In fact for sensitive materials Etox is the only acceptable sterilization method. It can be applied for a wide range of materials including those sensitive to heat and moisture, it represents a strongly effective bactericidal, sporicidal and virucidal activity agent. Two atoms of Carbon and one of Oxygen are kept together inside an unstable ring structure (Fig.9) that can open up launching the alkylation reaction [12].

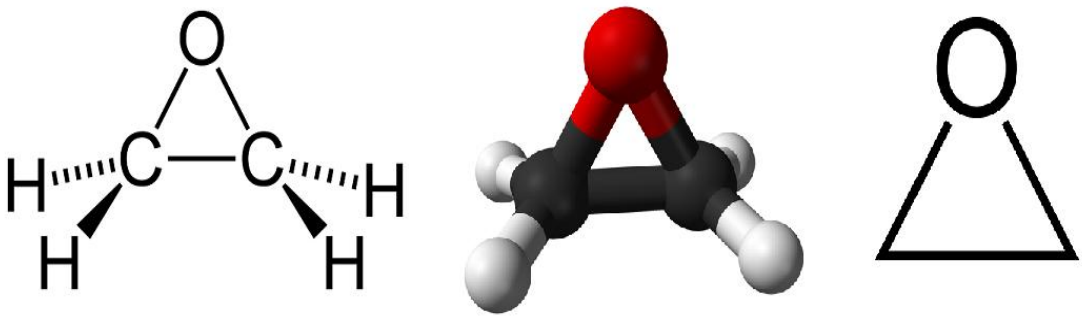

Figure 9. Three different representations of ethylene oxide

The efficacy in inactivating microorganisms resides in Etox high reactivity in combination with its high diffusivity allowing high penetration depth. Furthermore process flexibility given by the large number of control variables results in a great range of material treatable with this sterilization by just tuning process parameters (e.g. pressure, average temperature and humidity).

Etox action consists in a strong alkylation reaction with cellular components of organisms (such as nucleic acid and functional proteins) leading to their denaturation. This denaturation in DNA, RNA and proteins inside microorganisms occurs since alkyl groups bind easily to sulfhydryl, hydroxyl, amino and carboxyl groups. The result is the prevention of cellular metabolism and ability to reproduce, making the affected microbes nonviable [12,26]. Main MDs do not present the previously reported groups, therefore they do not undergo similar structural changes when they are exposed to Etox. Nevertheless this chemical agent presents several hazards to patients and everybody handling it, requiring high care when employed.

Even if MDs' structure does not generally include groups as those reported upwards, living beings can be affected by this alkylating agent, facing mutating and carcinogenic risks. However Etox can be considered a safe substance if used properly following certain safety procedures (indicated in Occupational Safety and Health Administration EO regulations). When these requirements are satisfied Etox can be considered a minimally hazardous agent.

In fact sterilization procedure must be followed by a certain time (aeration time) where the level of residual ethylene oxide can decrease. In their work Gunnigle MC et al. [27] relate the residual Etox and the L-cell toxic zone (where cells within this radius are dead) around the sterilized specimen. It is shown that Etox residuals lower than 900 ppm correspond to a 0 mm toxic zone. Silicone shows a quicker dynamic in the removal of toxic residues with respect to other plastic material (PVC and Polyether-polyurethane), in fact only 2 hours are enough in the described work. Even if 2 hours would be enough to avoid immediate toxic response by the surrounding cells/tissues (toxic zone with null radius), much longer aeration time is required in order to avoid any hazard in the long-time implantation. Indeed at least 48 hours of degassing process with 50-60° C into constrained ventilation systems are generally used [12].

In fact the risk is not directly associated only with entrapped Etox, but also to some of its derivatives. Examples of toxic derivatives are ethylene chlorohydrin, appearing when chloride ions are present, and ethylene glycol, generated through Etox reaction with water [26]. All these considerations about direct and indirect risks for patient health associated with MDs sterilization by Etox make residue controls compulsory.

In the last years the equipment related to Etox deeply improved and became more efficient, collecting lots of investments in order to achieve these improvements. Nevertheless discussions and debates about the actual safety of Etox have continued even if its application got more and more frequent.

2 Aim of the work

The present thesis deals with the sterilization of PDMS by Etox. Cochlear industry in Mechelen uses this material for the encapsulation of the housing containing a microchip in cochlear implants. The implantation of the material requires its sterilization before surgery to avoid infection risks. This industry employs Etox for such purpose. Despite its widespread use in the medical device industry, only few sources deal with Etox treatment on PDMS and little data have been published about its effect on mechanical properties of this material. Literature sources often do not supply details about the employed PDMS and its curing process, reporting terms as “silicone rubber” or “silicone” without any specific definition of the used material. Moreover some studies sometimes present contrasting results for the same properties or parameters, suggesting further investigation to clarify these mismatches. Most sources focus on single Etox sterilization, whereas few ones concern the effect of repeated sterilization cycles on PDMS. Thus little significance has been granted to the possibility of sterilizing PDMS implantable devices by Etox more than once. The unknown effects of multiple treatments compel medical industries to get rid of devices which may actually be still used. This way objects displaying contamination suspect after sterilization, unknown sterility status and sterilized products requiring extra-manufacturing or label addition (package opening requires a new sterilization) could be saved and still employed.

Thus, the present thesis aims at selecting test and the required samples to document the effects of Etox sterilization on PDMS properties. Bulk and surface properties after this treatment require investigation, in addition cytotoxicity test enriches this research. 8 experiments in total are carried out resulting in a wide range of information about this process. Result analysis wants to detect eventual material changes, trying to hypothesize potential reasons for registered behaviors. Statistical analysis assesses whether test outcomes are reliable and trustworthy. However as this material is quite variable in its behavior during test performances some results are expected to be statistically not significant according to an insufficient number of samples. However a greater sample number would result extremely expensive because of the test amount (both for molding and sterilization procedures).

3 Material and Methods

3.1 Description of the employed material

The material under inspection is MED-4860P (Fig.10), a Pt-cured silicone produced by NuSil (United Kingdom).

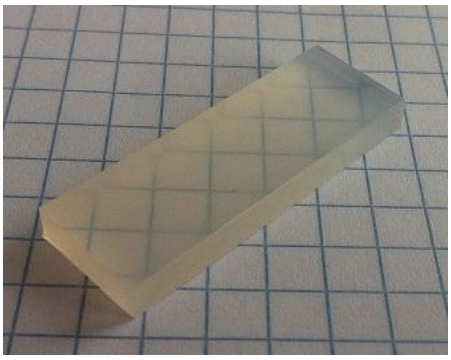

Figure 10. MED-4860P is a highly flexible and transparent material for thin thickness, these features decrease for higher thicknesses.

The advantages of Pt-curing with respect to peroxide-curing have already been listed in the previous chapter, nevertheless the absence of by-products after Etox sterilization for the first PDMS type is here quickly remarked. MED-4860P main properties are reported below in Tab.3.

Properties	Average Result	Standard
Uncured:		
Appearance	Translucent	ASTM D2090
Specific Gravity	1.15	ASTM D792
Durometer, Type A	60	ASTM D2240
Tensile Strength	1350 psi (9.3 MPa)	ASTM D412
Elongation	530%	ASTM D412
Tear Strength	255 ppi (45.0 kN/m)	ASTM D624
Stress @ 200% Strain	600 psi (4.1 MPa)	ASTM D412, D882
Tissue Culture (Cytotoxicity Testing)	Pass	USP <87> ISO 10993-5
Elemental Analysis of Trace Metals	Pass	ASTM E305

Table 3. Datasheet of the material investigated in this thesis (MED-4860P). For each row the parameters/properties with the respective average values and standards are reported.

This silicone rubber is designed for use with injection molding equipment and is suitable for overmolding, making it indicated for encapsulation purposes. It is obtained by mixing two parts (part A and part B) with a 1:1 ratio for 72 hours under vacuum deaeration procedure, curing with heat via addition-cure chemistry for 5 minutes at 165°C. In addition to pure vinyl-functionalised PDMS, parts A and B contain both amorphous silica (30%), whereas a 5% of Dimethyl, Methylhydrogen Siloxane Copolymer (CAS # 68037-59-2) is contained exclusively in part B. This second component (Fig.11) is used as crosslinker for vinyl-functional silicone polymers for the manufacture of addition curing (the key in its action resides in high-active Si-H) [28,29].

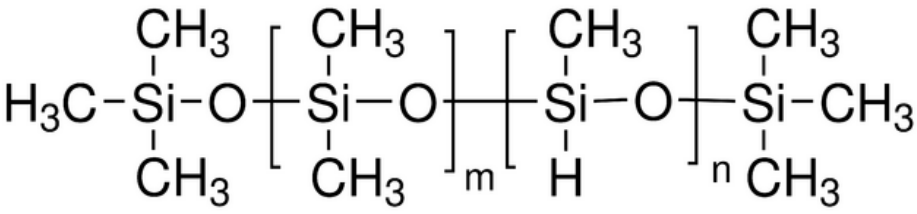

Figure 11. Chemical formula of Dimethyl,Methylhydrogen Siloxane Copolymer. It is composed of a long chain presenting Si-H bonds which are high-active, allowing the crosslinking between the 2 parts (see paragraph 1.1.1).

Silica is used as filler material in PDMS suspensions: before curing occurs, Tg (glass transition temperature) is not affected by the amount of silica, whereas Tc (cold crystallization temperature) may shift slightly leftwards with increasing amount of silica [30]. Once the cured elastomer is obtained no effect on Tm_2 (second melting transition temperature) can be recognized, whereas Tc peak and Tg step get less visible proportionally to the amount of silica [30]. All these parameters here quickly mentioned will be resumed in the paragraphs dealing with DSC analysis.

Sample types and shapes are initially chosen according to the selected experiments they are going to be employed in. However the sample preparation committed to a molding industry failed in being supplied on time. Thus this delay turned into the necessity to employ already available samples instead. This unavoidable choice obviously results in ignoring sometimes ASTM's sample requirements (anyway a certain compatibility with what

described in standards must be respected). Due to this hitch some experiments may produce results a bit different from those reported in procedures following ASTM standards. As specified in the upcoming paragraphs, the following experiments employ samples different from those specified by test standards: uniaxial tensile test, DMA and hardness test.

Test samples are sterilized by Andersen Products® (United Kingdom) one month before experiments are performed, keeping them in protective packaging away from heat, light and moisture. The samples are inspected after the reception and prepared at 23 °C and 35% humidity minimum. After that they undergo sterilization. Each cycle lasts 16 hours with an average temperature of 52° C and humidity varying from 40% to 90% during the different cycles and 50 Pa pressure. 10.6 g of gas are released on average in each cycle, whereas aeration time lasts from 50 to 100 hours with temperature ranging from 23° C to 53° C. Microbiological tests are carried out during the process with a minimum of 10^6 Bacillus atrophaeus after a minimum incubation time of 48 hours each. These steps do not show any growth, meaning the check tests are passed.

In this thesis the experiments are performed on samples which are sterilized once, four and ten times. These samples will be referred to as respectively C1, C4 and C10 hereafter. The choice of these values depends on the following items:

- The literature presents several examples of PDMS undergoing a unique Etox sterilization cycle and a large part of the sources agrees about the effects induced in the material. Nevertheless some sources are in contrast about some parameter changes (Young Modulus and Ultimate Elongation for instance) meaning that a new check of material behavior should be performed to clarify these mismatches and confirm the other results.
- Some sources deal with a maximum of 3 cycles instead of only one. Thus 4 cycles may be considered as a border which no confident behaviors and results are available beyond so far. Furthermore this value can be considered a reasonable number of sterilization repetitions in clinical/practical applications for implantable devices assuming post-sterilization operations.
- One source analyzes 100 cycle samples focusing only on few parameters [16]. This value is certainly extreme and no product would undergo such a high number of sterilizations as 10 cycles is thought to be already an unlikely number of repetitions to reach in practice.

As the present work focuses on comparing different exposures to the same sterilant, unsterilized samples are not generally employed. Indeed silicone cannot be employed for medical purposes without previously being sterilized. However one cannot ignore completely the unsterilized material as term of comparison in analyses dealing with material research. Therefore a basic comparison between unsterilized samples and sterilized ones is carried out during the uniaxial tensile test (see paragraph 4.1.5). This comparison reveals a certain compatibility between these two classes of materials.

3.2 Test modalities

The following paragraphs describe all the tests performed during the inspection of MED-4860P

3.2.1 Uniaxial tensile test

This mechanical test is performed following ASTM D412 on an Instron 5985 testing machine with a maximum cell load of 1KN and 2 different strain velocities. This machine is chosen depending on the attended high strain and small load in the samples during the experiments. Dogbone samples are employed: they show a central narrow part where the strain concentrates mainly, whereas the two large sides for clamping are assumed to contribute marginally to the strain of the whole sample. Sample shape and dimensions are shown in Fig.12. According to ASTM D412 the shape of the specimen for uniaxial tensile test on elastomeric material should present the narrow central part shorter than that used in dogbones for non elastomeric material [31]. Nevertheless this shape could not be produced by the molding industry on time: already available specimens with the shown design were employed instead. ASTM D412 reports 500 mm/min strain rate for elastomeric materials, however PDMS is a viscoelastic material, meaning its behavior is strain rate dependent. Thus the behavior for 100 mm/min strain rate is investigated as well in addition to the traditional 500 mm/min.

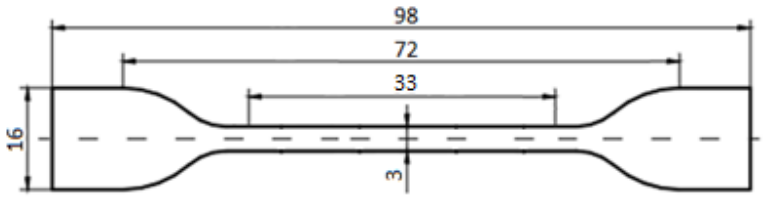

Figure 12. Shape and dimensions of the dogbone employed in the uniaxial test. Its shape is a bit different from what ASTM D412 indicates, in particular the central narrow part should be shorter as the material like silicon rubber can stand a huge deformation before breaking down.

8 samples on average per case are used and few ones are used to take some preliminary tests instead. In fact the correspondence with literature and datasheet values is checked and the suspected slippage during the test is investigated as well. According to the small changes attended after 1 cycle, some 1 cycle samples were sacrificed for these purposes.

During each test sample width and thickness are measured by a caliber (average thickness = 1,26 mm; average width = 3,01 mm). Dogbones are clamped (by pneumatic vises) with 61,5 mm distance between the 2 clamps (Fig.13), paying attention in setting the specimen symmetrically to distribute uniformly the tension over the cross-section [31]. The experiment is performed at 24° C. Clamps move in opposite direction according to the selected strain rate up to sample fracture. Data about extension and load with respect to time are collected in an Excel worksheet.

For each case the points registered after fracture (those with null load in the final part) are deleted whereas sections of the central part, stresses and strains are then calculated. Secondly UTS, Ultimate Elongation, E_lin and E_200_are identified in each experiment's Excel datasheet. UTS and Ultimate Elongation represent respectively the greatest stress and strain in the stress-strain curve.

Figure 13. Dogbone clamped in vises 61,5 mm far from each other. The specimen should be blocked as symmetric as possible in order to have uniform distribution of tension and to obtain comparable results.

Dealing with the elastic modulus, as demonstrated in Fig.14, elastomeric stress-strain relation is characterized by a first part approximately linear, followed by a less steep monotone curve. Due to this particular shape the secant modulus of elasticity can be employed instead of the classic tangent modulus (slope of the first linear part in the Fig.14). Secant modulus represents the slope of a line connecting the origin to any chosen point on a stress-strain curve. Common strains used for this modulus are 100, 200 etc. [12]. In the present work E_200 (secant modulus for 200 % strain) is chosen. Furthermore the tangent modulus (E_lin) is used as well to have another term of comparison. E_lin calculation is performed by considering the slope of graphs up to 30% strain, where the curve exhibits a linear behavior: for each case a graph from 0 to 30% strain is created and the dots are interpolated linearly, reporting the interpolate's slope as E_lin (Fig.15).

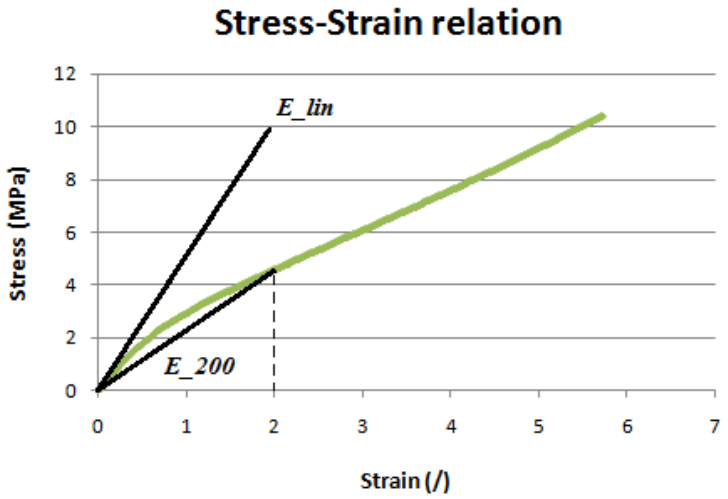

Figure 14. Stress-strain curve of the PDMS under investigation. The typical monotone pattern of elastomers (green curve) exhibits two different parts. The first one is steeper and shorter, the second one less steep but longer. The black lines represent respectively the tangent modulus (E_lin) and the secant modulus (E_200) used in the present work.

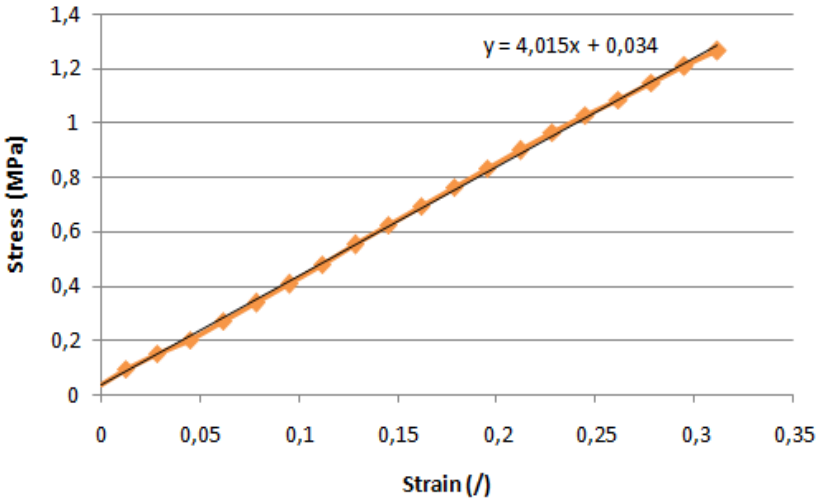

Figure 15. Dots up to 30% strain in the stress-strain graph are used in linear interpolation, the slope of the obtained line is reported as E_lin. This calculation is quite common but is actually used for materials withstanding only limited strains in general.

For the calculation of the strain, ASTM D412 suggests to draw two bench-marks on the dogbone in the narrow part and to track the distance between them during the test. The strain is calculated as the ratio of the distance between the two marks (with respect to the time) and the distance before the experiment is run. However this operation would result time-consuming considering the number of tests, furthermore laboratory instrumentation cannot satisfy this procedure. Instead of that, another approach is thought. Instron5985 and its dedicated software report the total extension of the two clamps (0 mm at the beginning) which contains also the extension due not only to the narrow part but also to the side parts with bigger width. Thus a calibration procedure is created in order to directly relate the registered extension to the real strain (which would be reported by the bench-marks method). Bench-marks are used for this purpose but only on two unsterilized dogbones, which are marked in the narrow part with two bench-marks 30 mm distant from each other, then the experiment is normally run at 100 mm/min. Thanks to the slow strain photos are taken every 10 mm extension until the rupture of the sample. Then photos are elaborated by a freeware software able to calculate distances on pictures (SketchUp, Trimble Navigation Ltd, USA). These measurements are therefore used to determine ratios between the digital distances and then real distances are estimated.

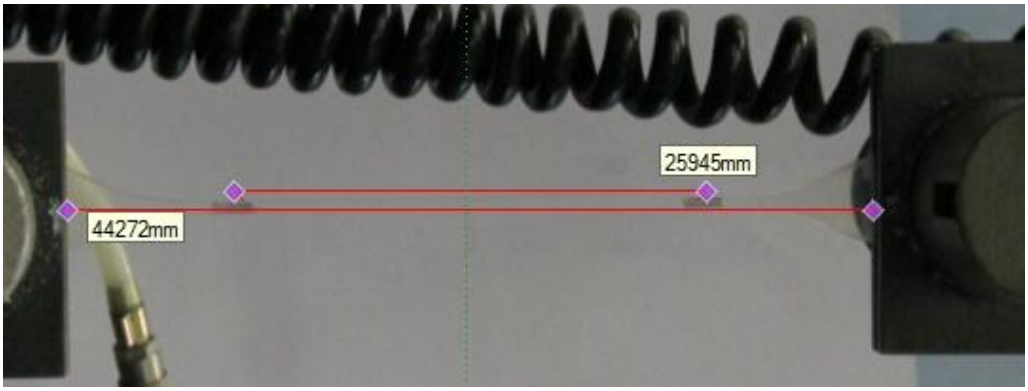

Figure 16. Picture of the dogbone between the two clamps (on the sides) when the extension equals 90 mm. The two bench-marks (dark rectangles connected by the upper red line) are marked by pen on the dogbone with a 30 mm distance. The image refers to a 90 mm extension and is here illustrated horizontally even if the experiment is performed vertically with one clamp (the left one) kept fixed whereas the other one (on the right) moves upwards.

For instance considering the relative distances between the 2 bench-marks (25945 units) and between the two clamps (44272 units) in a photo related to a 90 mm extension (Fig.16), their ratio equals 25945/44272 = 58,6 %. As the total distance between the clamps is known to be 61,5 + 90 = 151,5 mm, one can calculate the distance between the two bench-marks (in this case 151,5*0,586= 88,8 mm) in a certain photo.

This procedure is repeated for each photo so that the knowledge of the total distance between the clamps is used to calculate the distance between the two bench-marks every 10 mm of clamp extension. Once bench-marks distances are known, they are employed for the calculation of strain according to its definition. Thus two conversion tables relating the extension and the strain (referred to the bench-marks) are created. A final conversion table is created by averaging the strains associated with the same extension and then a linear interpolation is performed (Fig.17). The conversion factor results 0,020 mm^{-1}, therefore all the extensions stored in the Excel worksheets can be converted into strain values (for example a 25 mm extension corresponds to a 50% strain).

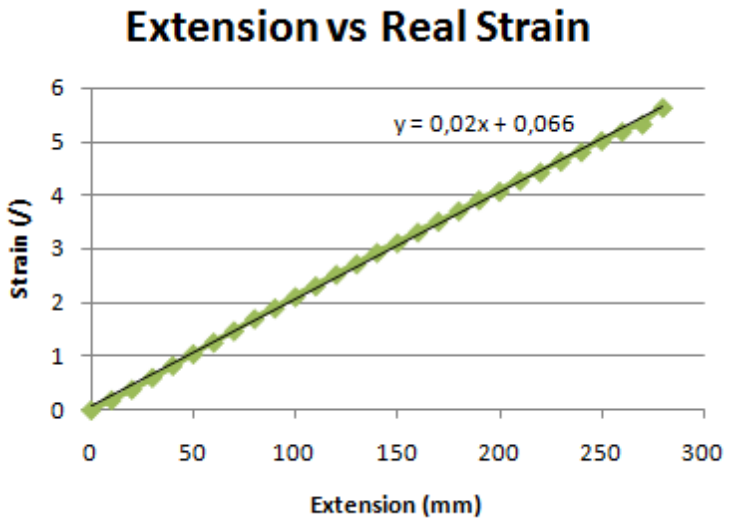

Figure 17. The strains in the two tests associated with a common extension are averaged, then the obtained mean values are plotted obtaining approximately a linear trend. A linear interpolation is therefore employed, drawing the conversion factor of 0,02 mm^{-1}between clamp extension and strain.

This procedure seems to return quite accurate strains. One may wonder whether direct comparison among extensions would not result already sufficient to evaluate changes in materials, however this additional step allows reliable results and comparisons with the values reported on the datasheets.

The mean value and standard deviation are calculated for each parameter and test type (for instance C4 samples with 500 mm/min strain rate). For each strain rate the 4 parameters are compared among the 3 sample types. An additional term of comparison is represented by uniaxial tensile tests performed later on unsterilized dogbones (C0). Their employment adds a fourth class to suggest and better recognize possible trends. Material datasheet often reports values which are slightly different from those recorded for C0, probably depending on mismatches in dogbone shape. Thus one may assume the values of unsterilized samples as corresponding to those indicated on the datasheet and rescale C1, C4 and C10 values. However mean values do not obviously represent straightforward terms of comparison according to the small sample availability and different conditions in lab environment (temperature and humidity may be a bit different from those in the first sterilized test group).

In addition to the mismatch between the available samples and those specified in ASTM D412, another source of error is given by sample slippage along the clamps when the extension reaches high values. Uniaxial tensile test is ideally considered with no slippage conditions, meaning that the strain should refer only to the part originally free from clamps. Nevertheless clamp action may not be completely effective so that a certain percentage of the sample which is initially blocked in the clamp may partially slide. This part of sample can bear now the strain as the central part (intended to be the only one doing that) does. This behavior would turn into an inaccurate calculation about the ultimate elongation which will result higher with respect to the real value. Two dogbones sterilized once are tested: a line is drawn on the sample along the clamp edges, then the normal experiment is run and clamps are briefly blocked at 180 mm extension (which is really unlikely in breaking the dogbone). A photo is quickly taken at this moment, than the two clamps are brought back to default distance and a new photo is taken. Photos are elaborated with SketchUp similarly to the procedure used to evaluate strain with unsterilized dogbones.

3.2.2 DMA

Dynamic Mechanical Analysis is a non-destructive technique which can measure several parameters in the samples, in particular Storage and Loss Moduli (E' and E'') can be investigated. The combination of these two parameters allows tanδ calculation (tan δ = E''/E') where δ (Fig.18) represents the phase angle (indicating the delay occurring between the applied force and the deformation).

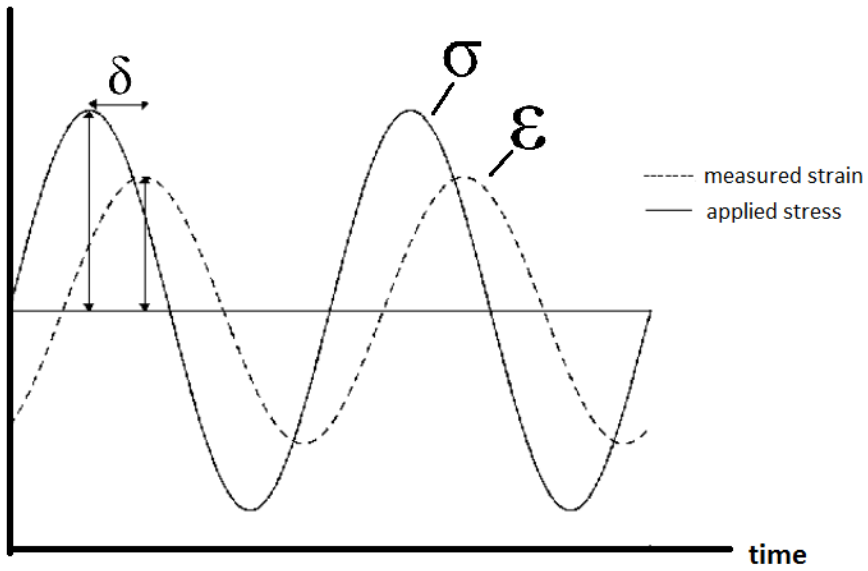

Figure 18. Sinusoidal stress and strain curves with respect to time. A perfectly elastic material would present a null delay among the peaks (δ = 0), whereas a viscoelastic material has δ ≠ 0.

Due to Etox treatment Storage and Loss moduli might change according to potential chain degradation or crosslinking, even though polydimethilsiloxane is known to have low chemical reactivity and to be particularly resistant to degradation in many cases.

The measurements are carried out on DMA Q800 instrument (TA Instruments, USA) with shear sandwich clamp (Fig.19). This type of clamp is generally used for the analysis of elastomers above the glass transition point. Clamping procedure is performed without a torque wrench which allows to check the employed torque in clamping. Instead the clamping is carried out by hand trying as much as possible to achieve the same clamping with the screws along the claws. The impressed force should be carefully balanced since two wrong cases may occur instead: insufficient tension results in sample fall from the housing (due to shrinking during cooling phase), whereas an exceeded action may break

the holding apparatus or overestimate material properties. Unfortunately results are known to be dependent on clamping conditions: the stronger the samples are clamped, the higher the calculated storage modulus in general.

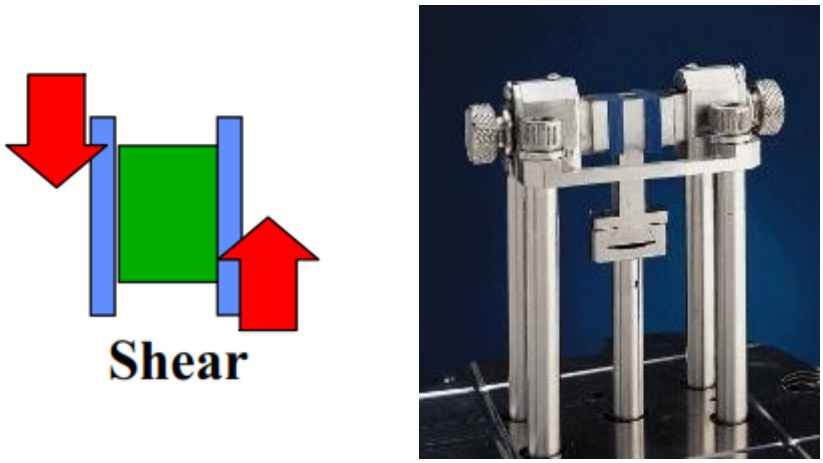

Figure 19. On the left the principle of shear mode is displayed (two surfaces in contact with the same sample move in opposite directions keeping themselves parallel to sample surface). On the right the shear sandwich apparatus (the same employed during the present test) can be observed: it consists of two fixed cantilevers on the sides and a vertically floating beam whose surfaces stay between the two cantilevers. Two samples at a time are inserted in the gaps between the metal surfaces.

Sample similarity and perpendicular faces are essential to achieve well distributed stresses and to maximize the compatibility among test outcomes, thus molded samples are preferable. Instead samples are cut from silicone bars (15 samples per case, 5 from each bar). Each sample is approximately a 10x10x3,75 mm parallelepipedon. The 15 cm long bars have 3,75 mm thickness, so that no cut is required to obtain the reported thickness. In order to increase the variability in analyzed samples, 5 samples are cut away from different positions along each bar: 3 samples belong to the central part and 2 are directly cut from the extremities. Cutting is performed inside MTM's Workshop at KU Leuven by using a sharp Gillette razor. Obviously this procedure results in samples less similar to each other, pre-tensioned areas, residual strains and surface damage. On the other hand this cutting technique avoids the exposure to modifying elements employed by other cutting technologies (e.g. laser-cut, waterjet). For each category samples are compared in order to

divide them into 6 couples trying to maximize the similarity among all the couples. However few samples perfectly match each other, indeed they often have at least one side slightly higher than 10 mm (the dimension of the vise face) and some cut faces are not perfectly perpendicular but slightly slanted. These flaws certainly result in lower precision in the measurements. For each experiment the two coupled samples are measured by a caliber, their face dimensions are averaged (the lower one in one sample with the lower of the other one) and their thicknesses are summed.

The furnace of DMA Q800 covers the cantilever structure, then the chamber is equilibrated to -50°C and 3 minutes of isothermal phase are allowed. After that a heating ramp with 3°C/min is run up to 100°C. During the heating ramp properties are investigated: 50 μm oscillations of the floating beam are continuously performed by switching sequentially the employed frequency (1 Hz, 50 Hz and 100 Hz). E' and E'' are the investigated parameters in this test. Tg is initially planned to be analyzed as well in order to obtain information by two different analyses (the other one employed is DSC) allowing a comparison between their outcomes. However the investigation of Tg (expected approximately around -125° C) compels an extreme liquid nitrogen depletion by DMA Q800 for such low temperatures. Probably this problem is due to the large space inside the furnace, which is definitely smaller in DSC chamber (showing reasonable liquid nitrogen consumption).

3.2.3 Hardness test

Surface mechanical answer to an indenter can be estimated by following ASTM D2240. According to that, hardness of materials with rubber property should be investigated by a Shore A indenter (Fig.20). This pocket-portable instrument has a flat base with a protruding tip in the middle which partially returns inside when the instrument is pushed against a flat surface. In order to achieve good measurements the samples must lean on a hard surface. The penetration of the pin into the investigated material is balanced by material resistance, so that an estimation of surface's answer can be carried when spring stiffness in the durometer is known. Thus the amount of penetration is converted into hardness (which ranges from 0 to 100 Shore A units) [32].

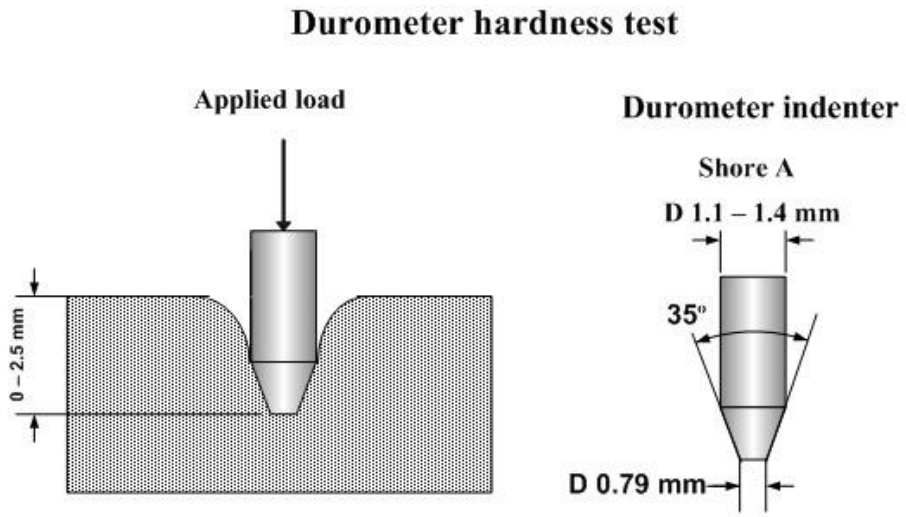

Figure 20. Shore A indenter presents a flat surface with a pin protruding outside. When the instrument is pressed on a surface the pin returns inside the device according to the balance between the instrument spring and surface deformation (material elasticity). The hardness can be calculated if the spring stiffness is known. Different Shore indenters are available and rubber-like materials are tested with Shore A indenter whose pin has the dimensions specified in the right picture.

ASTM D2240 specifies that samples should be at least 6 mm thick and measurements should be taken at least 12 mm from any edge. Nevertheless ASTM standard details that the samples can be arranged as a pile in order to reach the minimum thickness of 6 mm if the single sample is thinner than this value [33]. According to the lack of the commissioned samples, a parallelepipedon with dimensions 36x33x7,5 mm is composed by joining 6 large parts of the bars cut away during the preparation of DMA samples as illustrated in Fig.21 (3 parts in width and 2 parts in height).

Although ASTM standard allows to superimpose samples, it does not mention anything about putting samples next to each other along their sides. However this alternative approach is the only procedure compatible with the available samples, allowing perfect contact between the whole parallelepipedon surface and the indenter base (which the pin protrudes from). Indeed the face of a single sample would not allow complete contact with the instrument. Measurements are performed at 28°C by a Zwick&Co Pruefmaschinen Shore A. The instrument is smoothly pressed on the substrate till its base surface adheres firmly to the PDMS parallelepidon and measurement is taken after 1 second in order to stabilize the penetration of the needle. The tip is not pressed against the connections among the samples composing the parallelepipedon.

Fig.22 summarizes the strategy to obtain several measurements without sampling continuously from the same piece in the parallelepipedon. 3 measurements are acquired on the central sample in the upper parallelepipedon face, in points approximately 5-7 mm far from each other. Then the sample cluster is flipped and the measurements are repeated on the new upper face. To investigate a new part the parallelepipedon is decomposed and a new one is built so that every vertical block is shifted on the right (passage from the second to the third case in Fig.22). The measurements are now repeated until all the 6 pieces are sampled. In total 18 measurements are performed for each type of samples.

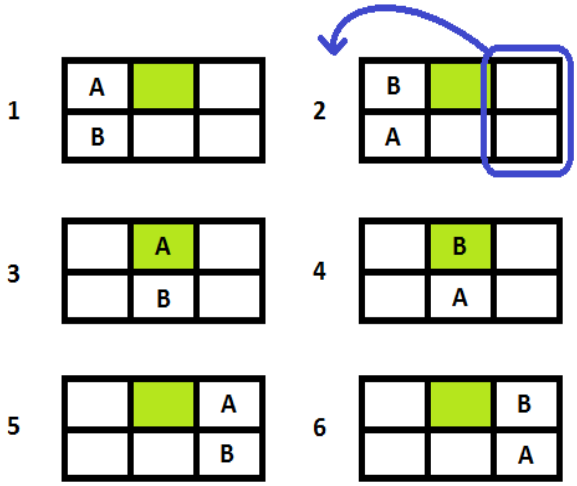

Figure 21. Picture of the Zwick&Co Pruefmaschinen Shore A used in the hardness test and the PDMS parallelepipedon assembled as specified in the sequence in Fig.22. The surface which the sample leans on must be rigid (hard wood in this case).

Figure 22. Schematic representation of the method employed to create a sample suitable for hardness test. 6 parallelelpidons are not singularly thick and wide enough to get a good contact with surface indenter, thus they are put together to create a bigger parallelepipedon. Following the sequence in building and switching the components, all the 6 parts are sequentially sampled (yellow part).

3.2.4 DSC

Differential Scanning Calorimetry (DSC) is a thermal analysis technique which allows to determine heat flow and temperatures associated with thermal transitions in materials as a function of temperature, time and frequency. Tg is an important parameter in polymers since at this temperature amorphous (noncrystalline) material turns from brittle and glasslike to flexible and rubberlike. Actually Tg does not identify a true phase transition but one that involves a change in the local degrees of freedom [34,35]. The measurement consists in comparing the heat flow of the specimen with a reference material so that both materials are at the same temperature. Increments or decrements in heat flow are associated to transition processes so that these changes are used to estimate the amount of heat absorbed or released during the undergoing transitions. For this experiment a DSC Q2000 (TA instruments, USA) is used with sapphire employed as reference material (Fig.23). PDMS Parallelepipedons with approximately 2x1x1 mm dimensions and 23 mg average weight (obtained from material scraps after DMA sample preparation) are taken as specimens. A first group of tests is run from -150° C to 0° C as the Tg is expected to be around -125°C. Chamber is therefore equilibrated (slow cooling rate) at -150 °C by liquid nitrogen and hold at this temperature for 5 minutes, then heated with a 3° C/min ramp up to 0° C. In addition to the detection of Tg, the enthalpy associated with the fusion peak (transition related to the Tm) is investigated. Universal Analysis 2000 software is used for transition detection purposes. A second group is later analyzed since first group's outcomes result unsuitable for determining the Tg. As many peaks of PDMS' characteristic thermogram are not visible as well, also the cooling curve is acquired. In this second case samples are first equilibrated at 20°C and kept at this temperature for 5 minutes. Then the chamber is brought to -160° C with a 30°C/min cooling rate, followed by a 5 minutes isothermal phase and a heating ramp (10° C/min) up to 20° C. Also in this case the analysis of the Tg is carried out on the PC by Universal Analysis 2000 software.

Figure 23. In DSC Q2000 already analyzed samples are removed and replaced automatically. Close to that a sapphire sample is housed. According to temperature transitions, heat flow variations with respect to the reference material occur to keep both materials at the same temperature.

3.2.5 ATR-FTIR

This technique allows the investigation of eventual changes in surface chemical structure. Chemical bonds on PDMS surface can be investigated therefore.

1 disk with 10 mm diameter and 1 mm thickness per case is used. Analysis is carried out by using an Agilent Cary 620 FTIR microscope (Agilent, USA) with ATR slide-on, Ge-crystal (128 scans). Background is acquired as preliminary step in order to exclude as much as possible CO_2 and H_2O contributions on the resulting Absorbance graph. The experiment is performed by the Centre for Surface Chemistry and Catalysis (Department of Microbial and Molecular Systems at KU Leuven). Spectra are recorded between 4000 and 400 cm^{-1} and are later analyzed in collaboration with the Centre for Surface Chemistry and Catalysis.

Figure 24. The Agilent Cary 620 FTIR microscope.

3.2.6 Wettability

Silicone has been described as an hydrophobic material but changes may be suspected after sterilization. Wettability test helps recognize this eventual variation by the size of the contact angle of a droplet on the surface: as illustrated in Fig.25 high contact angles are related to hydrophobic surfaces.

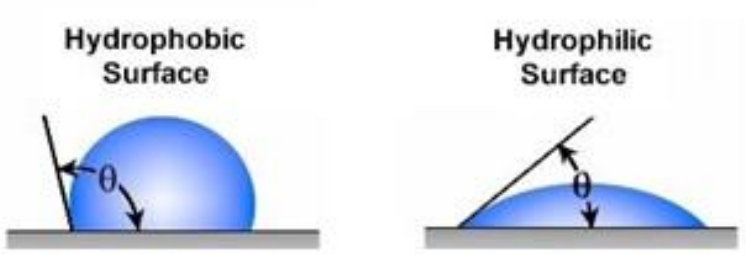

Figure 25. Difference in the behavior of a drop leaning on two different surfaces. Hydrophobic surfaces do not allow the drops to spread and flatten on the material, therefore the angles between the surface and the tangent to the drop in the contact points are higher than 90°. In contrast hydrophilic surface exhibits an angle lower than 90° so that drops flatten on the surface.

5 samples in total (10 mm diameter disks with 1 mm of thickness, 0.1 g each) per case are tested at 27° C. Each disk receives 3 drops on average, taking care of making them lean not next to the edge where surface is generally slightly bent upwards. Water is chosen as liquid for this experiment with drops of 1,1 µl average volume, air is used as gas phase. The test apparatus consists of a syringe with a high precision gear on the plunger able to create hanging droplets with highly controlled volume. Water drop is then brought closer to the substrate as much as possible (by lowering the syringe) without touching the PDMS. A camera with a light source positioned in front of it takes a first photo where the dark reflection on the substrate can be used to determine the baseline for the software calculation (Fig.26A). Then the drop is gently leaned on the surface and the syringe is immediately pulled upwards so that the drop detaches without altering its spreading on the PDMS. 5 photos are acquired every 30 seconds starting from the moment after syringe removal (Fig.26B).

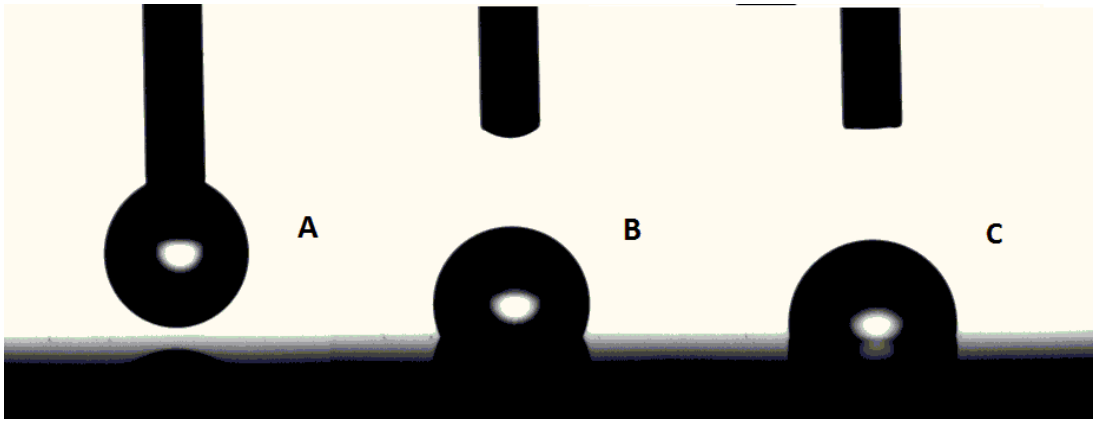

Figure 26. Phases in the wettability experiment. Firstly a hanging drop is created on the needle tip and is slowly brought close to the surface (A). When the drop gets in contact with the surface the needle is gently pulled upwards (B) so that the drop can start to flatten. However due to material hydrophobicity it cannot exactly flatten, resulting in a slight spreading while gradually reducing its contact angles (C).

The average contact angle (between right and left side) and volume with respect of the time are saved in an Excel worksheet. All the cases where water drops exhibit high asymmetry after touching the surface, where they accidentally fall or too much time elapses between contact and recording start (drops quickly modify contact angles during the first seconds) are discarded. Due to the large number of measurements in this test, the highest and the lowest values are not considered in order to further discard eventual bad cases. In addition to these sources of error also evaporation of water and electrostatic attraction forces (between pending drop and PDMS before touching while lowering the syringe) contribute to alter the measurements. Quality camera, calibration procedure and recording conditions are fundamental settings to acquire precise angle measurements.

3.2.7 Swelling test

According to the literature PDMS severely struggles to absorb water even if completely immersed [36,37]. Parallelepipedon samples are prepared from bar scraps, paying attention to obtain similar dimensions (15x12x3,8 mm) so that they have similar weights (0,8 g on average). 5 samples for C1 and C10 and 6 samples for C4 are prepared and each of them is scaled before swelling. The selected samples are immersed separately in 300 ml of partially demineralized water (6,25 < pH < 7 measured by color-fixed indicator sticks, conductivity below 2 µS/cm, room temperature) and allowed to swell to equilibrium over a

1, 2 and 9 weeks period at room temperature. The samples lean on the bottom of large beakers so that they do not stick to each other (in order to maximize the potential exchange). Sample weight in the swollen state is determined by removing the sample from the water, gently drying the surface with a paper towel to remove any liquid remaining on the surface and recording the weight. A Mettler AE240 (Mettler Toledo, Switzerland) with a 10^{-5} g resolution is used in sample scaling. Each sample is then immersed again. Swelling Ratio is calculated as the ratio between the weight in the swollen and the sample in unswollen condition.

One may hypothesize sample swelling might result different for samples presenting different faces. In fact some faces were directly exposed to Etox when sterilized, whereas other surfaces are created by blade cutting and they may show surface properties different from the previous ones. Thus the outcomes provided by this test cannot be considered completely straightforward and some outliers might be expected.

3.2.8 In vitro cytotoxicity testing

In vitro indirect cytotoxicity tests are performed at the Laboratory of Biocompatibility and Cell Culture "BioCell", Department of Chemistry, Materials and Chemical Engineering "G. Natta", Politecnico di Milano. This study aims at determining the possible release of cytotoxic products by PDMS samples exposed to Etox sterilization. In vitro cytotoxicity of the extracts of PDMS samples is assessed by using the L929 murine fibroblasts cell line (ECACC No. 85011425). The extracts were obtained according to standard ISO-10993. This standard asks for 0,2 g of specimen per case, therefore two samples (10 mm diameter, 1 mm thickness, approximately 0,1 g each) for each combination of sample type and incubation time are required. PDMS samples are immersed in Dulbecco's Modified Eagle's Medium (DMEM) with 10% fetal bovine serum (FBS) and 1% penicillin/streptomycin, maintaining a material/medium ratio of 0.2 g/ml. After 3 hours, 1 and 3 days of incubation, medium extracts are collected and put in contact with L929 (cell density = 5×10^4 cells/ml) in a 96-well tissue culture plate (TCPS). Cells are cultured for 24 hours and cell morphology is investigated by optical microscopy (Leica). As controls, complete DMEM incubated for 3 hours, 1 and 3 days and fresh complete DMEM, seeded with the same cell density for 24 hours, are considered. Tests were performed in triplicate.

3.3 Statistical Analysis

The analysis of the collected data is integrated by statistical analysis: depending mainly on the number of samples, test results are analyzed with different statistical methods. They return the probability that two or more classes of materials (after different exposure to Etox) can be considered equal (further details about these concepts and comparisons are provided below in following subparagraphs).

The statistical analysis is performed with Minitab, a software dedicated to data analysis and statistical methods. During each experiment data are initially stored in Excel worksheets and then copied into Minitab worksheets after their refinement.

Each experiment generally deals with a different number of samples (due to problems in receiving specimens from the molding house). Thus a first distinction can be established between statistical analysis performed on several and few samples respectively. In the first case a t-test is generally suitable if distribution normality is assessed, whereas non parametric methods are more suitable for groups with few values.

Distribution normality should not be evaluated exclusively according to the single group under inspection: in fact groups with few samples are more likely not to exhibit normality. Previous data and all available ones should be taken into account as well (or even included in certain cases) while judging dataset normality. In fact what matters is the distribution of the overall population, not the distribution of a specific sample group [38].

In some tests certain values referring to different test parameters (e.g. different strain rates in uniaxial tensile test) may be put together in a unique bigger dataset. In order to use such a technique the comparison of mean values and standard deviations among the different groups should show similar values (at least mean values, better if also standard deviations are compatible).

3.3.1 Analysis by t-test

A 2-sample t-test can be employed in order to check whether the means of two independent groups are different (meaning they belong to different materials) or not. In the present work datasets are generally classified as independent, however certain experiments rely on measuring the same samples before and after certain treatments (e.g. sample weight before and after immersion in swelling test). In these cases groups are classified as

dependent, so that a paired test should be preferred instead. Nevertheless if comparison is established among groups exclusively after the same treatment (immersion), the groups result now independent (these example will be resumed later).

When independence is assessed, normality of data groups has to be proved before applying t-test. Firstly one should remember there is no absolute minimum sample size for a t-test as this method was initially designed for small sample size and then extended to bigger ones. However as datasets get smaller, the test increases its sensitivity to the assumption that both samples belong to Gaussian populations. For large group of data (for the present work 10 samples at least are decided, even if many statistical forums suggest 30 as effective minimum size) normality can be evaluated by Anderson-Darling Normality test, by Shapiro-Wilk elsewhere. If a data distribution cannot be assumed Gaussian (generally due to very far outliers or many values concentrating in extremities of the value range) a non parametric test is chosen (Mann-Whitney) as for small datasets. Instead if normality condition is satisfied a comparison among C1, C4 and C10 samples can be established by t-test.

Two cases can be considered: the one-tailed and the two-tailed tests. The first one is used when the mean value of a data collection (μ_1) is suspected to be higher/lower than the mean value of another collection (μ_2). In this case only one side in the probability profile is taken into account (Fig.27A). On the other hand a two-tailed test focuses on understanding whether the mean value of a data collection equals the mean value of another collection. In this second case both sides of the probability profile are considered and the p value is split between both sides. (Fig.27B).

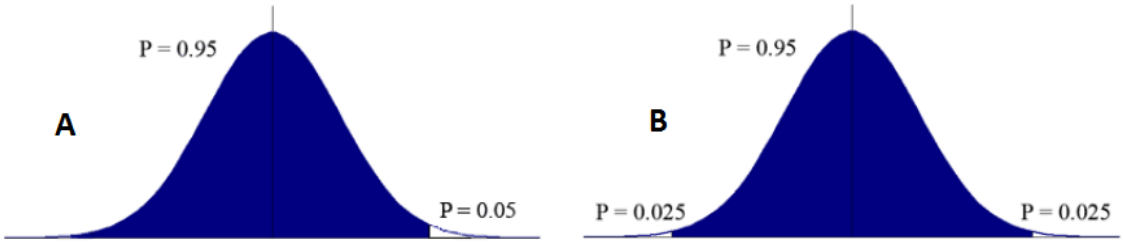

Figure 27. In both cases, shaded regions indicate the area represented by the null hypothesis ($\mu_1 = \mu_2$), whereas unshaded regions represent the rejection of the null hypothesis: $\mu_1 > \mu_2$ for 1-tailed test (A), $\mu_1 \neq \mu_2$ for the 2-tailed test (B). In both cases a 95% confidence level is represented. To increase the stringency in rejection, an even higher confidence can be chosen even though 95% is generally the most used one.

The present study focuses on significative changes in material properties independently from the type of change, so the second case is chosen. The null hypothesis "$\mu_1 = \mu_2$" and the alternative hypothesis "$\mu_1 \neq \mu_2$" are set, where μ_1 represents the mean value of a data group (e.g. 1 sterilization with 500 mm/min strain rate) and μ_2 the mean value of a second one (e.g. 10 sterilizations with 500 mm/min strain rate). Thus an F-test is performed to check whether the variances (the squares of the standard deviations) of the two groups can be considered equal (null hypothesis $s_1^2 = s_2^2$). If this condition is satisfied the d.o.f. (degrees of freedom) in the calculation result higher with respect of unequal variances.
If F-test does not reject the null hypothesis the formulas to employ for t value and d.o.f. calculations are:

$$t = \frac{\mu_1 - \mu_2}{s_{X_1X_2} \cdot \sqrt{\frac{1}{n_1} + \frac{1}{n_2}}} \qquad s_{X_1X_2} = \sqrt{\frac{(n_1 - 1)s_{X_1}^2 + (n_2 - 1)s_{X_2}^2}{n_1 + n_2 - 2}} \qquad d.o.f. = n_1 + n_2 - 2$$

Instead, if equal variances cannot be assumed the following formulas are used (resulting in fewer d.o.f.):

$$t = \frac{\mu_1 - \mu_2}{\sqrt{\frac{s_1^2}{n_1} + \frac{s_2^2}{n_2}}} \qquad d.o.f. = \frac{\left(\frac{s_1^2}{n_1} + \frac{s_2^2}{n_2}\right)^2}{\left(\frac{s_1^4}{n_1^2(n_1-1)} + \frac{s_2^4}{n_2^2(n_2-1)}\right)}$$

where μ is the mean value, s the standard deviation, s^2 the variance and n the number of samples. Then the p value related to the calculated t (according to the d.o.f. rounded to the closer integer) is calculated. If this value (doubled due to the two-tailed t-test) is lower than the p value chosen for the analysis (0.05) the null hypothesis is rejected, otherwise it results that no difference between the two datasets can be inferred. In fact according to that, the discrepancy is due to random error only, because p = 0,05 represents a 95% probability that the samples are not different. Minitab directly checks dataset normality by "*Normality Test*", performs the F-test by "*Two Variances*" and the t-test by "*2-sample t*", reporting the corresponding p values (Fig.29). These analyses have to be enriched by statistical power calculation, which describes the probability that a statistical method

correctly rejects the null hypothesis when the null hypothesis is false. Generally an 80% power is required in order to have a significant statistical result. In Minitab this analysis is performed by the "*Power*" function submitting average sample size and standard deviation plus the difference between means. Although only high statistical powers can prove the reliability of statistical methods' outcomes, powers are expected to result quite low in all the cases dealing with few sample datasets whose mean values differ slightly with respect to standard deviations' size. In these cases for instance 5 or 10 samples are definitely not enough to reach the 0.8 threshold. Unfortunately many cases reports 50 samples at least (or even 100 sometimes) to reach the mentioned threshold (Minitab includes the estimation of sample size given a desired statistical power). This huge amount of specimens definitely exceeds the aims of the present thesis which wants to focus on a broad range of material investigations instead of focusing on few of them only. Indeed works whose purposes reside in getting stronger statistical reliability have to include more samples.

3.3.2 Analysis by non parametric methods

When few values are collected during a certain experiment, the assumption of normality results quite labile. Indeed common normality tests have little power to discriminate between Gaussian and non-Gaussian distribution in these cases. Some of them however are more effective for few data (e.g. Shapiro-Wilk test) than the common one (Anderson-Darling test). Even though normality is inferred, using a parametric test (related to normal distributions) with a distribution which is actually not Gaussian generally results in an inaccurate P-value. For this reason in general non parametric methods are preferred for few values. Comparison between two independent distributions with few data can be performed by Mann-Whitney test (Fig.29), which returns a p value associated with distributions' medians (instead of their mean values) [38]. In the previous paragraph parametric methods were said to be commonly integrated with statistical power, however in non parametric methods this analysis is less known and used even if some methods (e.g. Monte Carlo simulation) are mentioned in the literature [39]. As these methods are quite complex and Minitab does not include them an alternative procedure is preferred: the power associated with the t-test (even if the current method is a non parametric one) is reported beside the non parametric method's p value.

3.3.3 ANOVA analysis

This thesis deals with the comparison of 3 groups, however statistical methods listed so far allow the comparison of 2 datasets at a time only. ANOVA (Analysis of Variance) can compare multiple datasets (its theoretical explanation is beyond the interest of this paragraph). Although normality and homogeneity of variances have to be checked, ANOVA generally works quite well even when the assumption of normality is not valid [40]. ANOVA behaves as an exact test of the null hypothesis (no difference in level means) if the distributions of the errors satisfy 4 assumptions (constant variance, normality, null mean and independence) [40]. These 4 conditions can be checked by the residuals returned by Minitab (an example of this passage is illustrated in Fig.28). Finally ANOVA can be integrated with its statistical power (number of datasets, average sample number, standard deviation and maximum difference among means are requested). Actually statistical tests related to more than 2 datasets are suggested to employ a lower p value threshold (Bonferroni correction). However in the present thesis 0,05 will be used as threshold anyway.

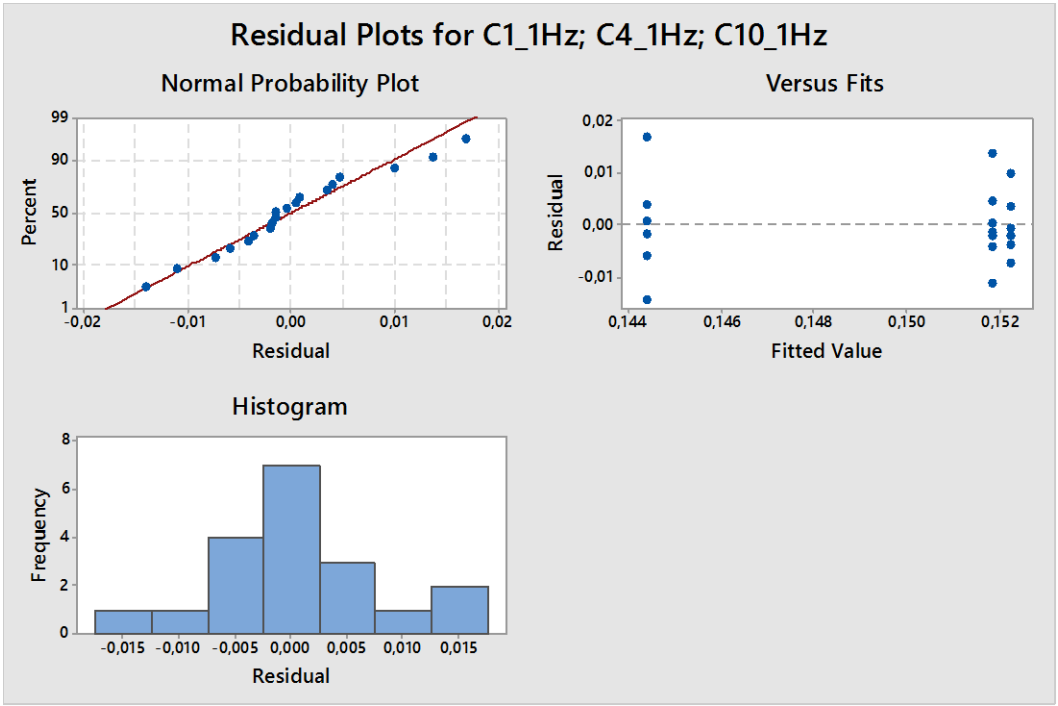

Figure 28. Analysis of the residuals returned after an ANOVA test performed on DMA data (Storage Modulus analysis for 1 Hz frequency). Normality and null mean are respected according to the left graphs, whereas the right graph suggests likelihood in variance equality. In order to assess this condition clearly the residual datasets are compared by F-tests which return p values higher than 0,25 in all the cases. Thus ANOVA method is expected to return a reliable outcome here as the assumptions result satisfied.

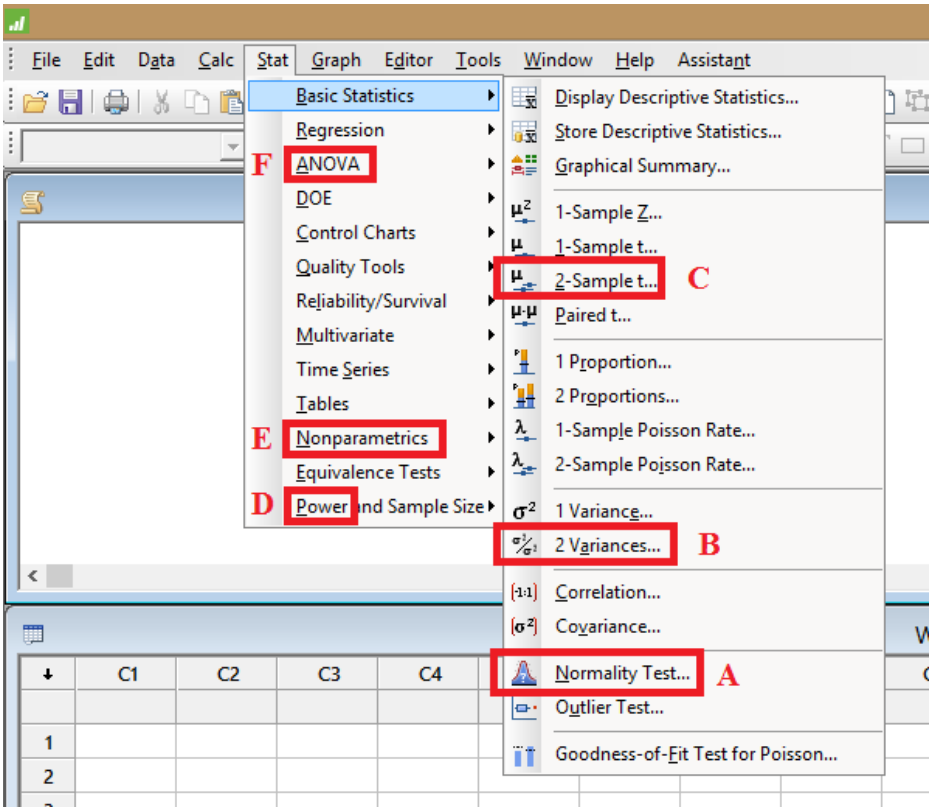

Figure 29. Minitab front panel presenting the mentioned functions and methods. Minitab can check distribution normality (A), perform an F-test between two datasets (B) and calculate the p value resulting from a t-test (C). This program implements the possibility to calculate the statistical power according to the chosen statistical method (D) and to employ non parametric methods (E). Finally ANOVA test is suitable for comparing more than two datasets together (F).

4 Results

4.1 Uniaxial tensile test

According to the great number of combinations between parameters and strain rates, each parameter is analyzed separately. Before listing all the considered parameters, one should remember that this material shows a very variable behavior which would require an amount of samples greater than that used in the present studies. However statistical power analysis evidences how in many cases the amount of specimens required to reach a 0,8 statistical power would abundantly exceed 50 units according to the standard deviations induced by the variability in test outcomes. Thus results are not expected to appear completely straightforward if no great alteration is achieved.

4.1.1 Ultimate Tensile Strength (UTS)

Tab.4 summarizes the resulting UTS values for 500 mm/min strain rate which does not show a clear trend (Fig.30). The highest mean value belongs to C4, however standard deviations are too high to establish an effective comparison among the mean values. Statistical analysis is performed by both t-test and Mann-Whitney test, even if non parametric methods should be preferred because of the labile assessment of dataset normality (due to few samples as explained in paragraph 3.3.2). Both tests do not reject null hypotheses (Tab.5), returning high p values except for the comparison between C4 and C10 (which is higher than 0,05 anyway).

	N	Mean (MPa)	StDev (Mpa)	Median (MPa)
C1 (UTS)	5	9,88	1,06	10,09
C4 (UTS)	9	10,39	0,86	10,38
C10 (UTS)	10	9,77	0,96	9,71

	MW p value	t-t p value	t-t power
C1-C4	0,505	0,931	0,15
C1-C10	0,854	0,99	0,05
C4-C10	0,131	0,913	0,27

Table 4 and Table 5. UTS means, StDevs and medians related to uniaxial tensile test with 500 mm/min together with p values and statistical powers.

Recorded UTS values for 100 mm/min strain rate (Tab.6) undergo the same statistical analyses described for 500 mm/min. C1 and C4 show similar mean UTS whereas C10 presents a lower mean value. On the other hand standard deviations for C1 and C4 are quite big, thus nothing can be inferred with precision (Fig.30). As C10 presents a lower standard deviation equal to the difference between C1 (or C4) and C10 mean values, UTS in C10 might actually be different from the other two classes. Statistical analysis (Tab.7) agrees with this idea: both non-parametric test and t-test report high p value between C1 and C4, whereas p value dramatically drops when comparing C10. However p values always result greater than 0,05.

	N	Mean (MPa)	StDev (Mpa)	Median (MPa)
C1 (UTS)	8	10,21	1,09	10,01
C4 (UTS)	8	10,17	0,90	10,36
C10 (UTS)	6	9,46	0,68	9,23

	MW p value	t-t p value	t-t power
C1-C4	0,958	0,946	0,05
C1-C10	0,175	0,168	0,33
C4-C10	0,081	0,132	0,34

Table 6 and Table 7. UTS means, StDevs and medians related to uniaxial tensile test with 100 mm/min together with p values and statistical powers.

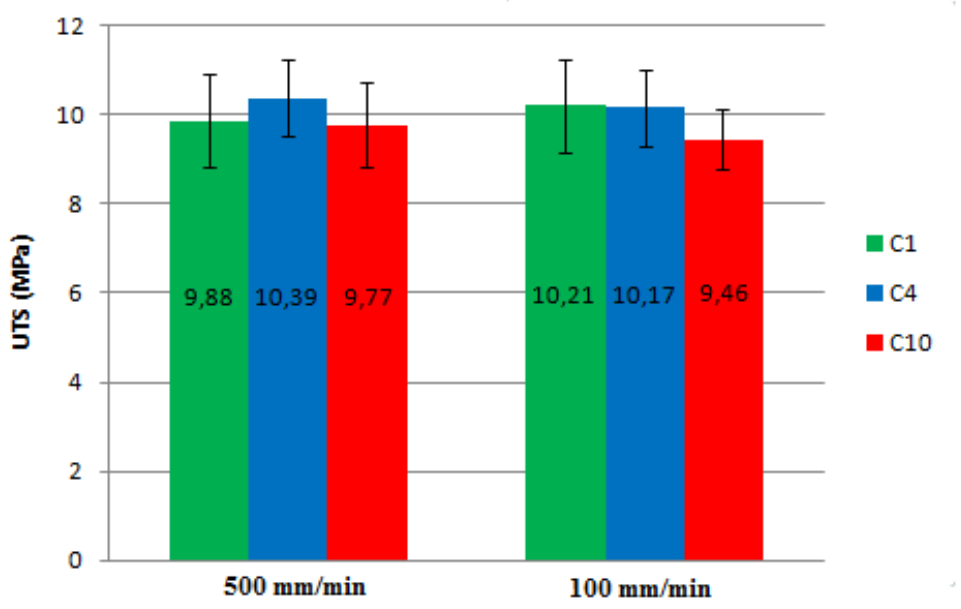

Figure 30. Comparison of UTS among C1, C4 and C10 groups according to the employed strain rate.

Thus the analysis of UTS depending on the strain rate shows different interpretations: in 500 mm/min case differences in mean values are small with respect to standard deviations, in 100 mm/min case one material class (C10) is suspected to differ but statistical tests cannot reject the null hypothesis all the same.

As both tests lack a high number of samples, comparisons and statistical methods result therefore quite labile. Then values associated with 100 mm/min and 500 mm/min are compared (e.g. UTS for C4 with 100 mm/min and 500 mm/min) in order to increase the number of dataset samples. Comparison between the mentioned datasets involves similar mean values and equal variances (F-test), plus distribution normality. Actually only C4 for 100 mm/min strain rate is not Gaussian according to Shapiro-Wilk test, whereas it is Gaussian according to Anderson-Darling test. Nevertheless because of the already mentioned property of considering not only the dataset under inspection but the whole population, one can assume normal distribution for this case as well.

Thanks to the proven compatibility between the data at the two strain rates, UTS datasets can be assumed to show similar behavior, therefore they can be merged. This method obviously just represents an approximation, however it helps results become statistically more reliable. Similarly, it is dutiful to mention how this approach cannot be repeated for the other 3 parameters which show different mean values for the two strain rates. After merging the three dataset couples (Tab.8), the sizes of datasets allow to employ only the t-test. The 3 data groups obviously present normality (by Anderson-Darling test) and equal variances. Results of this third analysis (Tab.9) confirm no appreciable difference can be inferred between C1 and C4, whereas equality between C4 and C10 is rejected with a 55% power. This statistical power is quite distant from the required 80% but it suggests C10 dataset may truly refer to a different material. The present method partially strengthens what was suspected from the analysis of 100 mm/min strain rate.

	N	**Mean (MPa)**	**StDev (MPa)**
C1 (UTS)	13	10,08	1,05
C4 (UTS)	17	10,29	0,86
C10 (UTS)	16	9,65	0,85

	t-t p value	**t-t power**
t-t C1-C4	0,561	0,09
t-t C1-C10	0,236	0,22
t-t C4-C10	0,042	0,55

Table 8 and Table 9. UTS means and StDevs related to uniaxial tensile test after 100 mm/min and 500 mm/min datasets are unified, with p values and statistical powers.

ANOVA tests are finally employed, returning 0,355 (SP = 0,17), 0,282 (SP = 0,24) and 0,143 (SP = 0,37) for 500 mm/min, 100 mm/min and the two cases together respectively. The first two values confirm the weakness in demonstrating a change with few samples, whereas the third case confirms p value decrease and statistical power increase when more samples are employed in statistical analysis.

Finally a comparison with the UTS reported on the datasheet has to be mentioned. All the listed mean UTS deal with values higher than 9,3 MPa so that a direct comparison of datasheet UTS with the recorded ones cannot be established. This disagreement is probably due to sample shape which is not exactly the one reported in the ASTM D412. In order to overcome this hitch, unsterilized dogbones with the same shape are employed (Tab.10). Their values can be immediately recognized to be much higher than all the other ones even if they are performed in the same laboratory environment (which however can present a slightly different temperature and humidity). Also in this case standard deviations are quite big, therefore direct comparisons are quite misleading to apply. However if we consider the two strain rates together for all the data (Tab.8 for C1, C4 and C10 and Tab.10 for the unsterilized samples), one may guess a decreasing curve as possible trend in UTS behavior depending on Etox cycles (Fig.31). Only for indicative purposes, ANOVA test applied to the four means and standard deviations returns a p value of 0,064 (SP = 0,58). This value is very close to the limit, however the differences in the values registered between sterilized and non-sterilized samples (in particular for C1 which should be reasonably quite similar to unsterilized specimens) have to be taken into account.

	N	**Mean (MPa)**	**StDev(MPa)**
UTS (500mm/min)	6	10,56	0,74
UTS (100mm/min)	4	10,60	0,81
UTS (all)	10	10,58	0,73

Table 10. UTS means and StDevs related to uniaxial tensile test for 100 mm/min and 500 mm/min strain rates on unsterilized dogbones.

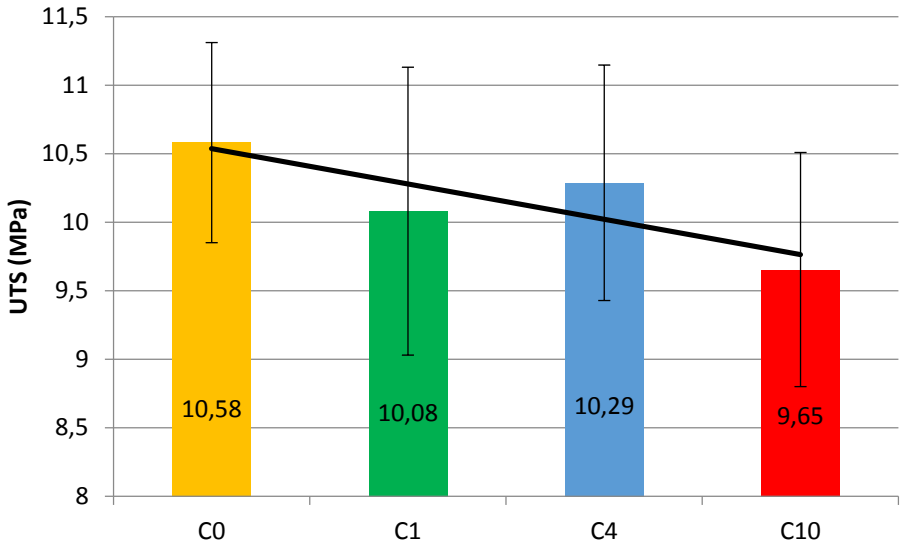

Figure 31. The 4 columns (100 mm/min and 500 mm/min together) do not allow to infer any straightforward conclusion due to the high standard deviations. However a possible interpretation of the whole behavior might be a progressive drop in UTS when Etox exposure increases.

4.1.2 Ultimate Elongation (UE)

500 mm/min strain rate case (Tab.11) reports C4 mean values as the highest one and C10 as the lowest one. C1 and C4 values are different but their high standard deviations (Fig.32) do not allow to infer any sure conclusion. Indeed statistical analysis never rejects null hypotheses as Tab.12 displays. Normality and equal variances are demonstrated for both 500 and 100 mm/min.

	N	Mean (%)	StDev (%)	Median (%)
C1 (UE)	5	5,10	0,59	5,21
C4 (UE)	9	5,34	0,49	5,33
C10 (UE)	10	4,98	0,54	5,05

	MW P value	t-t p value	t-t power
C1-C4	0,594	0,440	0,12
C1-C10	0,894	0,843	0,07
C4-C10	0,251	0,236	0,28

Table 11 and Table 12. Ultimate Elongation means, StDevs and medians related to uniaxial tensile test with 500 mm/min together with p values and statistical powers.

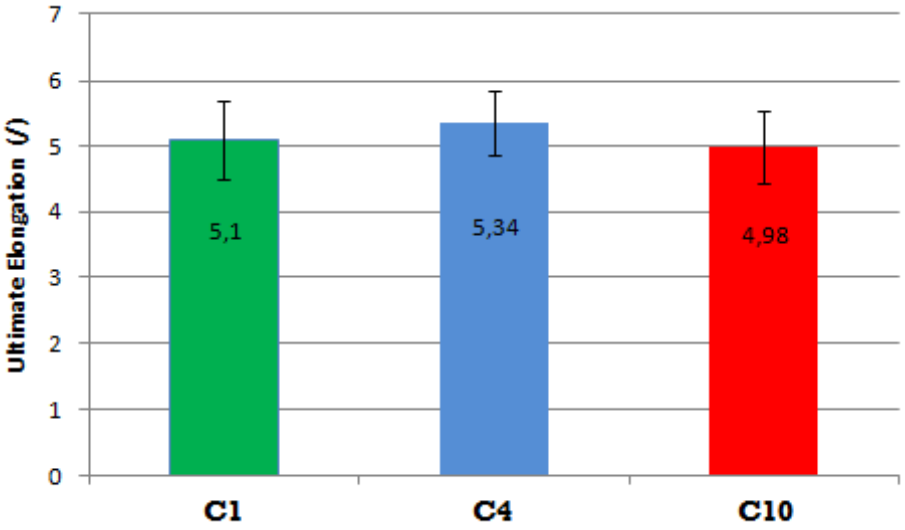

Figure 32. Comparison of Ultimate Elongation for 500 mm/min strain rate.

Considering 100 mm/min strain rate (Tab.13), similar values are reported for C1 and C4 whereas C10 exhibits a lower value (Fig.33). Even though standard deviation for C10 is smaller than the difference in mean values between C10 and C4, statistical approach (Tab.14) does not reject any null hypothesis. ANOVA tests in this case report p values of 0,478 and 0,209 for 500 mm/min and 100 mm/min respectively (SP < 0,35). Actually ANOVA outcome for the second case is not even suitable as residuals do not satisfy the requirements.

	N	Mean (%)	StDev (%)	Median (%)
C1 (UE)	8	5,67	0,58	5,43
C4 (UE)	8	5,69	0,49	5,77
C10 (UE)	6	5,23	0,44	5,06

	MW P value	t-t p value	t-t power
C1-C4	0,793	0,926	0,55
C1-C10	0,175	0,149	0,32
C4-C10	0,138	0,091	0,39

Table 13 and Table 14. Ultimate Elongation means, StDevs and medians related to uniaxial tensile test with 100 mm/min together with p values and statistical powers.

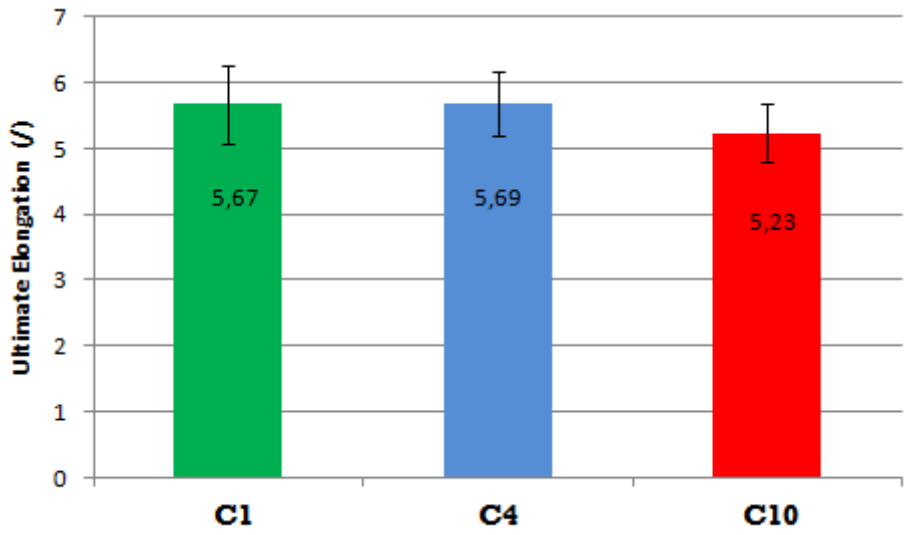

Figure 33. Comparison of Ultimate Elongation for 100 mm/min strain rate.

As explained in paragraph 4.1.1 the method of merging values belonging to 500 mm/min and 100 mm/min datasets can be applied only if compatibility among datasets is assessed. In this case this procedure is not possible due to the difference in the average values between the two cases.

4.1.3 Elastic Moduli

E_lin values (Tab.15) do not involve the rejection of null hypothesis (Mann-Whitney test) according to the small differences for both 500 mm/min and 100 mm/min strain rates (Tab.16). Also ANOVA test reports values higher than 0,3 for both cases (SP < 0,25). An outlier is removed from the C10 group with 100 mm/min strain (see paragraph 4.7 for details about this technique). According to the proven distribution normality and equal variances, t-test is also employed reporting similar results. Thus test outcomes suggest a negligible effect by Etox on this parameter (Fig.34).

E_lin case	N	Mean (MPa)	StDev (MPa)	Median (MPa)
C1 (500 mm/min)	5	4,05	0,09	4,02
C4 (500 mm/min)	9	3,97	0,10	3,95
C10 (500 mm/min)	10	4,01	0,10	4,01
C1 (100 mm/min)	8	3,84	0,10	3,85
C4 (100 mm/min)	8	3,79	0,08	3,81
C10 (100 mm/min)	5	3,80	0,05	3,79

E_lin case	MW p value	t-test power
C1-C4 (500 mm/min)	0,182	0,30
C1-C10 (500 mm/min)	0,462	0,12
C4-C10 (500 mm/min)	0,391	0,57
C1-C4 (100 mm/min)	0,270	0,19
C1-C10 (100 mm/min)	0,510	0,15
C4-C10 (100 mm/min)	0,826	0,32

Table 15 and Table 16. E_lin means, StDevs and medians related to uniaxial tensile test for both strain rates with p values and statistical powers.

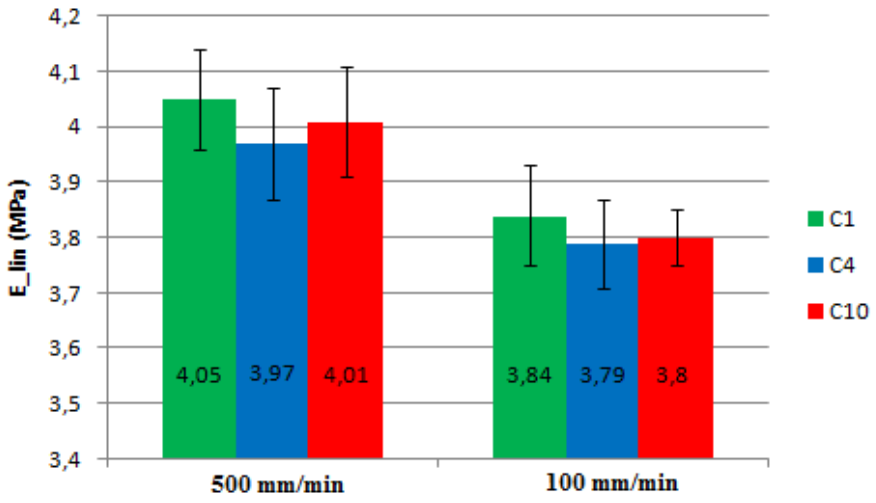

Figure 34. Comparison among C1, C4 and C10 E_lin according to the employed strain rate. The graphs confirm the quicker the strain is, the stronger the elastic answer of the material results (registered elastic modulus increases). The lack of time to rearrange its structure results in the material showing a tougher answer in the first case.

Secant modulus (E_200) presents a similar situation (Fig.35) with small differences between mean values with respect to standard deviations (Tab.17). Furthermore statistical analysis shows high p values in general for the Mann-Whitney test (Tab.18), whereas ANOVA test returns 0,681 for 500 mm/min strain rate and 0,468 for 100 mm/min strain rate (even if F test often rejects the hypothesis of equal variances among residuals) with SP < 0,20.

E_200 case	N	Mean (MPa)	StDev (MPa)	Median (MPa)
C1 (500 mm/min)	5	4,69	0,15	4,70
C4 (500 mm/min)	9	4,70	0,09	4,71
C10 (500 mm/min)	10	4,73	0,07	4,74
C1 (100 mm/min)	8	4,33	0,12	4,36
C4 (100 mm/min)	8	4,30	0,06	4,31
C10 (100 mm/min)	5	4,35	0,07	3,39

E_200 case	MW p value	t-test power
C1-C4 (500 mm/min)	0,790	0,06
C1-C10 (500 mm/min)	0,327	0,12
C4-C10 (500 mm/min)	0,488	0,11
C1-C4 (100 mm/min)	0,345	0,14
C1-C10 (100 mm/min)	0,847	0,07
C4-C10 (100 mm/min)	0,107	0,36

Table 17 and Table 18. E_200 means, StDevs and medians related to uniaxial tensile test for both strain rates with p values and statistical powers.

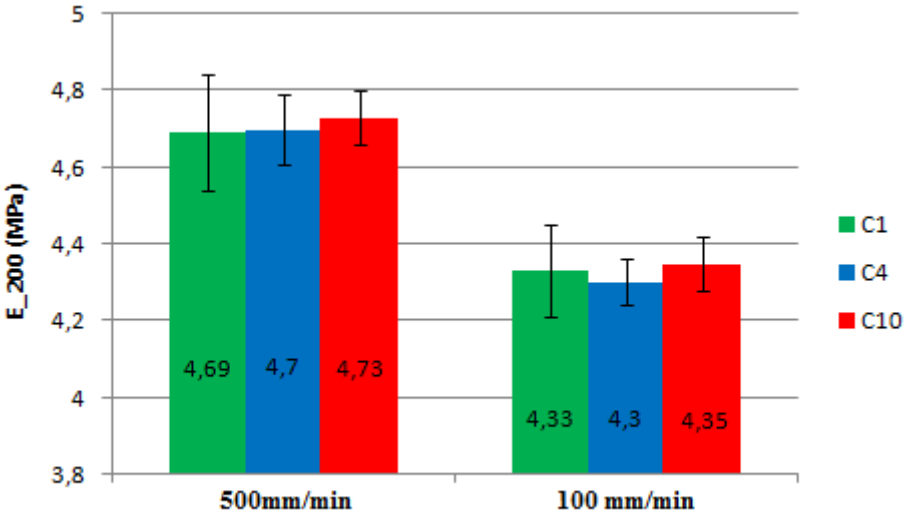

Figure 35. Comparison among C1, C4 and C10 E_200 according to the employed strain rate. The graph is in accordance with Fig.34 with the grater strain rate inducing a higher elastic modulus.

4.1.4 Slippage estimation

As explained in paragraph 3.2.1 slippage of dogbones extremities in the vises is a phenomenon which inevitably alters final results. Materials with high Ultimate Elongation are unfortunately more prone to this problem. Fig.36 and Tab.19 clearly illustrate the impact of slippage on the test: yellow lines (Fig.36A) indicate the edge of the clamps separating the blocked part from the unclamped one before the test is run. After the 180 mm elongation the clamps are brought back to the starting position so that the dogbone is not anymore in tension. In contrast, a bending in the narrow part can be seen (Fig.36B). The drawn lines (yellow lines in Fig.36A) appear now shifted away from the claws as the red arrows indicate. Calculation by SketchUp (the software already mentioned in the calculation of strain at paragraph 3.2.1) shows that from each side a 2,7 mm portion of clamped extremity slips out of the clamp (when clamps come back to the original position). When the extension is reported to be 180 mm, the photo acquired at this moment shows a 10 mm extension related to the shift of sample extremities (the 2 parts of sample outside the portion delimited by the red arrows).

	Before extension	**180 mm extension**	**After extension**
Slippage portion (per side)	≈0 mm	5 mm	2,7 mm

Table 19. Before the test is run the black straight line is approximately on the vise edge (Fig.36A), whereas it is not anymore along that in both moments when following photos are taken (Fig.36B).

However one cannot consider these 10 mm as a whole contribution of slippage: indeed a certain percentage is actually related to the strain of the portion between the lines drawn by pen and the exact clamp edges. However assuming this contribution to be negligible so that all these 10 mm are ideally due to slippage, this phenomenon influences the 5,5 % of the whole strain (at 180 mm). With respect to the strain at rupture reported on the datasheet of MED-4860P (525%) and assuming the 5,5% contribution to be constant after a minimum strain, this phenomenon might turn up to a 30% contribution (0,055*525%) overestimating

the real strain. According to that, one may consider this value (actually something less due to the neglected contribution explained above) as an error to take into account when looking at the calculated Ultimate Elongation. This calculation is merely indicative, therefore one may only take that into account as a partially affecting factor during result analysis. As the two elastic moduli deal with relatively small strains, slippage should not affect them significantly.

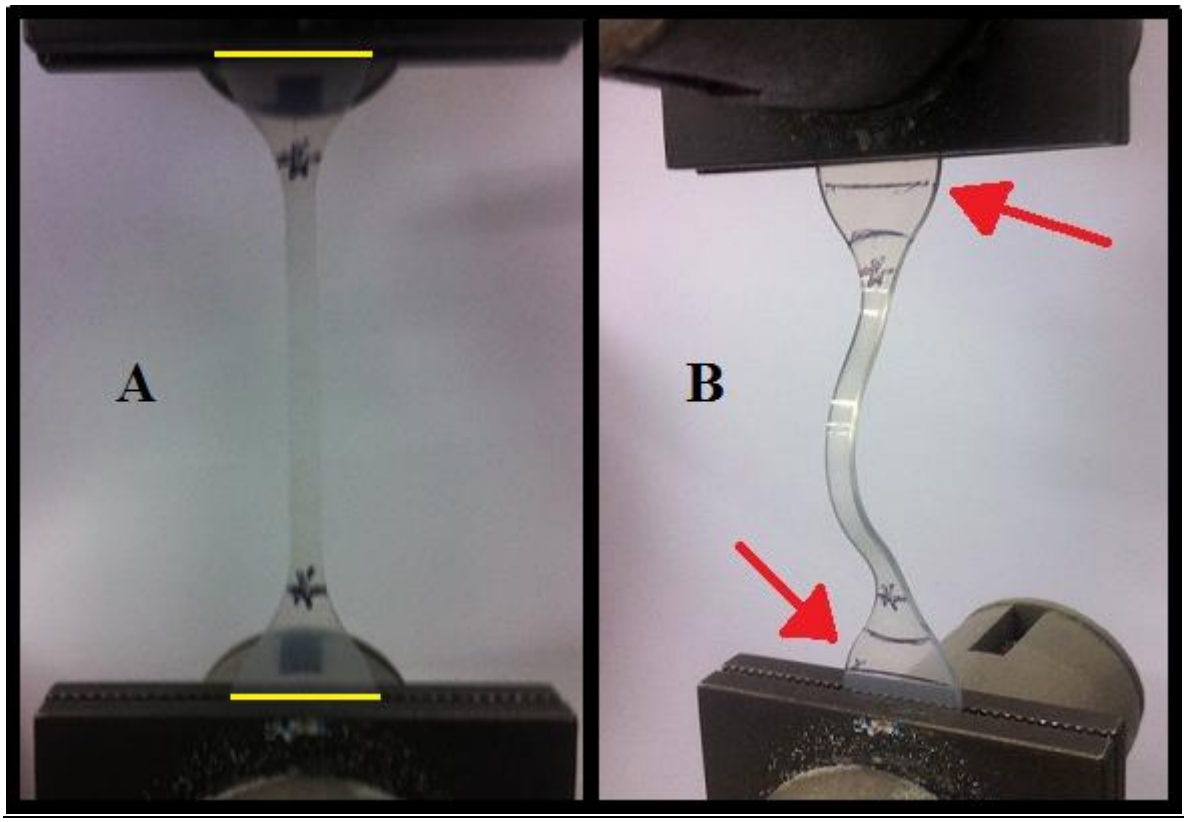

Figure 36. Photos taken before and after the uniaxial tensile test, the same lines (along the vise edges) drawn by pen are indicated by yellow line (A) and by the 2 red arrows (B). One may notice the curved lines between the red arrows and the asterisks. The central sample portion between these two curved lines represents the part which exhibits approximately the same width when a huge extension (180 mm indeed) is reached.

4.1.5 Compatibility with unsterilized samples

In addition to the comparison performed for UTS , the same experiment employed to collect C0 UTS data is used to compare C0 and the sterilized samples. The remaining 3 parameters in uniaxial tensile test are therefore analyzed by adding the C0 terms to the

tables reported in the previous paragraphs. As already mentioned only 6 samples are employed for 500 mm/min strain rate, whereas 100 mm/min case deals with 4 unsterilized specimens.

Ultimate Elongation for 500 mm/min (Tab.20) displays a situation similar to UTS at the same strain rate, whereas the same parameter for the second strain rate (Tab.21) results quite higher than both C1 and C4 (even though standard deviations are big). Dealing with the elastic moduli great compatibility can be observed for E_lin at high strain rate and E_200 at both strain rates (Tab.22 and Tab.23). Tangent modulus for slow deformation is definitely not compatible with C4 and C10 values according to their small standard deviations, instead C1 presents a higher standard deviation which would not return a p value < 0,05 in a statistical comparison.

UE (500 mm/min)	Mean (%)	StDev (%)
C0 (UE)	5,48	0,43
C1 (UE)	5,10	0,59
C4 (UE)	5,34	0,49
C10 (UE)	4,98	0,54

UE (100 mm/min)	Mean (%)	StDev (%)
C0 (UE)	5,95	0,43
C1 (UE)	5,67	0,58
C4 (UE)	5,69	0,49
C10 (UE)	5,23	0,44

Table 20 and Table 21. Comparison among C0 and sterilized specimens in uniaxial tensile test for Ultimate Elongation. Left and right values refer to 500 mm/min and 100 mm/min strain rates respectively.

E_lin case	Mean (MPa)	StDev (MPa)
C0 (500 mm/min)	4,04	0,13
C1 (500 mm/min)	4,05	0,09
C4 (500 mm/min)	3,97	0,10
C10 (500 mm/min)	4,01	0,10
C0 (100 mm/min)	3,94	0,15
C1 (100 mm/min)	3,84	0,10
C4 (100 mm/min)	3,79	0,08
C10 (100 mm/min)	3,80	0,05

E_200 case	Mean (MPa)	StDev (MPa)
C0 (500 mm/min)	4,64	0,10
C1 (500 mm/min)	4,69	0,15
C4 (500 mm/min)	4,70	0,09
C10 (500 mm/min)	4,73	0,07
C0 (100 mm/min)	4,32	0,08
C1 (100 mm/min)	4,33	0,12
C4 (100 mm/min)	4,30	0,06
C10 (100 mm/min)	4,35	0,07

Table 22 and Table 23. Comparison among C0 and sterilized specimens in uniaxial tensile test for elastic moduli for both strain rates. Left and right values refer to tangent modulus (E_lin) and secant modulus (E_200) respectively.

Apart from the small number of samples employed for C0 datasets, another fact affecting data outcomes for these groups may reside in the different sample stories. Unsterilized and sterilized groups are received in different moments so that materials are likely to be exposed to different conditions even if proper shelf life and shipping conditions are assured for them.

According to the displayed comparison and taking into account the limitations reported above, one may assume the similarity between C0 and C1 also for all the other experiments. Indeed Ethylene Oxide sterilization is known not to alter appreciably the samples made of silicone which however is a generic way to refer to a wide class of materials.

4.2 DMA

Data are collected for a wide range of temperatures, therefore only two of them are employed (freezing point for water and human body temperature). The analysis of obtained thermograms reveals that 2 C1 samples out of 6 (2 couples of samples actually) generate graphs including intervals with zig-zag shape instead of a smooth curve (Fig.37). Even though the number of samples is already quite limited (only 6 samples per group), these two cases have to be discarded (even though one of them may be interpolated in the zig-zag area, the resulting moduli would appear lower with respect to the other curves).

Thus Tab.24 and Tab.25 display test outcomes for 0° C and 37° C temperatures respectively. These data generally reveal small differences in mean values with respect to standard deviations, or similar at the latest. Graphic comparisons among C1, C4 and C10 show similar patterns with mean values slightly increasing with the number of cycles (but standard deviations have to be remembered to be big). Therefore instead of reporting the graphic comparisons for all the possible combinations (12 in total), only those returning the greatest and the lowest p values for ANOVA test (Tab.26) are graphically reported (Fig.38 and Fig.39).

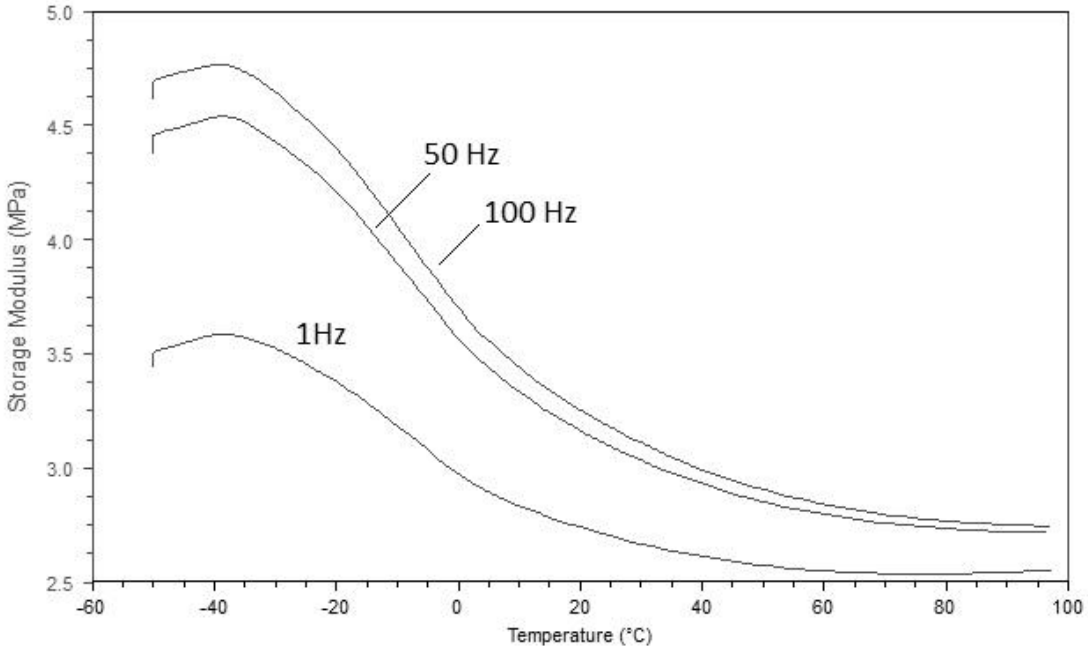

Figure 37. DMA thermograms related to three different frequencies. The curves generally appear smooth like the displayed shape, however for certain C1 samples, irregular parts can be seen.

The choice of ANOVA test instead of a 2 dataset-comparison (Mann-Whitney in this case) is taken due to the experiment procedure which is known not to be extremely precise (due to the lack of control in clamping). Indeed instead of comparing 2 datasets at a time, an overall comparison may be more effective since the experiments gather many sources of errors and differences with respect to standard and instrument requirements. According to that a comparison between two datasets may enhance the sensitivity to errors when statistical comparisons are performed.

		0° C		37°C	
	N	Mean (MPa)	StDev (MPa)	Mean (MPa)	StDev (MPa)
C1_1Hz	4	2,84	0,21	2,61	0,14
C4_1Hz	6	2,86	0,19	2,66	0,11
C10_1Hz	6	2,89	0,16	2,73	0,14
C1_50Hz	4	3,40	0,25	2,94	0,16
C4_50Hz	6	3,45	0,23	2,99	0,11
C10_50Hz	6	3,47	0,18	3,08	0,15
C1_100Hz	4	3,53	0,27	3,01	0,16
C4_100Hz	6	3,58	0,24	3,07	0,12
C10_100Hz	6	3,59	0,18	3,15	0,16

Table 24. Mean values and standard deviations for E' (storage modulus) depending on sample type, frequency and temperature.

		0° C		37°C	
	N	Mean (MPa)	StDev (MPa)	Mean (MPa)	StDev (MPa)
C1_1Hz	4	0,409	0,028	0,218	0,017
C4_1Hz	6	0,437	0,030	0,227	0,014
C10_1Hz	6	0,439	0,022	0,232	0,013
C1_50Hz	4	0,628	0,044	0,362	0,024
C4_50Hz	6	0,654	0,035	0,376	0,018
C10_50Hz	6	0,667	0,029	0,384	0,021
C1_100Hz	4	0,669	0,050	0,392	0,025
C4_100Hz	6	0,694	0,037	0,407	0,024
C10_100Hz	6	0,707	0,028	0,413	0,020

Table 25. Mean values and standard deviations for E'' (loss modulus) depending on sample type, frequency and temperature.

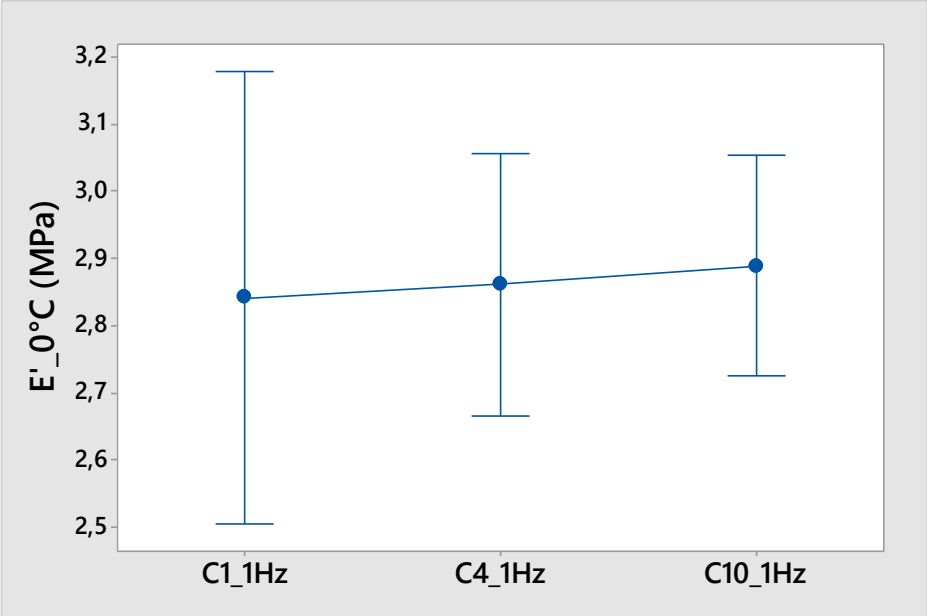

Figure 38. Comparison among E' values at 0° C for 1 Hz frequency. The ANOVA p value associated with this case is the greatest one (0,919) among the 12 cases.

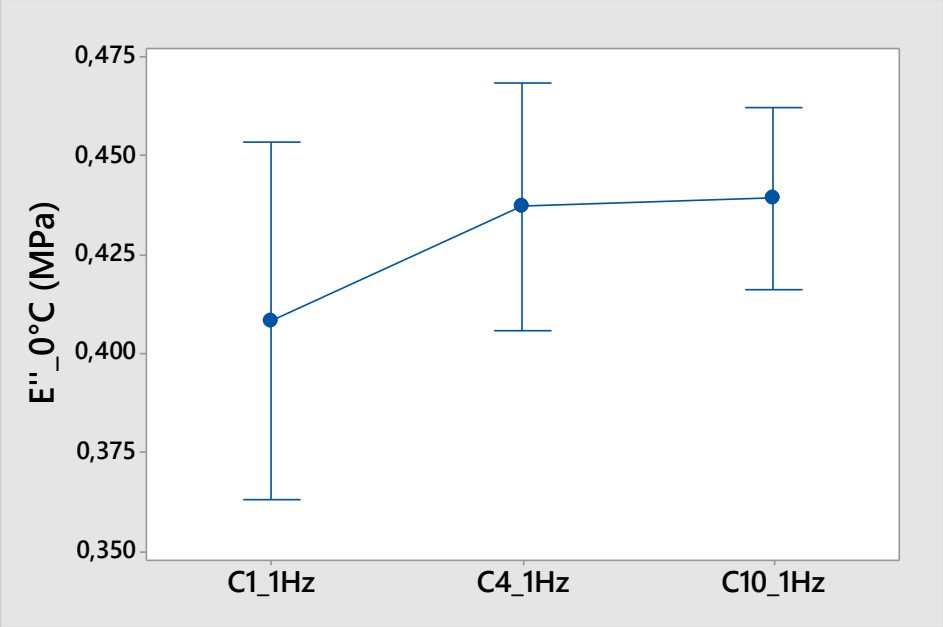

Figure 39. Comparison among E'' values at 0° C for 1 Hz frequency. The ANOVA p value associated with this case is the lowest one (0,193) among the 12 cases.

ANOVA test is run assuming equal variances and obtained p values never allow null hypothesis rejection as one may already infer from Tab.24 and Tab.25. Mann-Whitney test (Tab.27) is performed briefly also for those cases reporting a p value < 0,3 for ANOVA test. As the trend is similar for all the combinations and the relation C1 < C4 < C10 is always respected, only C1 and C10 datasets are compared. Resulting p values are still insufficient to reject null hypothesis also in this case.

	1 Hz		50 Hz		100Hz	
	p value	**SP**	**p value**	**SP**	**p value**	**SP**
E' (0°C)	0,919	0,06	0,903	0,07	0,915	0,06
E' (37°C)	0,338	0,19	0,319	0,22	0,316	0,20
E'' (0°C)	0,193	0,26	0,273	0,25	0,318	0,22
E''(37°C)	0,353	0,20	0,298	0,24	0,370	0,19

Table 26. Results (p values and standard deviations) of ANOVA tests (assuming equal variances) for E' and E'' with respect to temperature and frequency.

Parameter	**Frequency**	**ANOVA p value**	**ANOVA SP**	**MW p value**	**MW SP**
E'' (0°C)	1 Hz	0,193	0,26	0,134	0,39
	50 Hz	0,273	0,25	0,199	0,34
E''(37°C)	50 Hz	0,298	0,24	0,336	0,27

Table 27. All the cases exhibiting a p value lower than 0,3 for ANOVA test are repeated (only C1 and C10 are compared) with Mann-Whitney test.

4.3 Hardness

Collected data are used to calculate the mean values and standard deviations summarized in Tab.28 and illustrated in Fig.40. According to the graph, hardness increases with the exposure to Etox even though less than 1 Shore A difference is suggested. All the three values are higher than 60 Shore A, which is the value indicated on the material datasheet.

	N	Mean (Shore A)	StDev (Shore A)
C1	18	61,389	0,431
C4	18	61,736	0,397
C10	18	62,014	0,481

Table 28. Hardness data (mean values and standard deviations) for the three material classes.

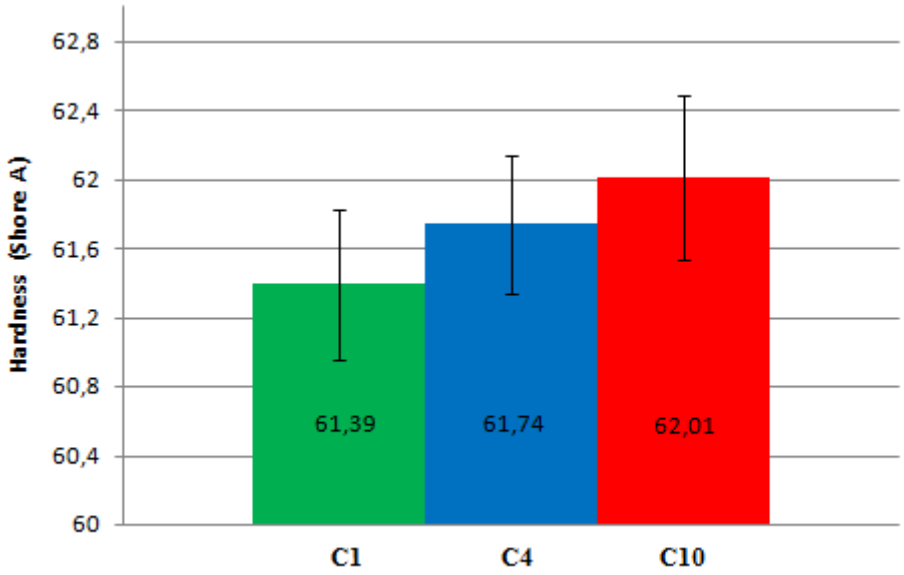

Figure 40. Hardness for C1, C4 and C10 groups. Even though standard deviations are quite big, the trend suggests that Etox exposure entails hardness increase.

Statistical analysis shows that all the distributions can be considered normal and F-tests do not reject null hypotheses. Thus 2-sample t-test is employed, its outcomes for the three sample comparison are reported in Tab.29. As its first column shows, C1 has certainly a different mean value with respect to the other two groups. Statistical powers in comparisons dealing with C1 give reliability to this consideration. On the other hand the comparison between C4 and C10 reports a p value slightly higher than 0,05 and the statistical power does not reach 50%. This behavior is unsurprising according to the large standard deviations of C4 and C10 with respect to the difference between their mean values. According to that the null hypothesis is not rejected but this result lacks reliability and even more samples should be employed (Minitab estimates 40 samples for 80%

power). Thus ANOVA test is performed as well in order to obtain a whole analysis: returned p value is approximately 0 with a statistical power of 97%.

	P value	Power
t-test C1-C4	0,017	0,69
t-test C1-C10	0	0,98
t-test C4-C10	0,067	0,45

Table 29. Statistical analysis by t-test for C1, C4 and C10 hardness values.

4.4 DSC

Test results given from the first test group show a common pattern (Fig.43) with a big negative (endothermic) peak around -44° C whereas the typical step used for Tg recognition is not visible. The second test group exhibits a different shape where also the Tg step in the baseline is present in addition to the endothermic peak (Fig.47). The differences between the two cases reside in the different cooling rate according to literature. Past studies dealing with PDMS analysis by DSC [30,41,42] report pure PDMS has thermograms (in the heating curve) quite easy to analyze due to sharp changes in the line (Fig.41), whereas crosslinked PDMS is more prone to show only the endothermic peak related to Tm_2.

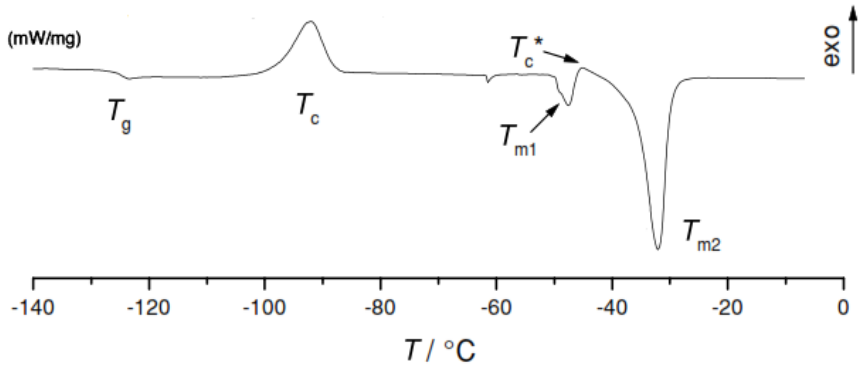

Figure 41. Typical heating curve thermogram for pure PDMS. One can notice the presence of 5 baseline changes. The step in the baseline (Tg) due to glass transition and an exothermic peak (Tc) because of the cold crystallization are the first ones from left to right. In particular the second transition is due to chain reaccomodation when they reach enough mobility. Consecutively there are two melting (endothermic) peaks, Tm_1 and Tm_2 (whereof only the latter is quite big) and finally a second small exothermic peak (Tc).*

Cooling rate is known to strongly affect the degree of crystallinity of semicrystalline materials [30,41]. In fact a temperature rate smaller than 10°C/min is generally not sufficient to make these transitions clear in the thermogram. Due to crosslinkages, slow cooling results in amorphous regions having the time to arrange themselves into crystalline structures during cooling procedure, with crosslinkages acting as guides to crystallization. Thus slow cooling process enhances the crystallinity, on the contrary quick cooling (rate higher than 10°C/mm, a very good value is 50°C/min) leads to the formation of an amorphous glass. That happens because amorphous areas have not the time to rearrange themselves before getting brittle. Thus the structures fastest in assembling and growing (rather than those with the lowest free energy) lead the process influencing the final crystallinity. As described a quick cooling (quenching) generally allows the detection of the step in the baseline whereas the exothermic peak for cured PDMS is reported to be negligible (Fig.42) [30]. These temperature transitions are now visible due to the amorphous parts which turn into rubber-like state (low energy status) from a brittle disorganized structure. In fact, as soon as temperature gets close to Tc, chains can arrange to form crystallites as they recover enough mobility due to viscosity decrease [30].

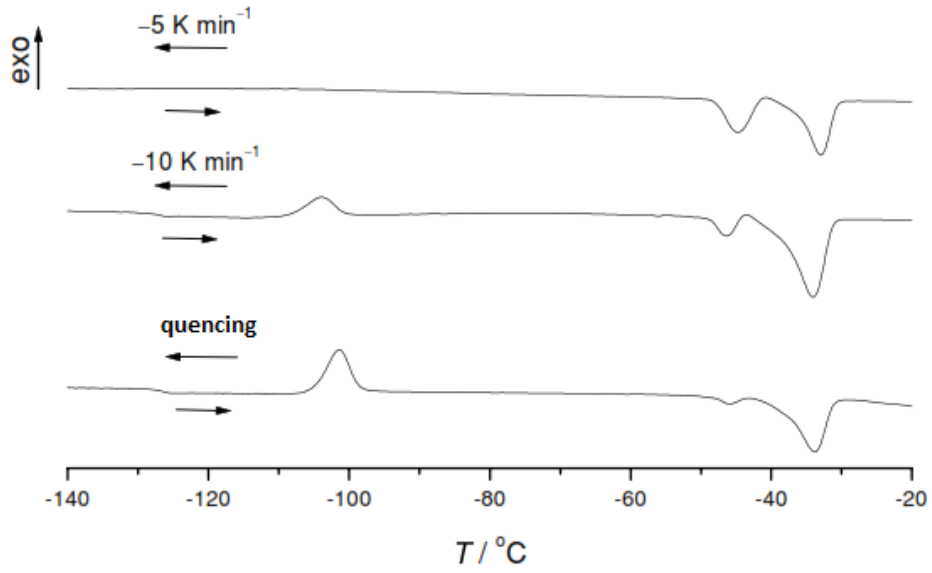

Figure 42. Influence of cooling rate on the resulting thermogram (heating curve) with the same heating rate in all the three cases. The first graph does not show neither any step in the baseline nor the Tc peak. Quenching (often 50°C/min cooling rate is used) allows the detection of the two elements thanks to the impossibility of rearranging chains in a well-organized manner. The presence of the Tc peak suggests this PDMS has low content of silica.

4.4.1 First DSC group (slow cooling)

The first test group is used to calculate the enthalpy associated with the endothermic peak (melting) and the Tm (temperature in correspondence of the peak tip). In fact all the thermograms (Fig.43) obtained during the first DSC show a single endothermic peak in correspondence of the Tm (for pure PDMS two peaks Tm_1 and Tm_2 appear instead).

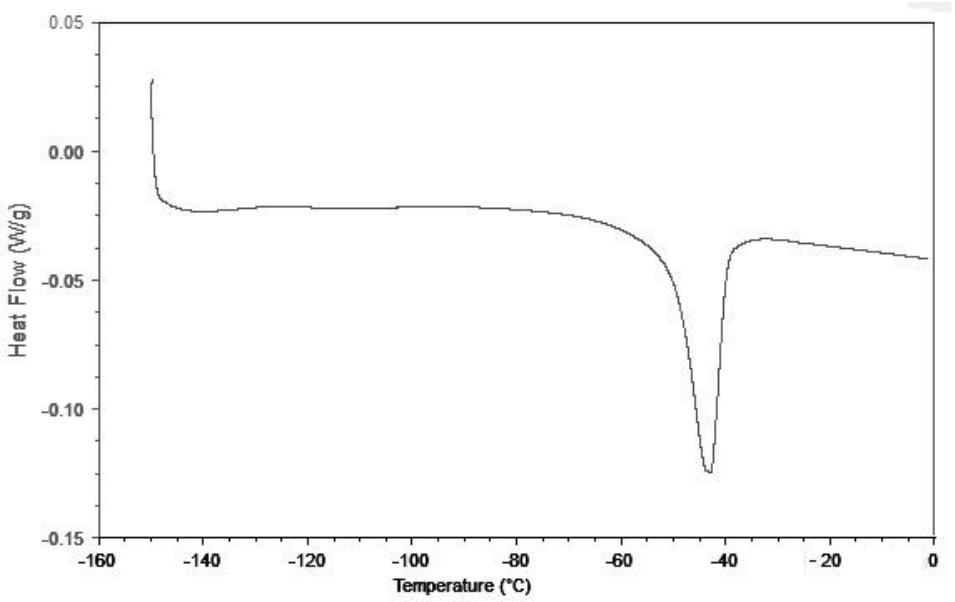

Figure 43. Thermogram (heating curve) of MED-4860P after equilibration (slow cooling) to -150° C. The only element which can be easily recognized is the endothermic peak (melting transition, Tm) around -44°C. Tg step in the baseline cannot be seen clearly (even though baseline shows some tremblings in that area).

Tab.30 displays compatibility for Tm among the three groups (Fig.44) with an average value of approximately -43,75° C, in fact ANOVA p value results 0,586 (SP = 0,18).

	N	**Mean Tm (°C)**	**StDev (°C)**
C1	6	-43,62	0,47
C4	7	-43,87	0,38
C10	7	-43,83	0,21

Table 30. Tm for C1, C4 and C10 calculated as the temperature in correspondence of the tip of the endothermic peak.

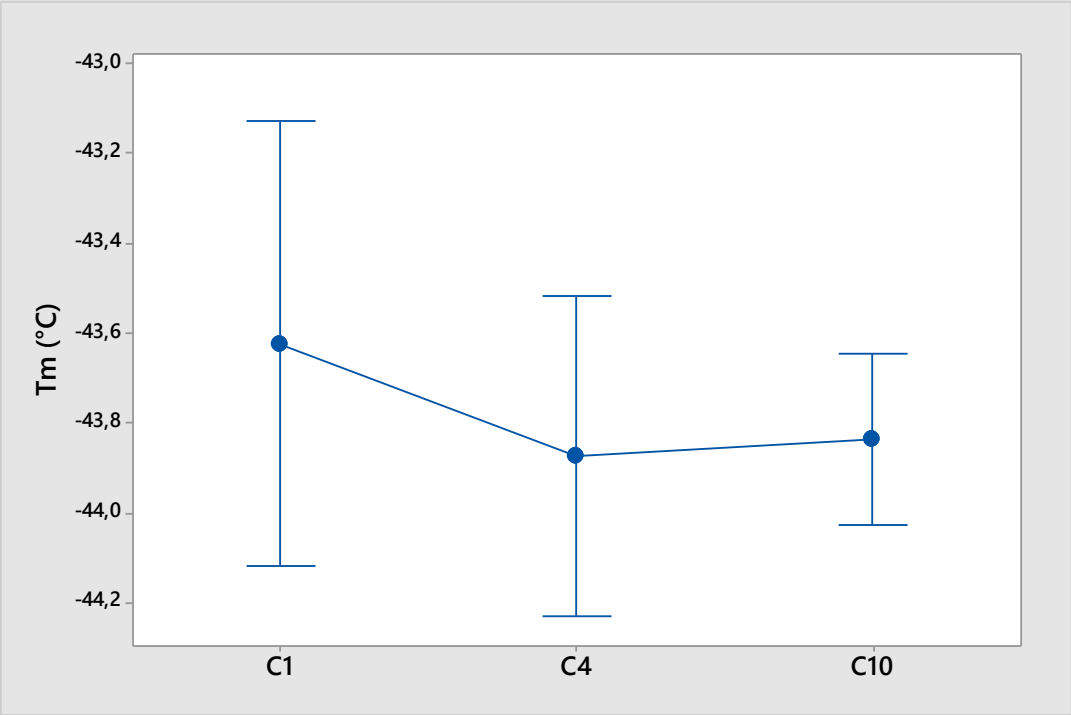

Figure 44. Comparison of Tm among C1, C4 and C10 (with slow cooling).

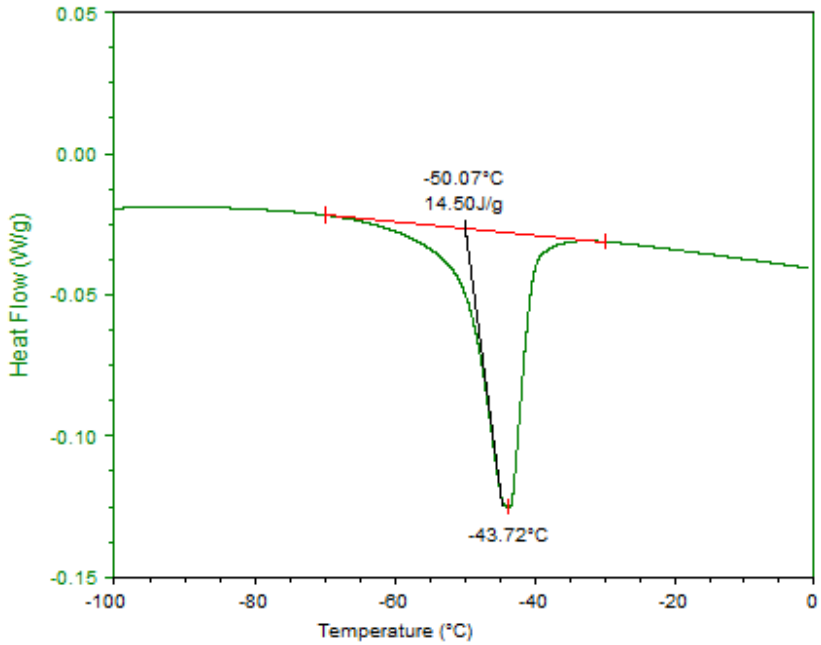

Figure 45. Universal Analysis 2000 can calculate the area (enthalpy) and two temperatures associated with the peak once the user sets the extremities of integration. As the two parts of the baseline before -70° C and after -30° C always appear aligned, the area is calculated with a linear segment (as element closing the area) connecting these two extremities.

On the other hand as Fig.45 displays, the integral of the peak with respect to the baseline (once two reasonable extremities are set) returns the value of the enthalpy. Indeed since DSC test is run at constant pressure, enthalpy changes equal the heat flow [43]. In order to enhance the compatibility among all the measurements, two extremities are set for all the integrations. For this purpose -70° C and -30° C temperatures are chosen since the two parts of the curve outside this integration interval always appear well aligned (Fig.45).
Tab.31 lists the obtained results for enthalpy in correspondence of the melting transition. Only ANOVA test is applied, returning a p value of 0,967 (SP = 0,05). Also Fig.46 shows how no specific differences among the different Etox exposures are seen.

	N	Mean (W/g)	StDev (W/g)
C1	6	14,78	0,28
C4	7	14,76	0,18
C10	7	14,75	0,19

Table 31. Enthalpy data for the Tm peak in the first DSC group (slow cooling).

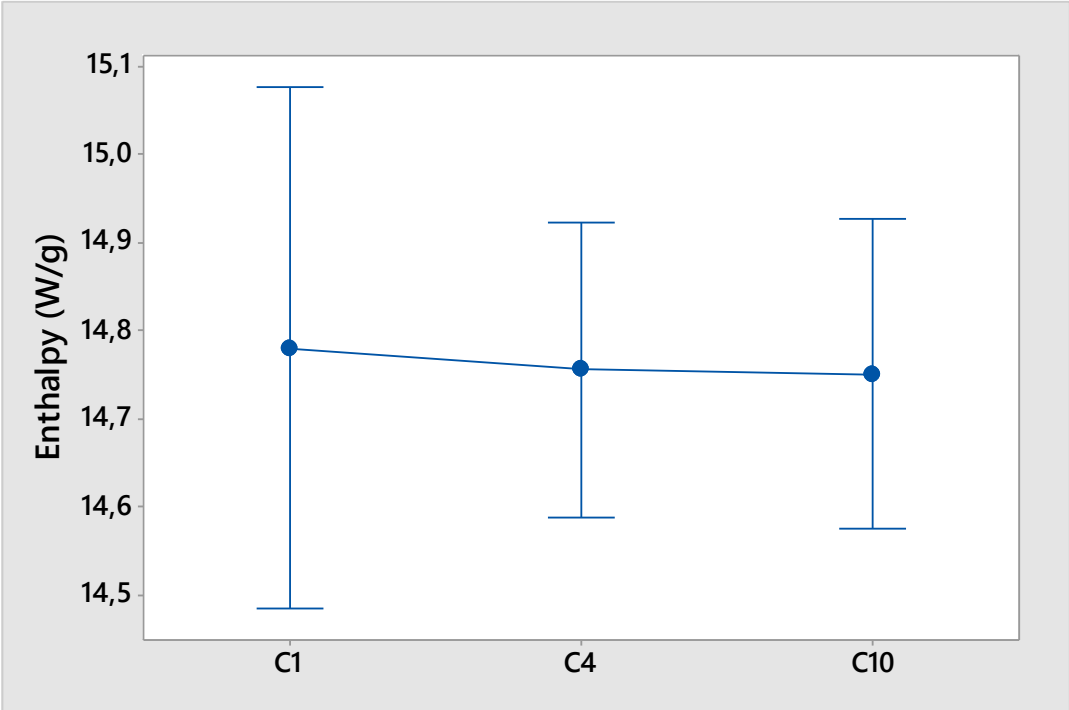

Figure 46. Comparison of C1, C4 and C10 enthalpies (for melting peak) in the first DSC group (slow cooling).

4.4.2 Second DSC group (fast cooling)

The tests associated with quenching show a different thermogram shape (Fig.47) for the heating curve, cooling curve is reported in this case as well. Melting transition is similar to the previous case but Tg step in the baseline can now be recognized whereas the cold crystallization (exothermic) peak on the right of the Tg step does not appear. However the crystallization transition can be seen in the cooling curve (exothermic peak) which furthermore reveals the Tg step as well (however the Tg calculation is run on the heating curve's step only since it results easier).

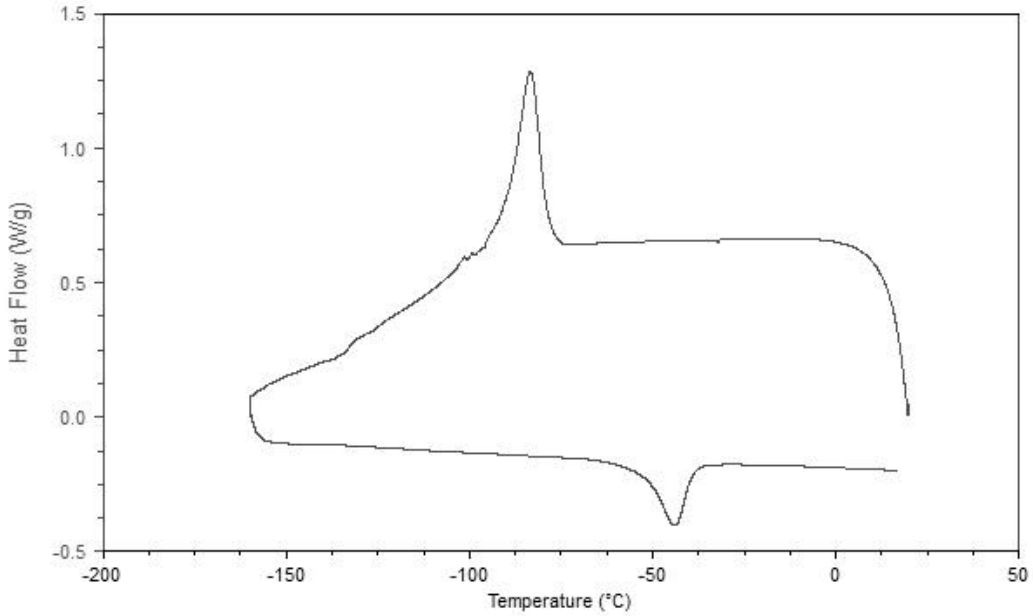

Figure 47. Thermogram of MED-4860P after fast cooling (30° C/min) up to -160° C. The cooling curve (the upper one) reveals the crystallization peak and the Tg step, whereas the heating curve (the lower one) shows both the Tm peak (around -44°C) and the Tg step in the baseline (approximately -134° C).The latter change in the baseline is better shown in Fig.48.

Similarly to the description of enthalpy calculation, Universal Analysis 2000 allows the identification of the glass transition temperature (Fig.48) once two interval extremities are set (so that they include a visible step). 3 temperatures are indicated along the step shape but only the central one (halfway point) is analyzed.

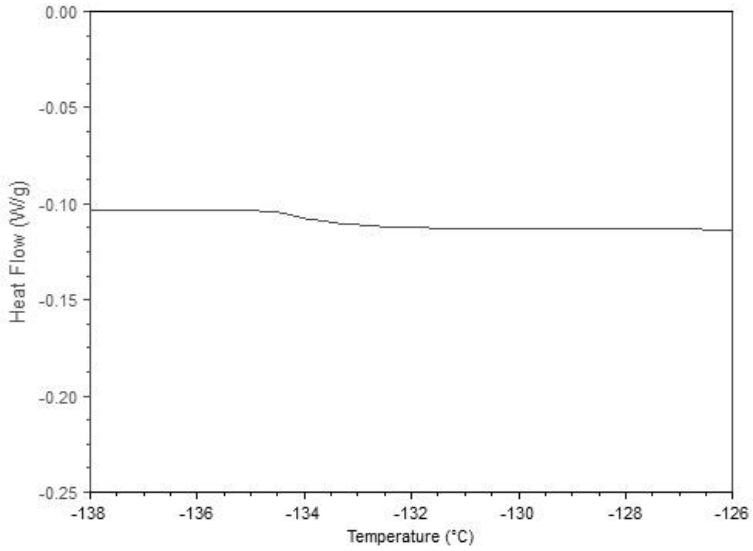

Figure 48. Particular of the heating curve in a thermogram related to quenching. The baseline exhibits a drop with the two parts separated by the step which are horizontal. This element could not be found in the thermogram with slow cooling rate instead.

Thus Tab.32 and Tab.33 report the analyzed data and their statistical analysis. ANOVA test is performed as well returning a 0,924 p value (SP = 0,06). As both Fig.49 and statistical analysis suggest the Tg parameter is not likely to change.

	N	Mean Tg (°C)	StDev (°C)
C1 (Tg)	10	-133,81	0,22
C4 (Tg)	10	-133,82	0,41
C10 (Tg)	10	-133,86	0,32

	t-test	Power
C1-C4	0,919	0,05
C1-C10	0,655	0,06
C4-C10	0,806	0,05

Table 32 and Table 33. Mean values and standard deviations for Tg related to fast cooling process, together with p values and statistical powers.

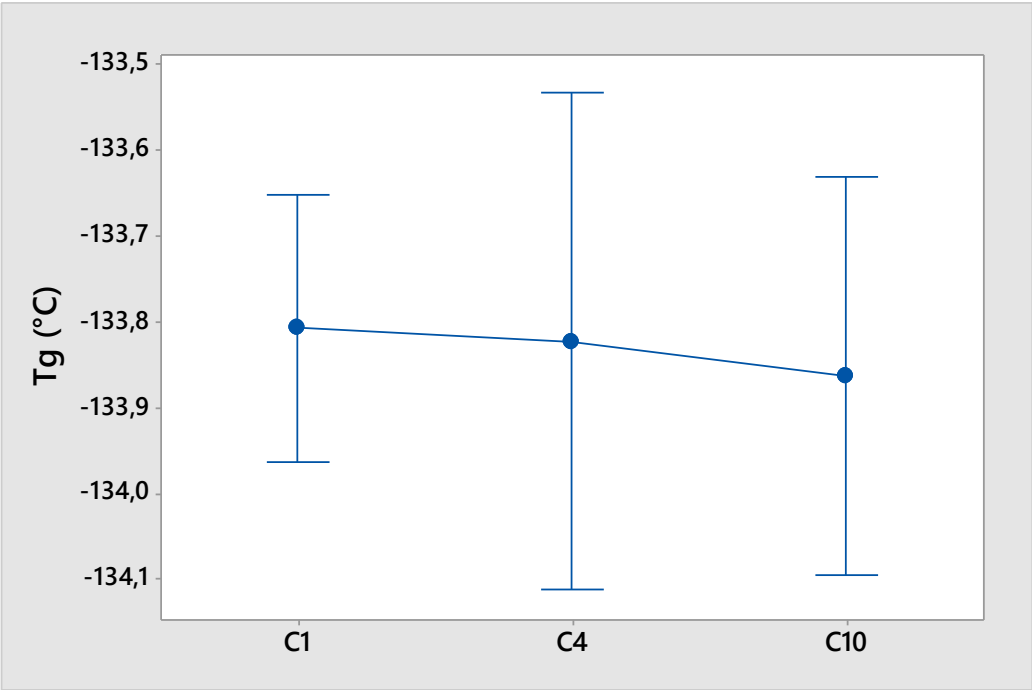

Figure 49. Comparison among C1, C4 and C10 based on their Tg.

Focusing on melting transition, the calculations of the enthalpy (with the same procedure described for the first DSC group) associated with the melting peak and the Tm are repeated in this case as well. Enthalpy reveals C4 and C10 with comparable variances, whereas C1 has a much higher one. Outlier test (Dixon's r11) is performed but it does not allow the removal of potential outliers (p value= 0,15). Indeed this p value cannot be extremely low as 2 values spread on the lower interval extremity so that the lack of rejection makes sense. However if also C4 and C10 values are included in this outlier test (since they display values concentrating in the 13,75-14 W/g interval as C1 mainly does) a Dixon's r22 test can be performed as well (similar approach is carried out for swelling data). In this case the lowest value is recognized as outlier (Fig.50). Fusion between C1, C4 and C10 datasets for such purpose is certainly not straightforward since these datasets are inspected to evaluate the potential difference among them.

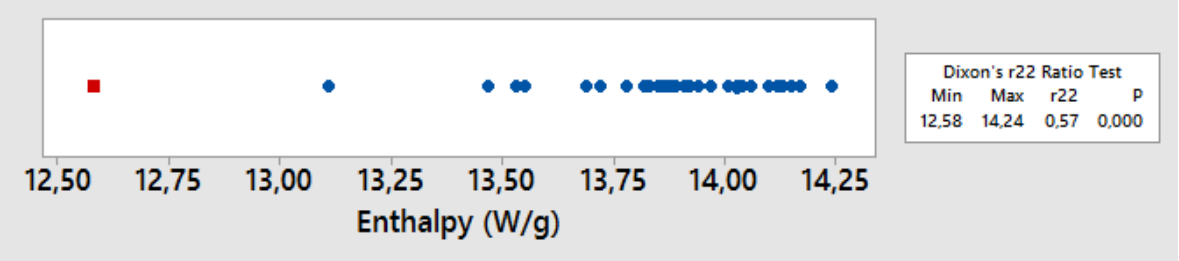

Figure 50. Dixon's r22 outlier test (suitable for datasets with more than 14 samples) for all the values together (dealing with the enthalpy of the melting peak). The lowest dot is recognized as outlier with respect to the selected dataset (30 values). Also the second dot on the left is quite far from the other ones and may therefore be suspected as outlier too. However taking two outlier tests sequentially has already been mentioned not to be recommended.

Depending on what mentioned above, Fig.51 reports the three canonical cases plus two datasets (C1* and C1**) where suspected outliers are removed. Without the two lowest values (C1**) the variances among the three groups results compatible.

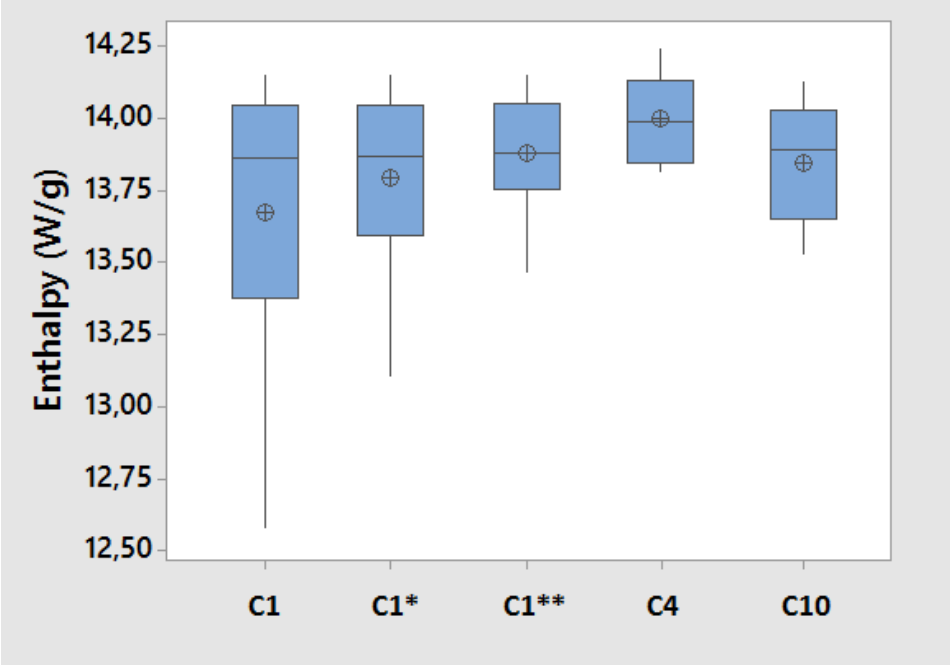

Figure 51. Boxplot comparison among the three canonical cases (C1, C4 and C10) with the addition of C1 (the lowest value is removed) and C1** (the lowest two values are removed) datasets for the enthalpy associated with the melting peak.*

Tab.34 shows the values for the five mentioned datasets. According to the high number of groups, ANOVA test is performed on the three possible combinations: C1-C4-C10, C1*-C4-C10 and C1**-C4-C10 (Tab.35). Actually for the first comparison the residuals struggle to satisfy ANOVA requirements. Finally t-test is performed among C1**, C4 and C10 datasets (Tab.36). Both these methods fail in rejecting the null hypothesis even though p values are generally close to 0,05.

	N	Mean Enthalpy (W/g)	StDev (W/g)
C1	10	13,68	0,49
C1*	9	13,80	0,33
C1**	8	13,88	0,22
C4	10	14,00	0,15
C10	10	13,85	0,21

Table 34. Mean values and standard deviations of the enthalpy associated with the melting peak in the second DSC group (fast cooling). For the C1 case the three datasets listed previously are reported.

	ANOVA p value	SP
C1-C4-C10	0,067	0,57
C1*-C4-C10	0,103	0,36
C1-C4-C10**	0,157	0,19

	t-test p value	SP
C1-C4**	0,181	0,25
C1-C10**	0,726	0,06
C4-C10	0,068	0,42

*Table 35 and Table 36. Statistical analysis on melting peak enthalpy by ANOVA test employing different C1 datasets and by t-test (C1** is used for samples sterilized once).*

The second parameter dealing with the melting transition is the peak temperature Tm (Fig.52). C10 dataset presents a value which is estimated to be an outlier (Dixon's r11 test with p value of 0,006), however C1 shows a similar behavior even if outlier test p value is not lower than 0,05. Merging all the datasets as described for the previous parameter returns C10's suspected value not to be recognized anymore as outlier. Indeed the test returns a PV = 0,148 which however is still quite low and labile considering the employed procedure. ANOVA test is therefore applied twice: in case the outlier is removed it returns

PV = 0,361 (SP = 0,42) or PV = 0,226 (SP = 0,23) otherwise, even though in the second case (Tab.37) the requirements for residuals are not well satisfied. Because of the lack of normality in C10 dataset (with the potential outlier), Mann-Whitney test is applied as well (Tab.38): p values never allow null hypothesis rejection (even if for C4-C10 comparison p value is really close to the threshold).

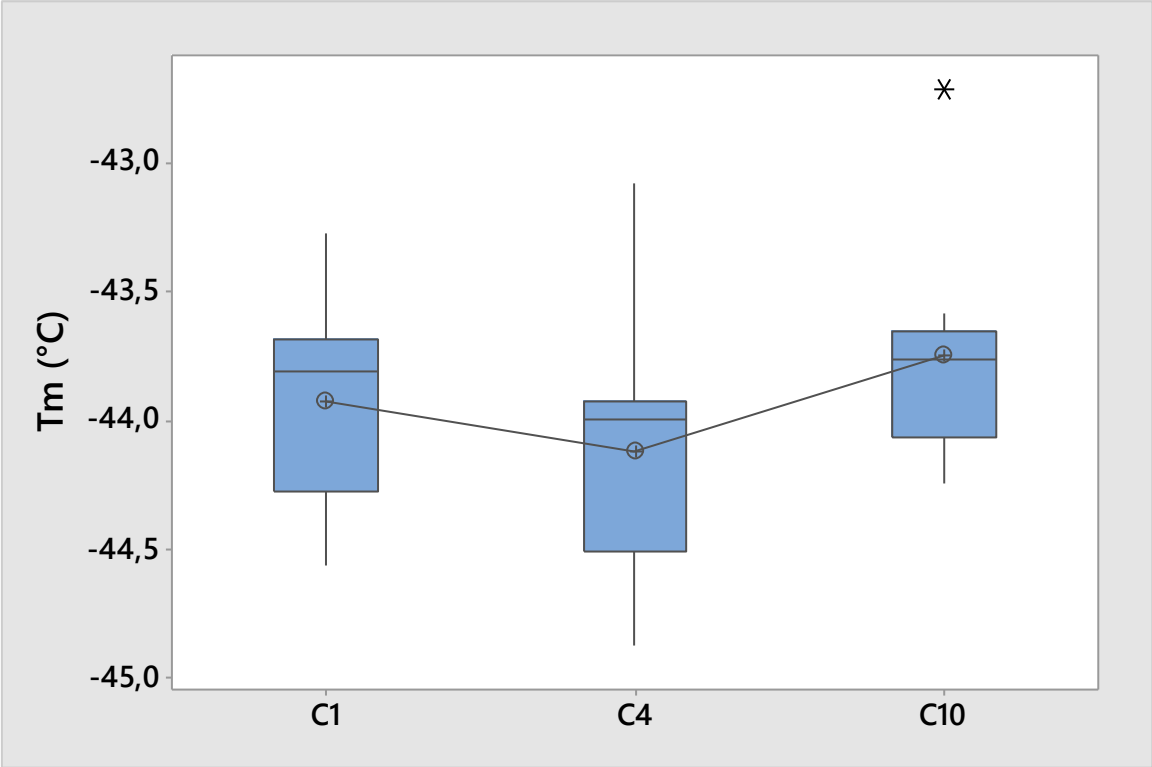

Figure 52. Boxplot comparison among Tm in the three groups. In correspondence of C10 one can notice the asterisk above which suggests the presence of an outlier.

	N	Mean Tm (°C)	StDev (°C)
C1	10	-43,92	0,41
C4	10	-44,12	0,50
C10	10	-43,74	0,42

	MW p value	SP
C1 vsC4	0,212	0,16
C1 vs C10	0,623	0,15
C4 vs C10	0,054	0,42

Table 37 and Table 38. Mean values and standard deviations of Tm (C10's outlier not removed) and statistical analysis (by Mann-Whitney test as C10 dataset with the potential outlier is not normal). In case one employs C10 without the outlier test outcomes are similar to the displayed data, with p values always higher that 0,05.

Finally the analysis of the positive peak in the cooling curve is performed, focusing on transition enthalpy and peak temperature. A preliminary smoothing (0,75° C resolution) is applied for enthalpy calculation as many thermograms report some trembling or small peaks on their left side (Fig.53). Quick attempts demonstrate smoothing with such a resolution does not influence significantly enthalpy calculation for already smooth peak.

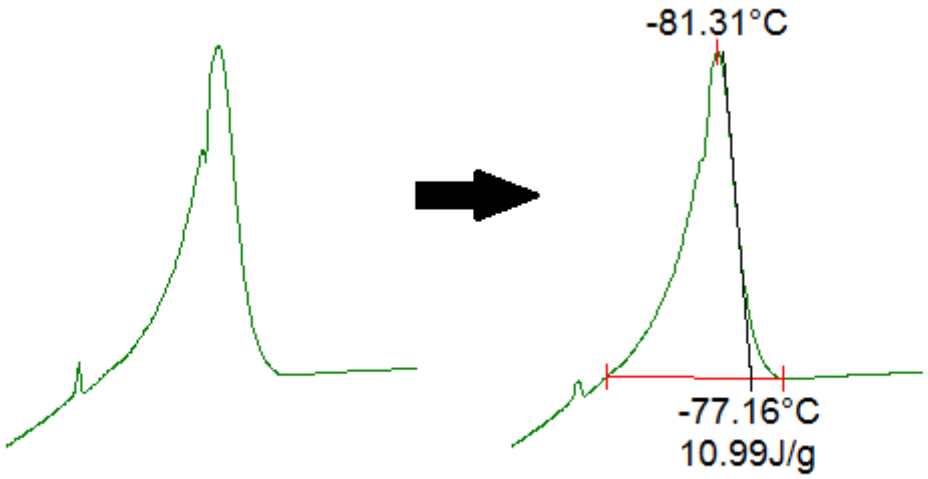

Figure 53. The peak presents some irregularities on its left side (left graph), thus a 0,75° C resolution smoothing is applied in order to obtain a more regular shape (right graph) in correspondence of these elements. Transition enthalpy is calculated as the area of the peak delimited by a horizontal line (aligned with the quite straight line on the right of the peak). As the left extremity of integration is often in correspondence of trembling regions in the cooling curve, the smoothing should help regularize the obtained area.

Firstly peak enthalpy is investigated (Tab.39 and Fig.54) showing variances which are definitely not suitable to be considered equal. ANOVA test is initially applied, returning a p value of 0,044 (SP = 0,59). According to the graph, Etox exposure increases the enthalpy associated with this transition.

	N	Mean (W/g)	StDev (W/g)
C1	10	11,08	0,65
C4	10	11,23	0,15
C10	10	11,50	0,28

Table 39. Mean values and standard deviations for enthalpy associated with the crystallization peak in the cooling ramp.

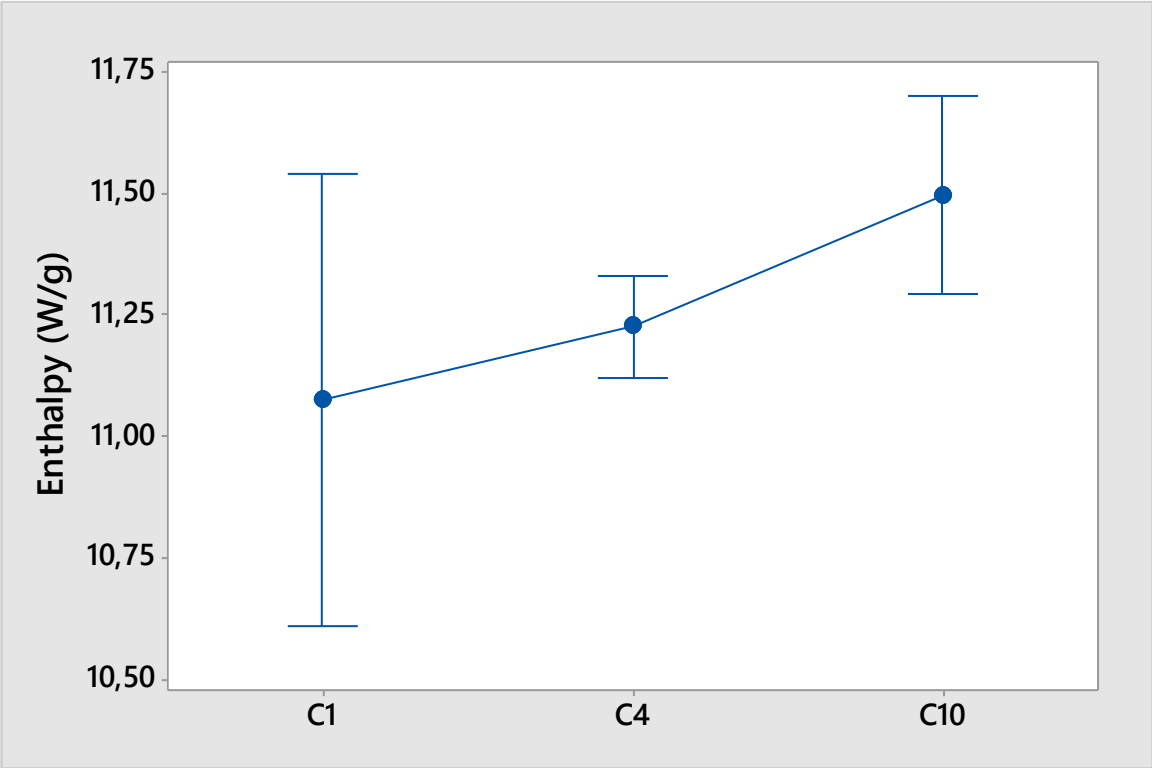

Figure 54. Comparison between C1, C4 and C10 enthalpies associated with the crystallization peak in the cooling curve.

However the strong discrepancies among variances in the residuals of ANOVA suggest to include t-test (Tab.40) in the analysis (datasets are normal). C1 (whose standard deviation is large) and C4 reveal a high t-test p value, meaning the difference in the three datasets may be ascribed also to C10 dataset. In fact t-tests including C10 dataset return p values lower or really close to the threshold, making the strong difference in variances not the only possible reason for low p values. Indeed t-test returning low p values show really

similar p values even when equal variances are assumed and the comparison between C4 and C10 presents a low p value with a considerable SP. Therefore statistical methods confirm what Fig.54 visually suggests: even though C1 and C4 show different variances, they are the only datasets between whom compatibility can be assumed.

	p value	**SP**
C1 vs C4	0,497	0,12
C1 vs C10	0,087	0,47
C4 vs C10	0,019	0,76

Table 40. Statistical analysis results by t-test on enthalpies associated with the crystallization peak in the cooling curve.

Finally the temperature in correspondence of this peak is investigated. As Tab.41 and Fig.55 reveal, this parameter displays strange outcomes: C4 dataset is not compatible with C1 and C10 and furthermore Minitab suggests the presence of two outliers for it. These outcomes do not allow to infer any particular interpretation for the parameter evolution. Obviously ANOVA returns a PV = 0 (SP = 0,95) even though equality among variances and null mean error are barely satisfied.

	N	**Mean (°C)**	**StDev (°C)**
C1	10	-81,74	0,91
C4	10	-83,72	0,76
C10	10	-81,46	1,50

Table 41. Mean values and standard deviations for Tc (cooling curve).

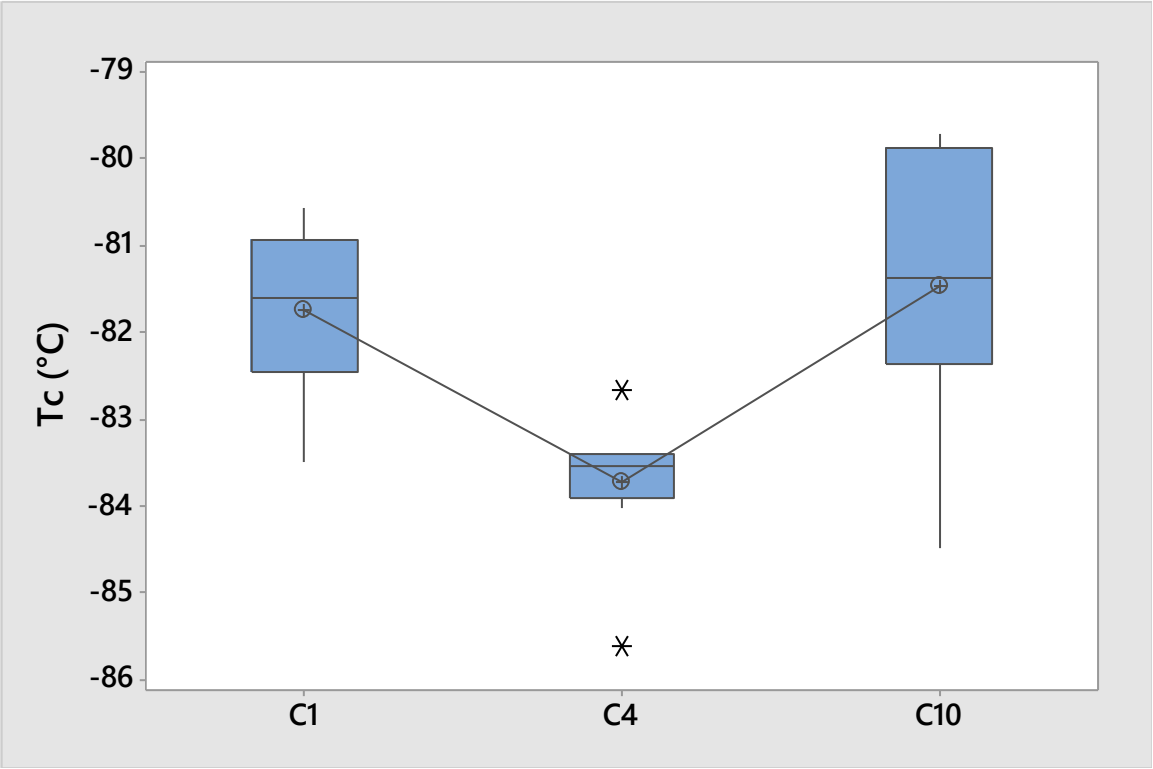

Figure 55. Boxplot comparison of Tc (cooling curve) for C1, C4 and C10 datasets. C4 appears with two outliers and a variance smaller than the other two datasets.

4.5 ATR-FTIR

Spectra acquired by this technique are shown in Fig.56. The graph shows good overlapping, in particular for the three big peaks on the left (790, 1012 and 1259 cm^{-1} respectively) whereas the 2962 cm^{-1} peak appears too weak to infer directly good overlapping. As the differences among the 3 samples for these wavenumbers appear very small in the graph, no alteration may be supposed because eventual changes would be expected to be already visible in this graph. However some parts clearly show trembling and furthermore some discrepancies may be hidden by the employed scale resolution). In order to quantify these potential differences and check spectra overlapping in correspondence of peaks Fig.57 is created. This graph displays the ΔAbsorbance among spectra with respect to wavenumber, with C1 spectrum chosen as reference so that differences between the reference and C4/C10 spectrum can be calculated (their absolute values are reported).

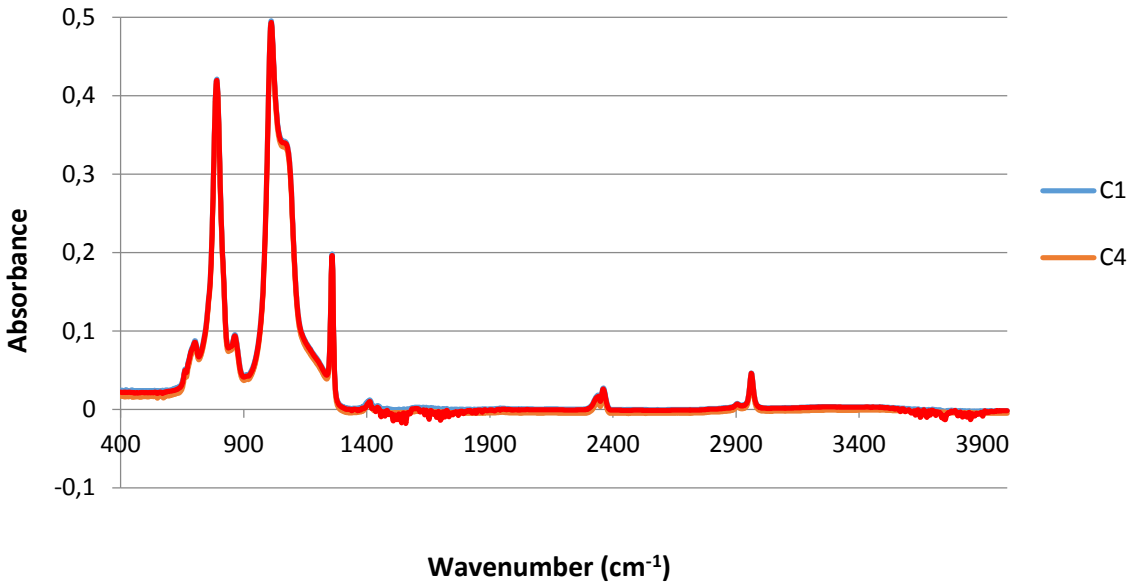

Figure 56. ATR-FTIR spectra for the three samples. The three spectra overlap very well in correspondence of the three strong peaks in the first part of the graph, whereas trembling can be clearly seen in two intervals (2000-1325 cm^{-1} and 3950-3450 cm^{-1}). These parts of the spectra have not to be ascribed to PDMS properties, instead C02 and H_2O are responsible for them. Background acquisition tries to limit as much as possible these undesired contributions which are better contrasted by in vacuum procedure.

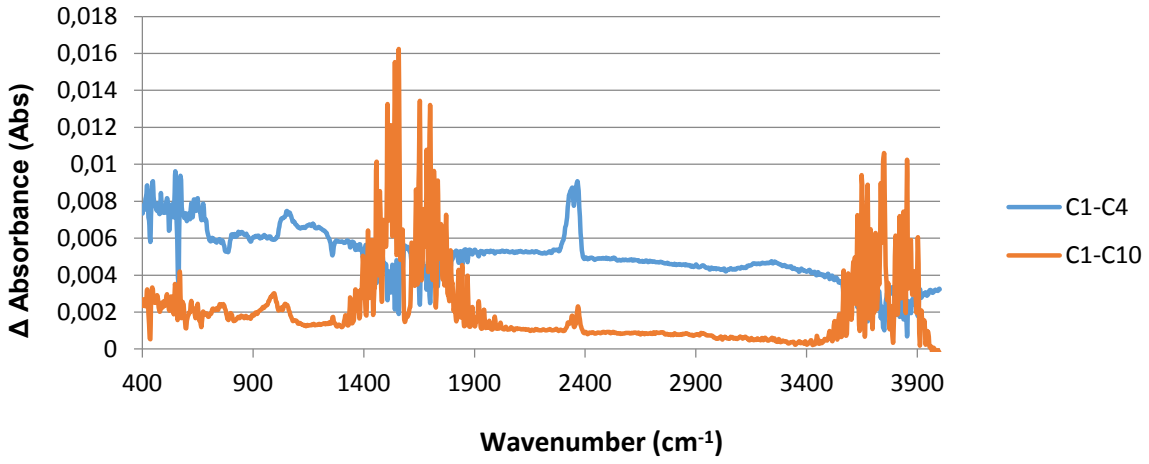

Figure 57. C4 and C10 Absorbances are subtracted from C1 spectrum (taken as reference) and the resulting differences are expressed as absolute values. In addition to the trembling regions at 2000- 1325 cm^{-1} and 3950-3450 cm^{-1}, one may notice the distance (approximately 0,004) between the 2 baselines of this graph.

In this graph 2000-1325 cm^{-1} and 3950-3450 cm^{-1} intervals exhibit the biggest discrepancies and variability. However Fig.56 indicates these parts correspond to almost null Absorbance where no peak is present. In fact this small irregular signal is ascribed to water. Background acquisition prior to sample investigation (which is then subtracted) allows the reduction of such effect, nevertheless a better method is represented by measurements in vacuum. Unfortunately the ATR-FTIR setup available in the department where the analysis is carried out does not incorporate this possibility. Finally also in proximity of 2300-2400 cm^{-1} interval one can see the presence of two-headed peaks. This phenomenon is related to CO_2 which results tricky to avoid completely. In both cases the respective influencing substances are not constant with respect of time (they will be listed in the next lines). Firstly the nature of the peaks and the analysis of the spectrum will be presented, then the comparisons among some peaks will be listed.

Beside of the already mentioned peaks, weaker peaks can be detected: on the sides of the 790 cm^{-1} peak 3 small peaks are visible at 663, 701 and 864 cm^{-1}, whereas the 1075-1055 cm^{-1} interval contain a big peak (approximately 0,34 absorbance) which partially merges with the 1010 cm^{-1} peak (Fig.58 and Fig.59).

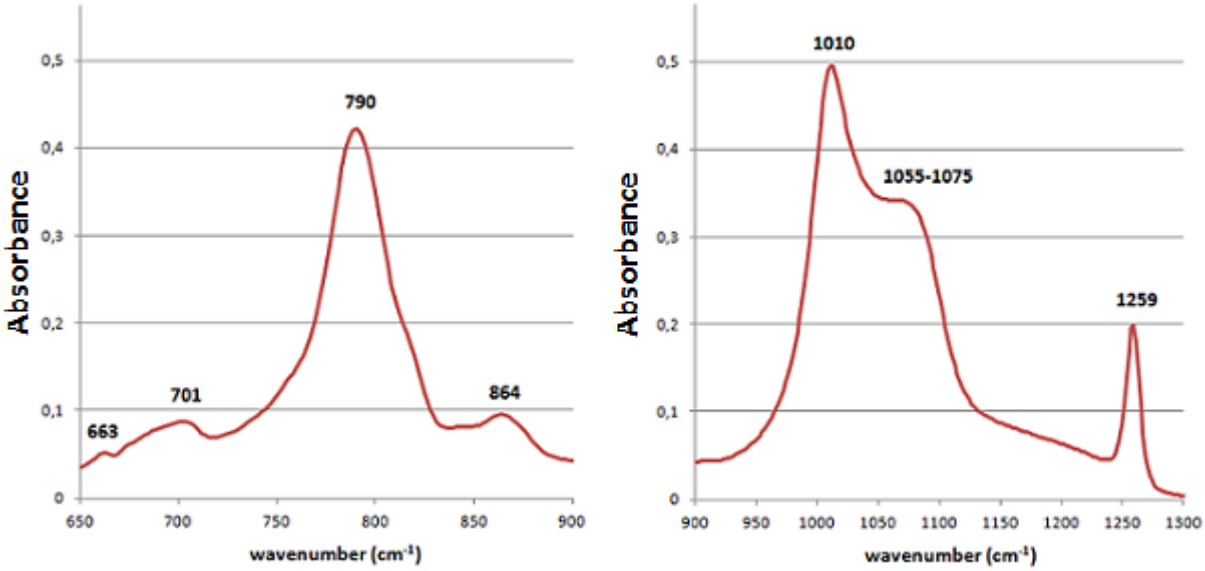

Figure 58 and Figure 59. Particulars of ATR-FTIR spectrum for the C1 sample inside the 1300-900 cm^{-1} and 900-650 cm^{-1} intervals. The greater scale resolution in wavenumber allows to visualize weak peaks around the stronger ones. Peaks which are close each other tend to partially merge or slightly lose their sharpness.

In order to ease the comprehension of the bonds and molecular vibrations mentioned hereafter, Fig.60 (a particular of Fig.5) and Fig.61 are reported.

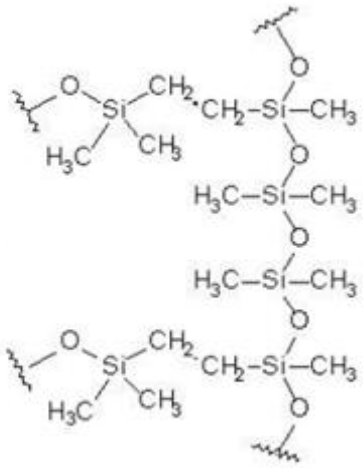

Figure 60. Chemical structure of a generic crosslinked PDMS (obtained by vinyl-functionalized chains) displays the bonds which can contribute to peaks into the FTIR spectrum: Si-CH_3 , Si-O-Si , Si-CH_2-Ch_2-Si , CH_3 , Si$(CH_3)_2$O and their eventual sub-grouping.

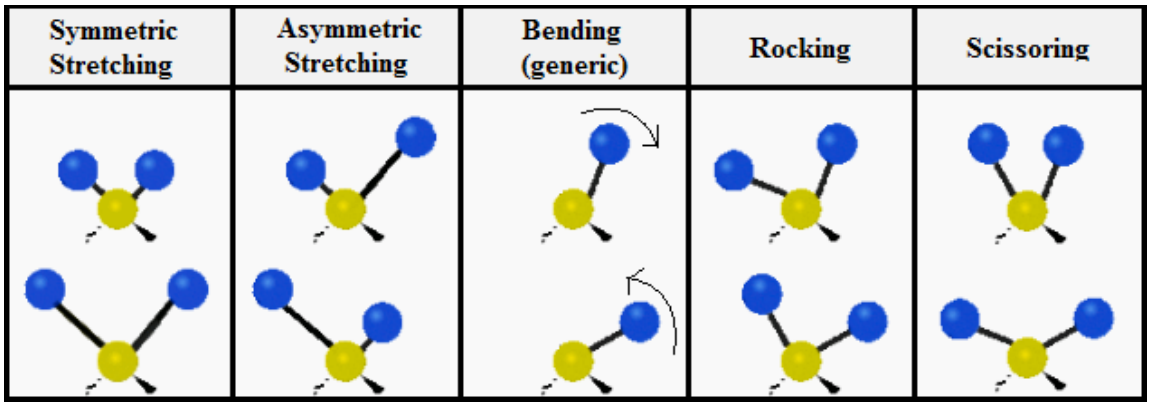

Figure 61. Main molecular vibrations described in the present paragraph. Rocking and scissoring are particular types of bending, in fact many sources generally refer to bond "bending" without specifying exactly which movement is performed (in addition to the already mentioned ones also twisting and wagging exist).

The isolated peak on the right (2962 cm^{-1}) represents the asymmetrical stretching mode in methyl groups (two C-H bonds of the methyl group are extending while the third one is contracting) [44]. Si-CH_3 can be recognized by the sharp peak at 1259 cm^{-1} which generally appears together with another one or more strong peaks included within the 865-750cm^{-1} interval [45]. In this case this description matches the high 790 cm^{-1} peak. A weak 860 cm^{-1} peak is indicated as effect of $Si(CH_3)_2O$ [45], indeed a small peak can be seen (then slightly shifted) at 864 cm^{-1}.

Siloxanes can be recognized in general by the 1300-1000 cm^{-1} interval in their spectrum. In fact Si-O-Si (mainly due to its stretching) entails one or more very strong peaks (1010 cm^{-1} peak) inside this range. However the longer and more branched the chains are, the more superimpositions appear and the more complex this part of the spectrum gets. Disiloxanes structure (R-Si-O-Si-R) are pointed to generate a signal in 1080-1040 cm^{-1} whereas 1110-1050 cm^{-1} can be related to Si-O-C stretching [45,46]. On the right side of the highest peak one may indeed notice the presence of another peak (or even more) around 1055-1075cm^{-1}. This spectrum shape is in accordance with what previously found in FTIR analysis literature. One may suspect the presence of something else between the 1075-1000 cm^{-1} band and the 1259 cm^{-1} peak as the spectrum does not reach the null value immediately showing a bend instead (approximately at 1125 cm^{-1}). Indeed the 1350-1150 cm^{-1} interval is reported to express out-of-plane bending of CH_2 (wagging and twisting). Thus probably some weak bands (absorbance < 0,1) superimpose to the spectrum in the 1250-1100 cm^{-1} interval [44].

The wavenumbers listed so far do not include the 2 weak and unsharp peaks on the left side of the spectrum and the previously mentioned trembling already ascribed to H_2O and CO_2. Indeed trembling in 3950-3450 cm^{-1} can be explained by the symmetrical (3652 cm^{-1}) and asymmetrical (3756 cm^{-1}) stretching by H_2O, whereas trembling in 2000- 1325 cm^{-1} is generated by H_2O scissoring (1596 cm-^{1}) and CO_2 symmetrical stretching (1340 cm^{-1}). The small peak at 661 cm^{-1} and the small two-headed group (2341 and 2360 cm^{-1}) can be explained by CO_2 scissoring (665 cm^{-1}) and CO_2 asymmetrical stretching (2350 cm^{-1}) [44].

Then the only peak still lacking of explanation is at 701 cm^{-1}. Literature lists methyl rocking (730 cm^{-1}) and CH_2 rocking (720 cm^{-1}) peaks occurring close to the recorded peak. However these values do not correspond exactly to the reported wavenumber in the spectrum, even if the proximity with other peaks (with partial merging as possibility) may

induce a 20 cm^{-1} shift. Another possible interpretation resides in the *Cis*-CH out-of-plane bending for alkenes presented as a wide peak at 700 cm^{-1}. The description of the peak perfectly matches the recorded spectrum even if Fig.60 does not display any C=C bond. However the reaction reported in Fig.5 shows how the siloxane oligomers present carbon-carbon double bond extremities which are used to connect to the crosslinking agent. Then if some oligomers remain unchained at one extremity (or they remain completely unchained exhibiting two free extremities instead of only one) they keep the C=C bond (it does not turn into a single bond) which allows the CH vibration previously described.

Wavenumber (cm-1)	**Appearance**	**Bond**
661	weak peak	CO2
701	weak peak	CH in C=C
790	strong peak	Si-CH_3
864	weak peak	$Si(CH_3)_2O$
1010	strong peak	Si-O-Si
1080-1040	hidden peak	R-Si-O-Si-R ; Si-O-C
1125	hidden peak	CH2
1259	strong peak	Si-CH_3
2000-1325	trembling	H_2O, CO2
2360-2341	two-headed weak peak	CO2
2962	weak peak	CH_3
3950-3450	trembling	H_2O

Table 42. Summary of the listed recognized bonds with the description of their appearance and related wavenumber.

Fig.57 does not give any idea about the relative magnitude of the spectrum differences (the ratio between difference and spectrum value for a certain wavenumber). As the elements this analysis focuses mainly on are spectrum peaks, the differences in correspondence of the main ones are divided by the respective C1 peak's value (Tab.43). This way the dissimilarities among peaks can be better estimated instead of dividing all the discrepancies by a unique value.

wavenumber (cm^{-1})	C1 Absorbance	ratio C1-C4 (%)	ratio C1-C10 (%)
790	0,419	1,260	0,372
1010	0,493	1,232	0,462
1259	0,194	2,621	0,833
2962	0,043	10,081	1,702

Table 43. The 4 strongest peaks in the spectra are investigated. C1, C4 and C10 values are measured in correspondence of each peak and the difference between C4 or 10 and C1 (reference) are divided by C1.

The three strong peaks (the first three ones) report a variation percentage lower than 3 % (and often even 1%) so that this step confirms what already inferred from Fig.56 where the three spectra seem to overlap. However the fourth and small peak at 2962 cm^{-1} displays a 10% change with respect of C1. This value may be considered relevant or still insufficient to assess a change depending on some interpretations. Indeed 10% generally represents a value which should not be neglected, however part of this difference may be ascribed to the distance between C1 (similar to C10) and C4 baselines. A certain gap lasts for the whole wavenumber axis (approximately 0,006 in the left part of the graph and 0,04 in the right one), in particular on the two sides of the fourth peak (3100-3000 and 2900-2800 cm^{-1}) its mean value equals 0,0044 (calculated by the differences between C1 and C4 spectra in these ranges). The gap between C1 and C10 at 2062 cm^{-1} results 0,0043 which equals the average gap between the two baselines on the sides. Then this difference should be ascribed mainly to this reason.

One may claim the same procedure should be repeated for the other peaks as the same factor may influence the estimation of the overlapping. However before doing that the relevance of peak intensity has to be underlined: the reported change variation is weighted more for weaker peaks with respect to stronger peaks when the gap between C1 and C4 curves for instance is the same (ratio with lower denominator).

For each peak the intervals on their sides are analyzed: absorbance values belonging to quite horizontal portions (approximately 20-50 cm^{-1} long) are averaged and the mean value between the two sides is taken as local baseline gap. This value is compared with curve difference in correspondence of the respective peak (peaks related to CO_2 or H_2O are not included here), with a 0,005 absorbance difference between them proposed as threshold

value. Results of this method are presented in Tab.44. This approach (which consists in a "local baseline shift") aims to separate potential contribution by the baseline gap from actual induced changes, however it fails in demonstrating a possible change as all the differences between local gaps and spectrum distances results to be between 0,1 % and 1 % which are values definitely too low to take into account a reliable and influencing change.

Wavenumber (cm-1)	**Peak intensity**	**C1-C4 diff.**	**C1-C10 diff.**	**local gap C1-C4**	**local gap C1-C10**	**chemical group**	**potential change**
702	0,088	0,0059	0,0018	0,0066	0,0022	CH in C=C	no
791	0,421	0,0054	0,0016	0,0061	0,0020	$Si\text{-}CH_3$	no
864	0,096	0,0062	0,0017	0,0062	0,0018	$Si(CH_3)_2O$	no
1011	0,495	0,0061	0,0023	0,0064	0,0016	Si-O-SI	no
1055-1063	0,342	0,0074*	0,0022*	0,0064	0,0016	R-Si-O-Si-R ; Si-O-C	no
1065-1074	0,341	0,0073*	0,0018*	0,0064	0,0016	R-Si-O-Si-R ; Si-O-C	no
1259	0,198	0,0051	0,0017	0,0062	0,0014	$Si\text{-}CH_3$	no
2962	0,047	0,0043	0,0007	0,0044	0,0007	CH_3	no

*Table 44. As already mentioned each wavenumber (or wavenumber interval) refers to a specific molecular vibration in a chemical group (seventh column). For each wavenumber the differences among the three spectra (C1 in the second column is taken as reference) are listed in the third and fourth columns, whereas the fifth and sixth ones report the baseline gap obtained by the procedure described in this paragraph (* = mean value in the indicated wavenumber interval). Changes might be suspected* (last column**)** *when the differences between spectra differences and local gaps exceed 0,005 (10% of the absorbance in weakest peak reported in the table).*

4.6 Wettability test

Tab.45 shows the variation of mean contact angles depending on the time and type of samples. C1 and C4 samples present slightly different values, with standard deviations often lower than 2,5°. In contrast, values in the third column are very different from the previous ones, even though the standard deviation is sometimes beyond 4°. This difference suggests a lower surface hydrophobicity independently of time instant, as evidenced by Fig.62. In particular this graph indicates the difference in mean contact angles should

increase with time ($\Delta\theta_{max}$_0s = 3,42 ; $\Delta\theta_{max}$_120s = 5,95). Other two graphs (Fig.63 and Fig.64) displays mean values and standard deviations for 0 s and 120 s only.

Statistical analysis focuses only on initial contact angles (t = 0 s) and final ones (t = 120 s). According to the large number of values the Anderson-Darling Normality test is performed, confirming the normality in the distributions. Null hypothesis in the F-test is rejected only when comparing C4 and C10. For this comparison t-test with unequal variances is performed, whereas t-test with equal variances is chosen otherwise (Tab.46).

	1 Cycle (N=17)		4 Cycles (N=21)		10 Cycles (N=13)	
Time (s)	**Mean Angle (°)**	**StDev (°)**	**Mean Angle (°)**	**StDev (°)**	**Mean Angle (°)**	**StDev (°)**
0	116,29	1,78	115,67	1,63	112,87	2,81
30	99,38	1,69	98,44	2,28	94,83	4,38
60	97,46	1,73	96,32	2,42	92,45	4,15
90	96,01	1,90	94,61	2,6	90,59	3,96
120	94,59	2,26	92,94	2,73	88,63	3,73

Table 45. Contact angles (mean values and standard deviations) according to the time elapsed before recording the parameter and the number of cycles the material was exposed to.

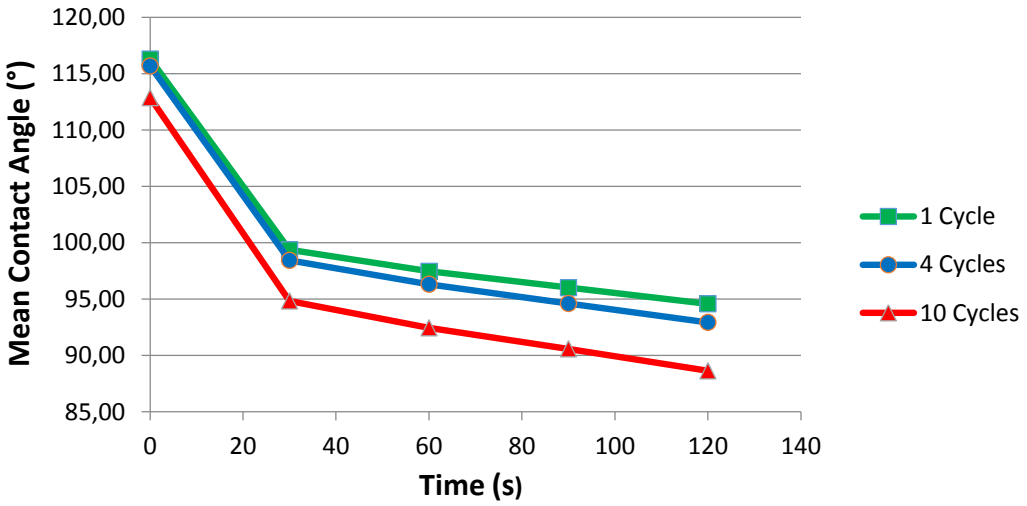

Figure 62. Mean contact angle evolutions with respect to contact time for the 3 classes of material. The 3 curves exhibit similar trends even though the gap between them is displayed to increase with time.

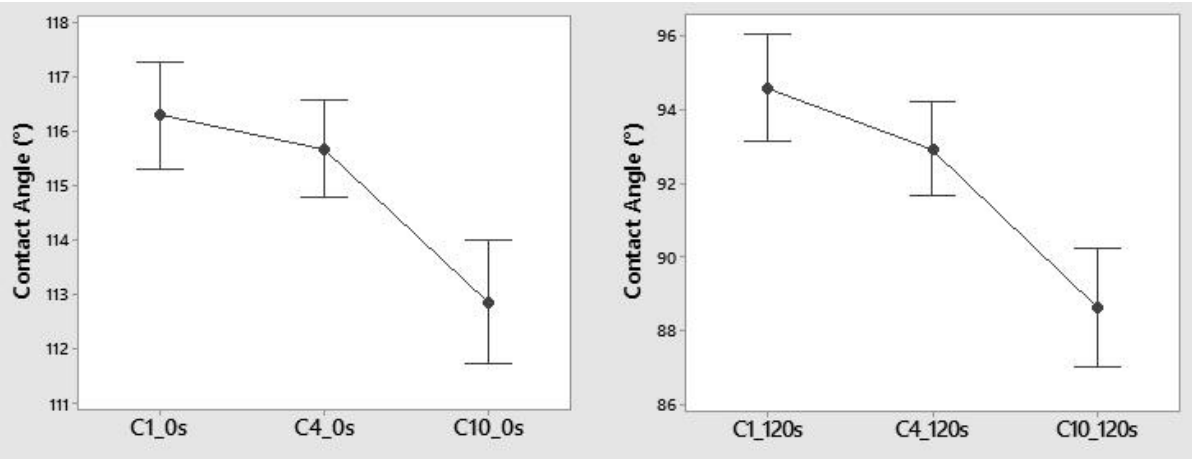

Figure 63 and Figure 64. C1, C4 and C10 contact angles immediately after contact with the material surface (0s) and after 120 s. Standard deviations are here included as their presence would make Fig.62 difficult to read.

As summarized in Tab.46, samples sterilized 10 times by Etox are different from the other two categories: the p value is lower than 0,05 and statistical power is 0,95 at least. In contrast, 4 cycles samples do not differ appreciably from those sterilized once even if after 120 s the p value results close to 0,05. However in this case statistical power results lower than the previous cases, in particular for the comparison at 0 s.

These results confirm how a good number of samples (approximately 20) is not totally effective when differences between mean values are lower than standard deviations. For instance Minitab estimates 119 samples to have a 0,8 power with a 0,62° difference and average standard deviation of 1,7°. Finally ANOVA tests confirm the difference among the three groups returning a null p value for both 0s and 120s. Following analyses demonstrate the 4 assumptions on residuals to be satisfied, meaning that the outcomes of ANOVA tests are reliable (SP > 0,95).

Test	P-value	Power
t-test C1-C4_0s	0,278	0,21
t-test C1-C4_120s	0,057	0,51
t-test C1-C10_0s	0	0,97
t-test C1-C10_120s	0	1
t-test C4-C10_0s	0,004	0,95
t-test C4-C10_120s	0,002	0,95

Table 46. P values and statistical powers for t-test employed with 0 s and 120 s contact angles.

4.7 Swelling test

A preliminary analysis of the data evidences how C4 distribution does not spread as a Gaussian (according to Shapiro-Wilk test), suggesting the presence of a possible outlier. Graphical summary of C4 distribution for 1 week immersion well evidences how one value is quite different from the others (Fig.65A). Since mean value in C4 distribution without this potential outlier results similar to C1, graphical summary is repeated by adding C1 values to C4 group (Fig.65B) and also C10 (Fig.65C). In fact even if C10 has higher swelling ratios than C1 and C4 (once the potential outlier is removed), these values are much lower than C4's outlier.

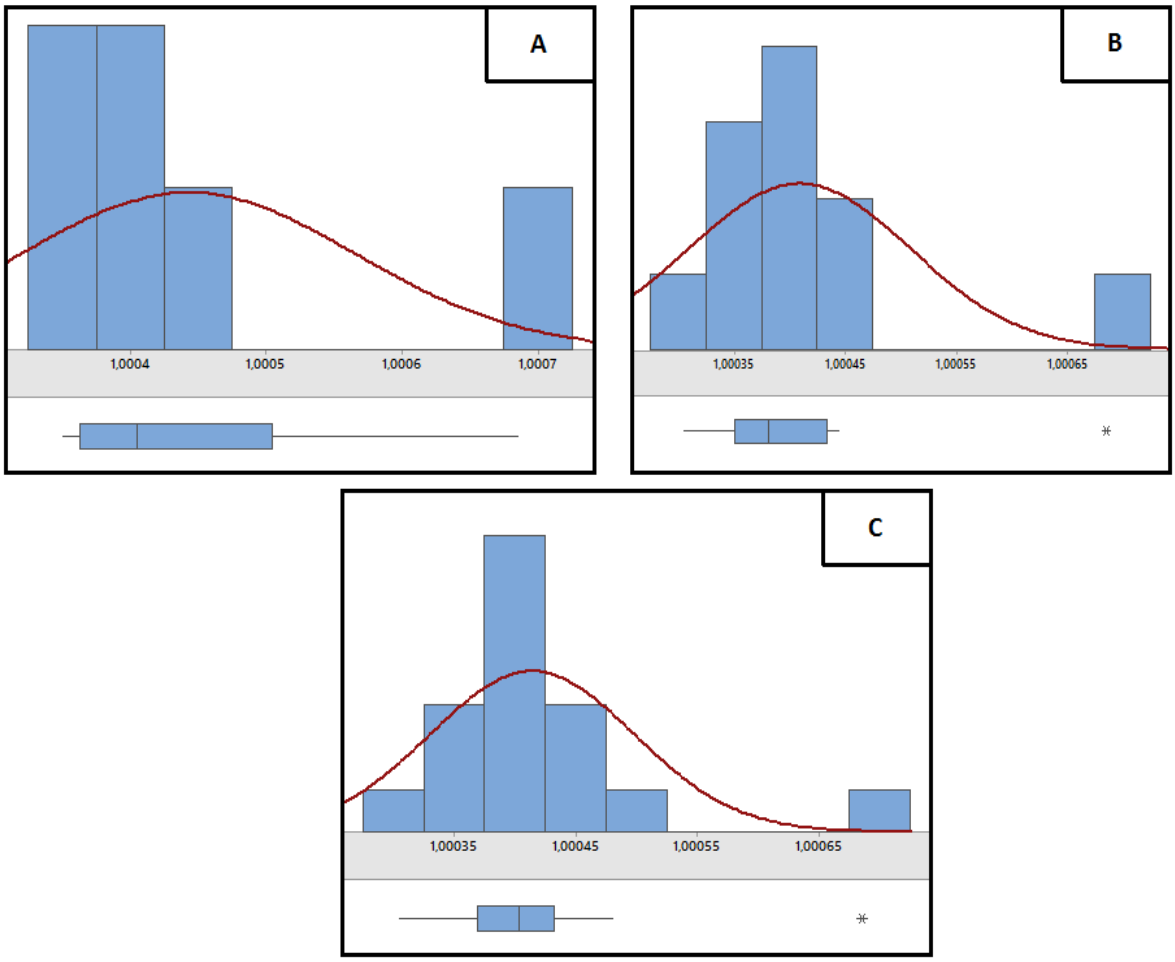

Figure 65. Graphical summaries of 1 week data related to C4 dataset (A), C1 and C4 together (B) and all the datasets together (C). This Minitab's feature displays the occurrence (height of the column) of a specific value (horizontal axis) for the analyzed parameter (Swelling Ratio in the present case). In the first case (A) the small number of samples does not allow the assessment of the outlier on the right side, whereas the other 2 graphs (B, C) better reveal the potentiality of this value as outlier (displayed as an asterisk).

Furthermore the function “Outlier Test” in Minitab (Fig.66) can confirm this interpretation by reporting a p value associated with the null hypothesis “the largest data is not an outlier”. Many outlier tests are available: Grubb’s test is not useful as normality is required, whereas Dixon’s test (Q-test) is indicated for sample size lower than 7. The calculated p value results 0,007. Then the same approach is used by merging C4 with C1 (Dixon’s r21 ratio test) and also C10 (Dixon’s r22 ratio test). These new outlier tests are reported to be more effective according to the sample size of the new investigated groups. They return 0,003 and 0,000 respectively as p values (Fig.66). Thus the outlier in C4 can be ignored according to test outcomes.

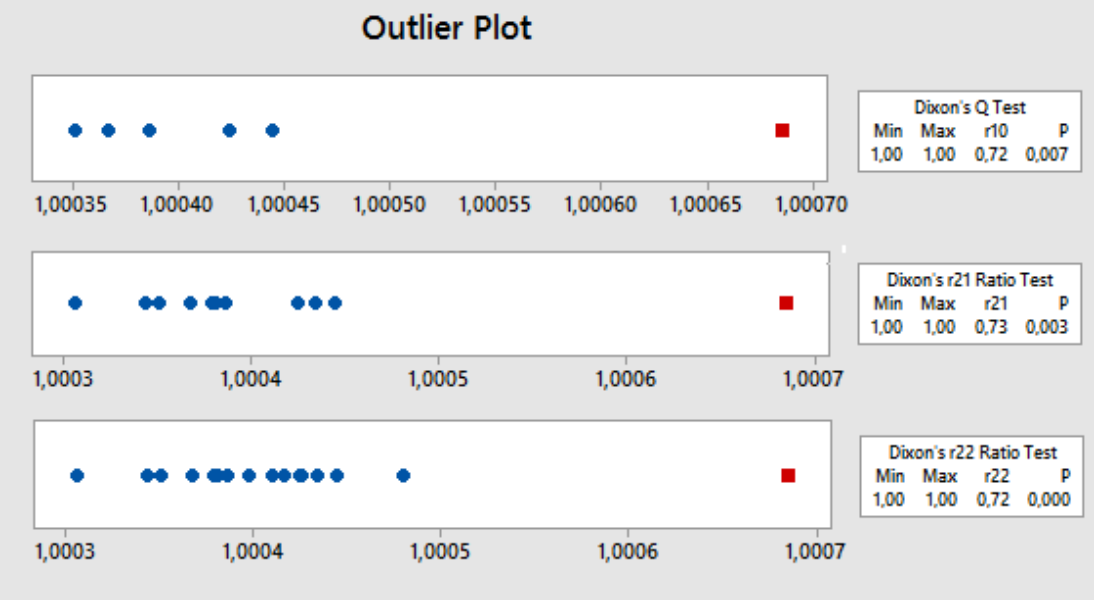

Figure 66. Comparison among the three outlier tests which analyze an increasing number of samples (as done in Fig.65). P value progressively decrements in accordance with what graphical summaries suggested before.

Swelling ratios for the different categories according to the immersion time are listed in Tab.47 whereas Fig.68, Fig.69 and Fig.70 display the comparisons for a set swelling time. Finally Fig.67 reports the average values for the 3 material with respect to the number of weeks (standard deviations are not reported, instead they are shown in Fig.68, Fig.69 and Fig.70).

	N	Mean Ratio (-)	StDev (-)
C1_1w	5	1,00037	0,00005
C4_1w	5	1,00039	0,00004
C10_1w	5	1,00043	0,00003
C1_2w	5	1,00026	0,00005
C4_2w	5	1,00033	0,00003
C10_2w	5	1,00035	0,00004
C1_9w	5	1,00010	0,00005
C4_9w	5	1,00018	0,00004
C10_9w	5	1,00011	0,00003

Table 47. Mean values and standard deviations for the Swelling Ratios after the outlier has been removed. 1w, 2w and 9w refer respectively to 1, 2 and 9 weeks of immersion of the sample into water.

As mentioned in the chapter dealing with statistical analysis (paragraph 3.3) comparisons related to a certain sample with respect to its time evolution rely on dependent datasets. However in this test comparisons are established for different samples at the same immersion time, then Paired Test is not required.

Mean values suggest 1 week Swelling Ratio to be proportional to Etox exposure as C10 samples absorb more water than C4 and C1 ones. This behavior may be expected as it recalls the results in wettability test, where increasing Etox exposure appears to lower surface hydrophobicity. Fig.67 reveals also how all the Swelling Ratios at the end of the second week are lower than those after 1 week. This behavior in such an experiment does not surprise as PDMS curing is a process unable to achieve 100% crosslinking and at least 5% of PDMS bulk remains uncrosslinked. These oligomers are generally low molecular weight species free to diffuse out of PDMS. During leaching tests or simply submerging the material, they diffuse from the bulk to surface [47], resulting in a decrement of the scaled weight (with respect to the 1 week swollen state). Also in this case C10 mean value is the highest, however C1 value exhibits a steeper decrease with respect to the other two material groups. Finally after 9 weeks one can notice how C4 results the group with the highest mean value, whereas C1 and C10 have comparable results. Similarly to what is

seen after 2 weeks, all the groups display a decrease in Swelling Ratios with respect to the previous weeks.

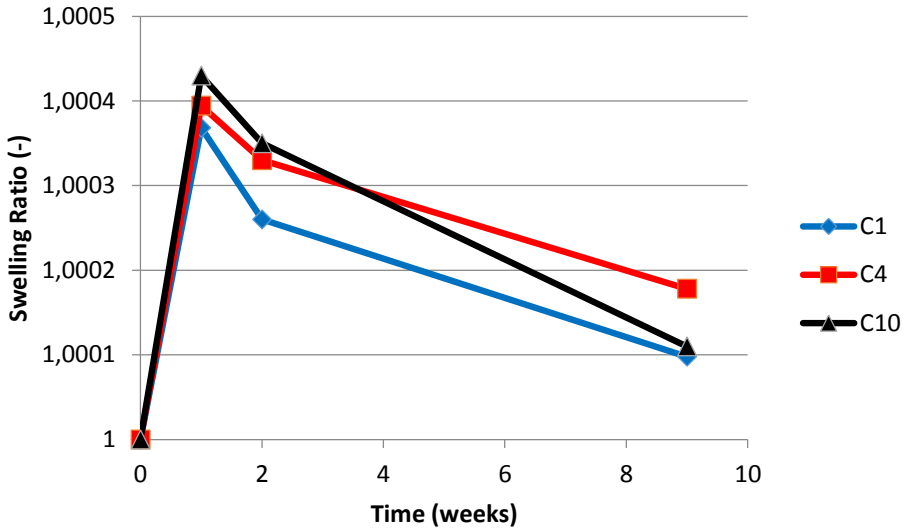

Figure 67. Swelling Ratios of the materials with respect to the weeks elapsed after first immersion. The values referring to 1 and 2 weeks reflect wettability test outcomes, where samples exposed to more sterilization cycles exhibit lower hydrophobicity. On the ninth week however C10's mean Swelling Ratio is displayed within C1 and C4's values.

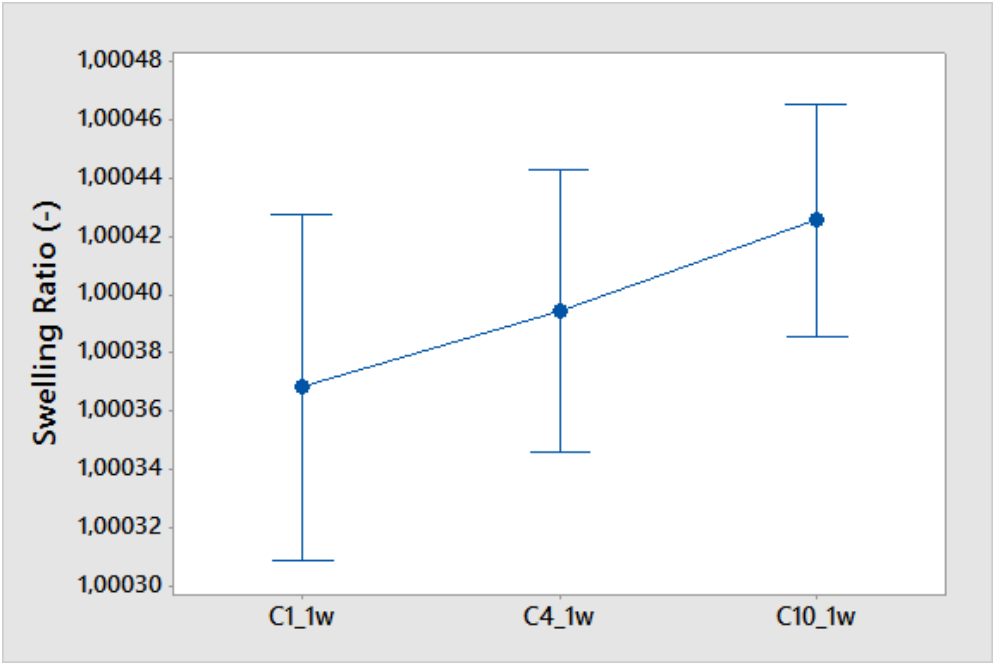

Figure 68. Comparison among the Swelling Ratios for the 3 materials after 1 week immersion.

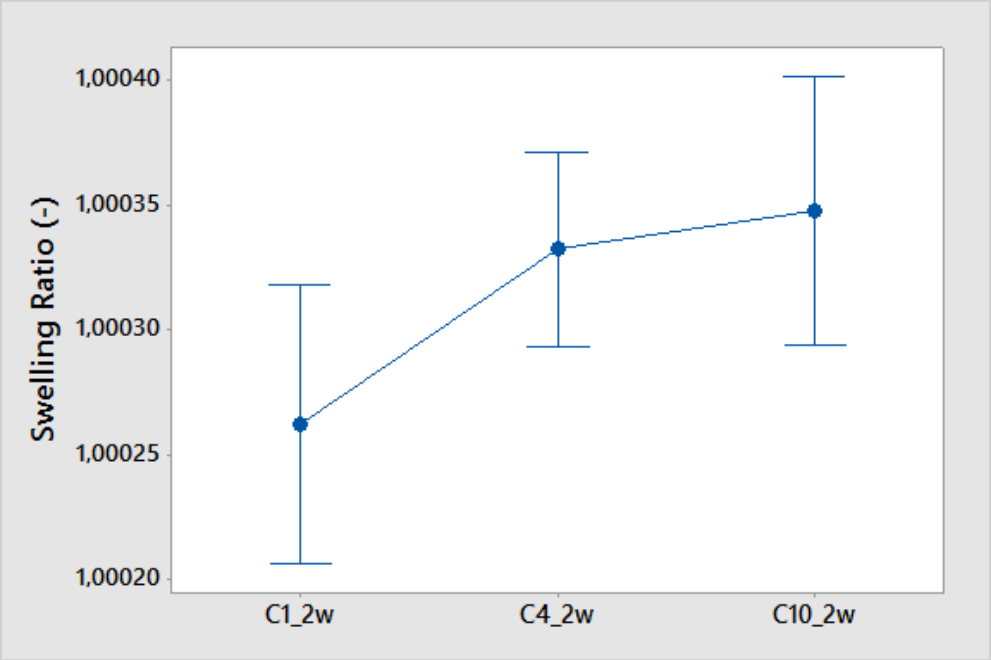

Figure 69. Comparison among the Swelling Ratios for the 3 materials after 2 week immersion.

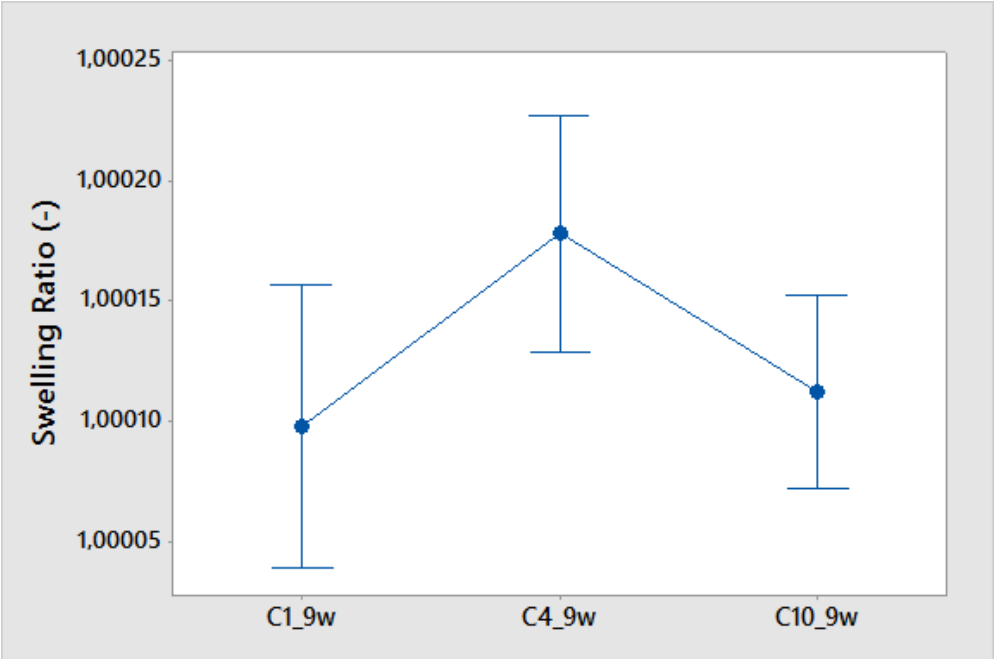

Figure 70. Comparison among the Swelling Ratios for the 3 materials after 9 week immersion.

Dealing with statistical analysis (non parametric methods), null hypothesis in Mann-Whitney test (Tab.48) is always accepted for samples which undergo 1 week immersion (even if p value is next to 0,05 for C1-C10). However the other cases often display the rejection of the null hypothesis together with high statistical power. ANOVA test is performed as well (Tab.49) since the requirements for its application are satisfied. Also in this case the values related to 1 week immersion result insufficient to reject the null hypothesis. On the other hand ANOVA tests for 2 and 9 week immersions return the rejection of null hypothesis with high statistical powers.

	pvalue_1w	**power_1w**	**pvalue_2w**	**power_2w**	**pvalue_9w**	**power_9w**
C1-C4	0,403	0,13	0,022	0,72	0,095	0,72
C1-C10	0,095	0,58	0,022	0,81	1,000	0,07
C4-C10	0,296	0,28	0,676	0,12	0,037	0,63

Table 48. Statistical analysis for 1, 2 and 9 week samples (by Mann-Whitney non parametric test).

	p value	**power**
ANOVA_1w	0,119	0,48
ANOVA_2w	0,013	0,81
ANOVA_9w	0,019	0,70

Table 49. ANOVA test for 1, 2 and 9 week immersions. SP results high for the second and third cases.

Beside of these statistical results normality cannot be assessed for C4_9w dataset as four values result to spread around 1,00016 value and the fifth one equals 1,00025. Outlier test in these cases is worthless and generally misleading because another outlier test has already been applied previously, then the same procedure is not performed. This fifth value may not be considered anyway responsible of C4 Swelling Ratio being greater than C10. In fact even without this value the mean Swelling Ratio would result to be higher than 1,00015.

4.8 In vitro cytotoxicity testing

Optical microscope observations are illustrated in the following pages (Fig.71, 72, 73, 74). Fig.71 reports the optical image of the L929 cells seeded in fresh DMEM (no incubation phase with PDMS samples but direct culture with cells) for 24 hours which represents a first term of comparison.

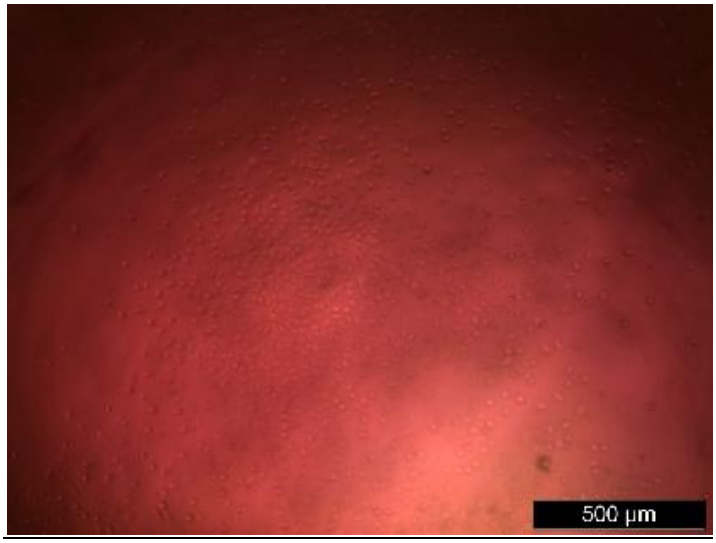

Figure 71. Optical image of 24-hours cultured cells with fresh DMEM (no contact with PDMS substrates).

Fig.72, 73 and 74 illustrate L929 cells seeded in DMEM incubated for 3 hours, 1 and 3 days respectively. As mentioned in the test description, in each case cells are cultured for 24 hours with the same cell density. In the right columns cells seeded in DMEM incubated with PDMS are displayed, whereas the left column shows the L929 fibroblasts cultured in DMEM which did not get in contact with PDMS. The reported images are only those of cells adherent onto the bottom wells in which L929 cells were cultured with the eluates obtained by the contact with the three types of sterilized PDMS samples for 3 hours, 1 and 3 days. According to these images acquired by optical microscope, the laboratory report that they qualitatively demonstrate all the PDMS samples considered in the in vitro indirect cytotoxicity test to be not cytotoxic. Thus no difference among samples seems to exist. Furthermore it is said that acquired images show a good cell adhesion, with the absence of dead cells in any culture well. Nevertheless this result is merely qualitative, lacking the quantitative detection of differences (a colorimetric assay would allow that instead).

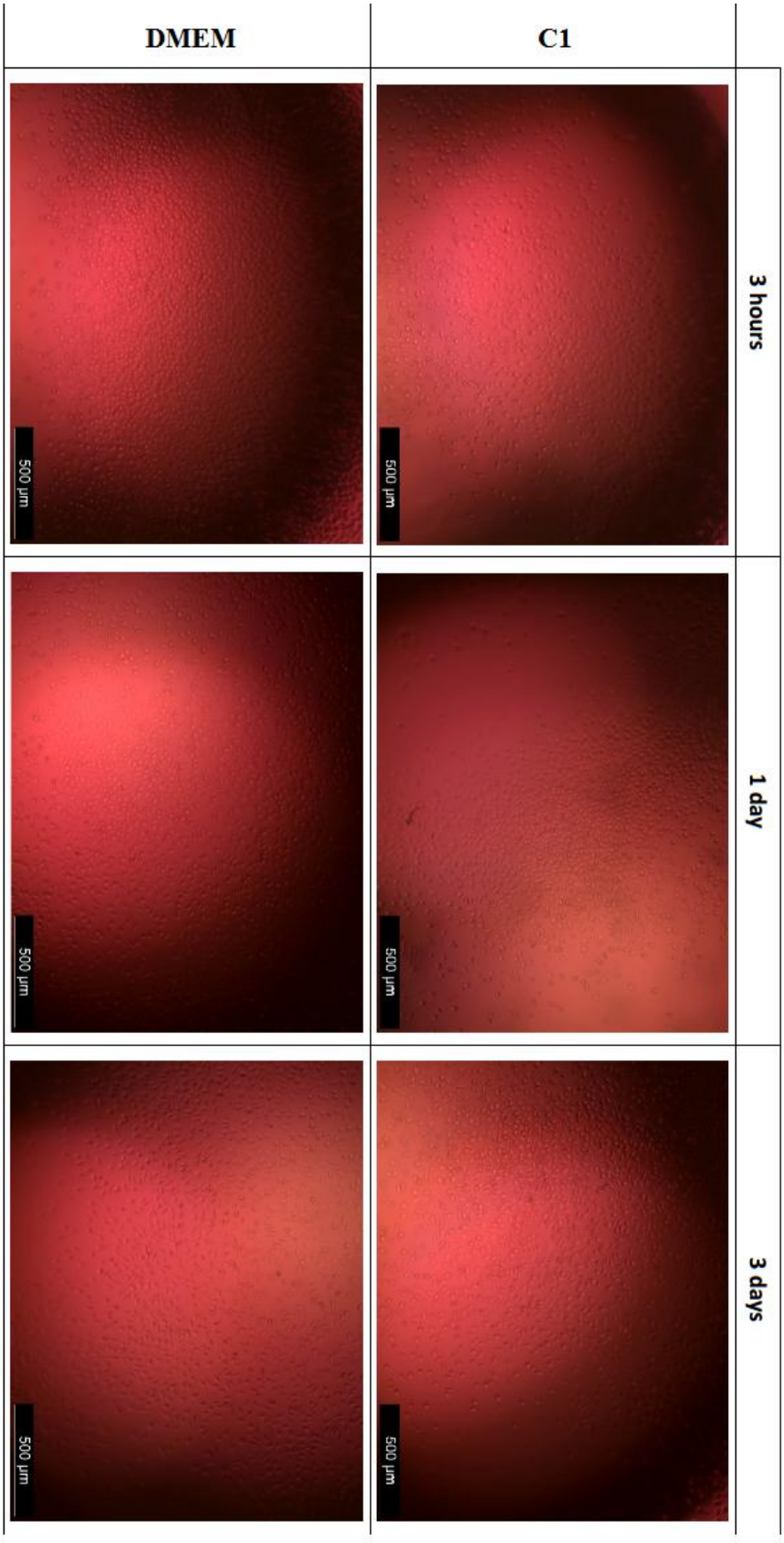

Figure 72. Optical microscope images of L929 cells seeded in the C1 eluate (C1-3h, C1-1d, C1-3dd) for 24 hours.

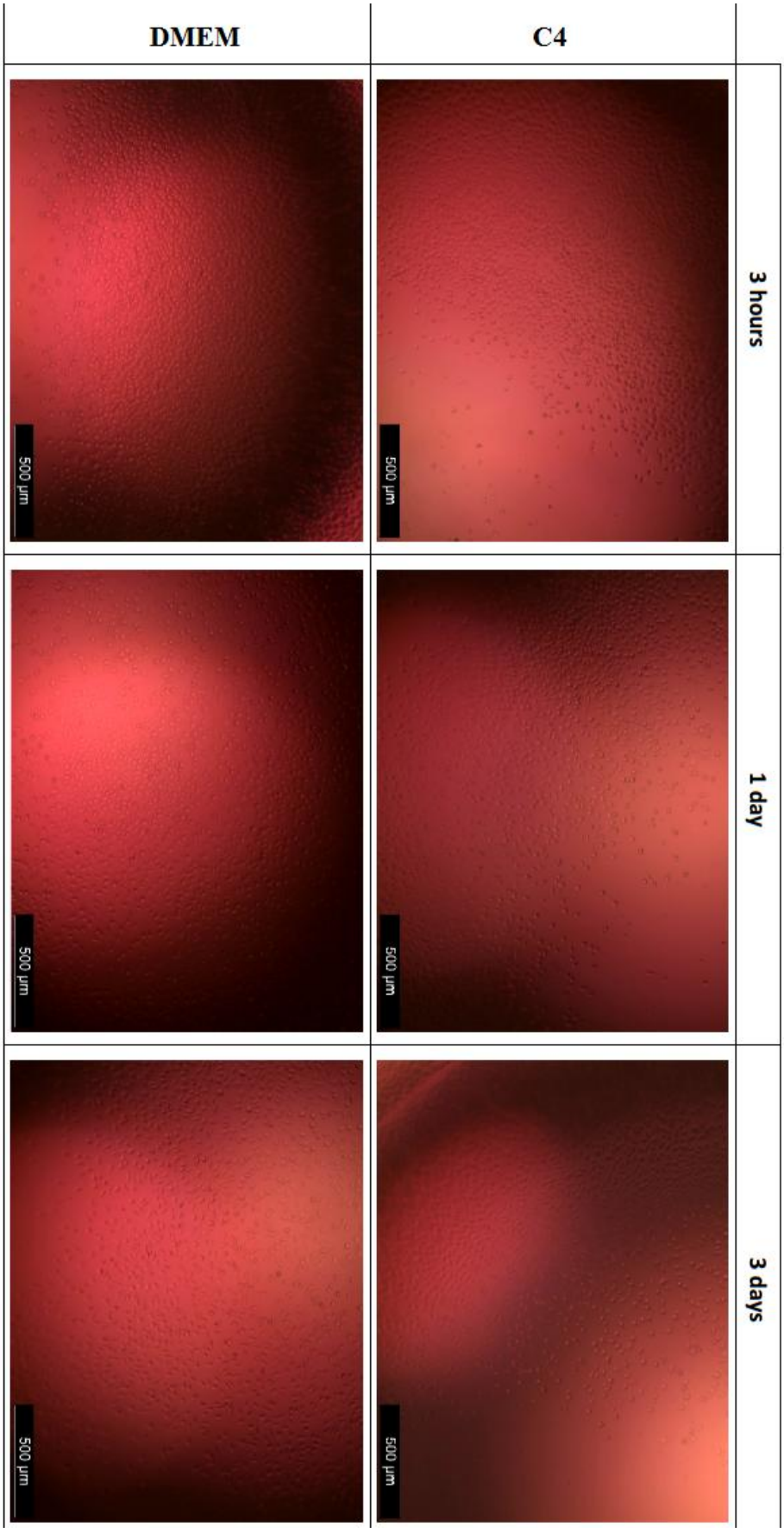

Figure 73 Optical microscope images of L929 cells seeded in the C4 eluate (C4-3h, C4-1d, C4-3dd) for 24 hours.

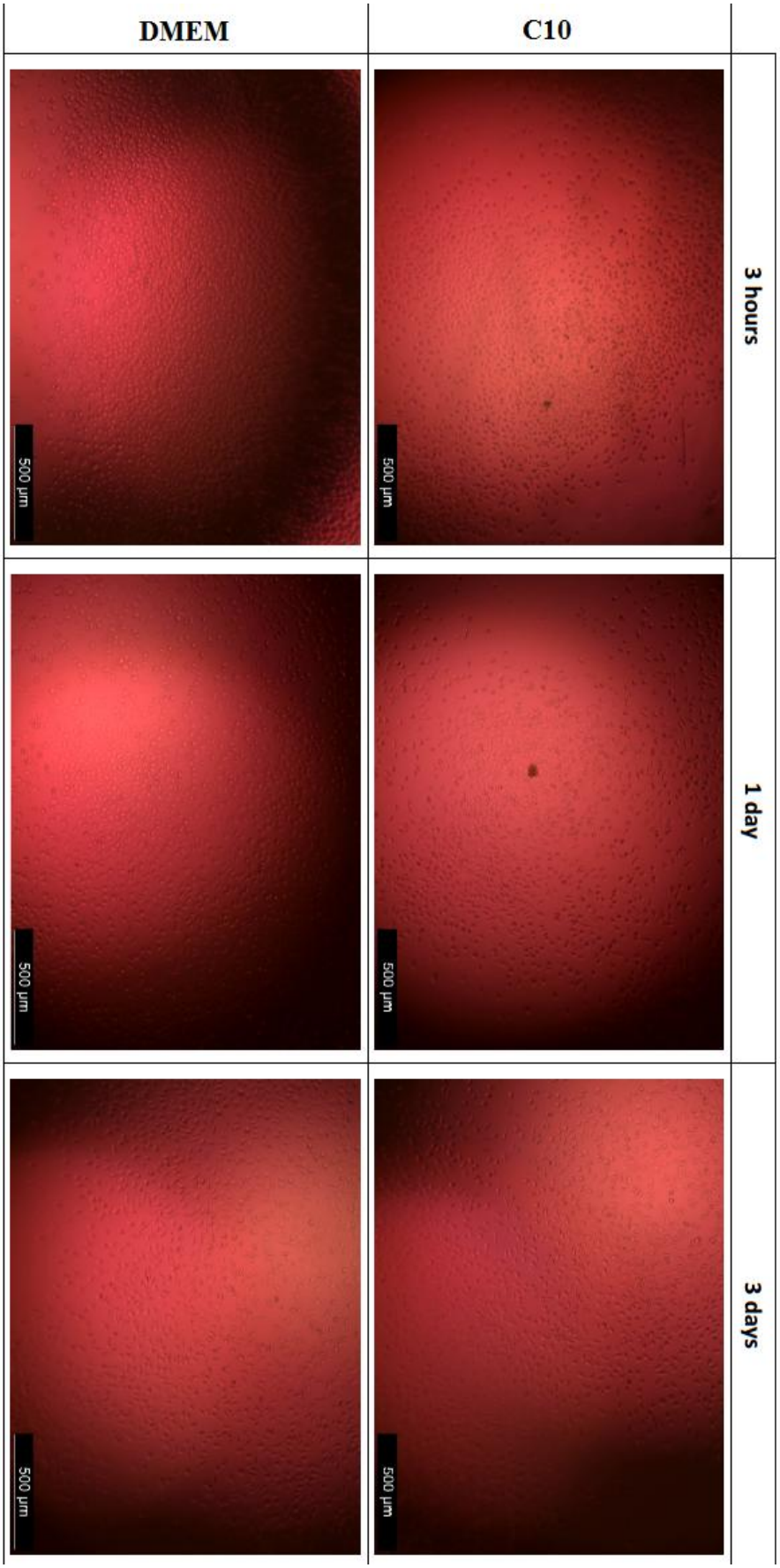

Figure 74. Optical microscope images of L929 cells seeded in in the C10 eluate (C10-3h, C10-1d, C10-3dd) for 24 hours.

5 Discussion

The first indication the present work reveals is the great variability in test outcomes when this material is employed. Indeed that turns in sources mentioning contrasting changes in material properties and showing large standard deviations. Elastomers are known to be materials not easy to investigate mechanically, therefore a huge sample amount is warmly suggested in order to neglect bad cases and lower standard deviations (for instance Minitab suggests 60 samples on average in uniaxial tensile test to reach SP = 0,8).

Test outcomes are compared with literature sources to see whether there is agreement between them and eventually justify the suspected parameter trends. One source has to be employed carefully when its results are used as comparison terms: Gautriad et al. [17] report many mechanical parameters after one 100% Etox sterilization cycle. This source presents certain values often not compatible with the other sources or at least quite surprising (with big changes after a single cycle, e.g. hardness test). Only 5 samples are used for parameter calculation, making that not suitable for complete reliability when comparing test outcomes. Apart from that as unsterilized samples are generally not employed, the generally accepted lack of difference between unsterilized silicone and that sterilized once by Etox is proven. In uniaxial tensile test not all the parameters perfectly match between C0 and C1 datasets, however many parallelisms may allow to infer equivalence between them also for the other experiments.

Finally possible interpretations for the observed phenomena are hypothesized.

5.1 Mechanical Testing

Acquired **UTS** data generally cannot demonstrate any statistically relevant change: null hypotheses are never rejected apart from one case (C4-C10 comparison considering the two strain rates together) although the related SP = 0,55 only. ANOVA test carried out on four datasets (C0 included) still returns a PV > 0,05. This case represents the one with most sample types, however the mentioned difference between C0 and C1 mean values makes it not the most suitable to come to a conclusion about the overall Etox effect. Despite the lack of statistical support, one may suspect a faint drop of UTS as the exposure to Etox

increases (Fig.31). This effect might become evident only after several Etox cycles and is less likely to reveal itself after few exposures.
This hypothesized behavior is compared with literature studies (related to a single Etox cycle) which however deal with contrasting outcomes. Terheyden et al. [48] report a 90%-100% value with respect to unsterilized silicone rubber, on the opposite Gautriaud et al. [17] register a 1 MPa increment in UTS. Finally Simmons et al. [10] compare P80A and E2A, two polyurethane materials with the second one enriched by small PDMS segments. E2A's UTS is observed to remain similar to the unsterilized value (even if standard deviations are not small), whereas P80A suffers a clear UTS drop. E2A is not pure silicone but confirms the stability potential PDMS can bestow to other materials by small amount addition. Thus the three sources suggest different UTS answers to limited Etox exposure. The second source has been mentioned to be not completely trustworthy whereas the other two ones may be compatible with the hypothesized weak drop as the number of cycles gets bigger.

Ultimate Elongation cannot be statistically demonstrated to be altered by Etox treatment, however trends and obtained p values in Ultimate Elongation and UTS (without merging datasets) suggest a certain parallelism between these two parameters. Therefore even if Ultimate Elongation datasets with different strain rates cannot be directly merged, one may suppose a faint decrease due to Etox exposure as hypothesized for the previous parameter. This interpretation is not supported by Gautriaud et al. [17] who observe a faint increment for this parameter, whereas Heiner et al. [16] report a slow decrease (approximately 0,6% strain per cycle). Similarly Simmons et al. [10] notice a drop for E2A, whereas P80A (no PDMS fragments) is not described to show a significant change in its Ultimate Elongation. Thus PDMS may be responsible of the weakening in this mechanical parameter.

Dealing with **Elastic Moduli**, E_lin and E_200 do not reveal any substantial change. Both cases confirm the greater the strain rate, the higher the elastic modulus is. Terheyden et al. [48] report a wide range of results (ranging from 85% to 105% of the original E_200) which anyway suggests a decrease should be more likely than an increment. Gautriad et al. [17] in their study do not notice any change in secant modulus at 100% strain, Heiner et al.

[16] report an extremely slow decrease for the elastic modulus of Pt-cured silicone (lower than 0,2 % for each cycle).

Results from hardness tests reveal a small increment in **Hardness** after Etox treatment: assuming a linear increase between C1 and C10 mean values, the increment would result approximately 0,06 Shore A/cycle. P values and their statistical powers supply complete trustworthiness to the analysis. Even though this investigation returns statistically relevant outcomes, one should remember the procedure employed to sample the material. ASTM D2240 specifies one should prove the absence of outcome differences between specified procedure and the employed one. This change is compatible with what Heiner et al. [16] find out in their experiment, where an increment of only 2 Shore A units is registered after 100 sterilization cycles (0,02 Shore A/cycle approximately). Gautriaud et al. [17] report a decrease of 0,5 shore A after only one sterilization cycle instead, contrasting strongly the previous source both in the quickness of change (single cycle to induce a measurable difference) both in the nature of the change (decrease).

5.2 Thermal Analysis

Independently from inspected temperature and frequency, E' and E'' calculated by **DMA** are never demonstrated to differ due to diverse Etox exposure. All 12 C1-C4-C10 comparisons show a common trend with C1 mean values slightly smaller than C4 and C10 ones which appear similar instead. Both ANOVA and Mann-Whitney tests never reject null hypothesis, resulting unable to give this trend any statistical relevance. Apart from the labile reliability because of the ways samples are produced and clamped, experiment outcomes and hypothesized trends are affected by the small sample number (only 4 samples for C1 due to the discarded 2 outcomes out of 6). Thus this experiment ought to get enriched by more specimens in order to return more trustworthy statistical outcomes. In fact doubling dataset dimensions by using twice each datagroup (by simply copying and pasting them into the same columns), ANOVA p value equals 0,038 for E''_0°C at 1Hz (0,193 in the original case). Certainly this consideration is not valuable enough to assess the reliability of an E' or E'' increase as Etox exposure grows, however the similarity among the trends in all cases may induce the reader not to discard this hypothesis.

According to the cooling rate, **DSC** experiments display two types of graph and slow cooling has been reported to enhance crystallinity in the frozen structure.

Endothermic peaks related to melting transition (approximately between -44,5 and -43,5 °C in both graphs) do not reveal any change for Tm and its enthalpy. Actually this result is reliable for the slow cooling case only (PV > 0,5 ; SP < 0,2), whereas the fast cooling one not only reveals many potential outliers but it also presents 3 ANOVA tests out of 6 returning p values extremely close to the 0,05 threshold. Therefore one may conclude Etox sterilization cannot influence the melting transition guided by the crystalline component (slow cooling procedure). On the contrary nothing precise can be assessed for fast cooling procedure also due to the potential outliers (Fig.51 and Fig.52). In this case for both parameters a good compatibility can be graphically observed between C1 and C10, whereas C4 distributions justify the low p values in the other comparisons.

Crystallization transition (Tc between -84° C and -80° C) is observed only in the cooling curves. ANOVA test rejects compatibility among the enthalpies for the three different datasets as the variance appears smaller for C4 than C1 and C10. In fact if C4 variance is assumed to be actually larger (similar to C1 or C10 cases), ANOVA would fail in rejecting instead (assuming equal variances PV = 0,095). T-test reveals compatibility between C1 and C4, whereas the low ANOVA p value can be ascribed also to C10 dataset which may effectively differ from the other two ones. Rejections of these null hypotheses suggest Etox increases the enthalpy associated with crystallization transition (as Fig.54 displays), with this effect becoming relevant only after several cycles (e.g. C10). Though the absence of variation in Tg, a change in this parameter would suggest an alteration of the components contributing to material crystallinity.

The comparison related to Tc instead reveals a great incompatibility among data. C1 and C10 present a certain similarity but the C4 dataset displays much lower mean value and standard deviation, reporting also two potential outliers. Apart from the obvious rejection of null hypothesis, the described situation casts doubts about the reliability of these obtained data. Therefore for this parameter the inclusion of new data or the repetition of this test may be suggested.

Finally the Tg is taken into account. This parameter is greatly valuable as it is strongly affected by the level of crosslinking in the material. In addition to Tm, also the damping

(linked to E'') and the slope of the glass transition are dependent on material crosslinking [49,50].

Statistical comparison among C1, C4 and C10 does not register any alteration and this outcome is statistically reliable (for all methods PV > 0,6 and SP < 0,06). Tg value obtained for MED-4860P results approximately -134° C, which is compatible with the value literature generally reports for PDMS (-125°C). The compatibility between the two values resides in the variability which the Tg can be calculated with. According to the chosen investigation technique a difference up to 25° C can be reached, for instance Tg by DMA is often reported to be 10° C higher than Tg obtained by DSC [51]. These mismatches result from the different ways the Tg is obtained. In fact glass transition actually represents a range of behaviors whose nature cannot be easily concentrated around a unique specific temperature. Different industries have used different points from the same data set. DSC, TMA, and DMA measure different processes and therefore return different values [52].

Crosslinking profoundly influences the Tg: indeed as crosslink density among polymer chains increases, Tg shifts to higher temperatures (rightwards along the temperature axis) [49,50]. Therefore the undetected change in Tg may suggest no substantial change in crosslink density when the material is sterilized by Etox. The lack of change in Tg is in accordance with the study of Zhang YZ et al. [53]. The Tg of the silicone rubber they analyze by DSC reports no changes after single Etox sterilization, indicating neither crosslinking nor chain degradation occur for such a limited exposure.

Apart from Tg, Tc is reported to be included in the -90/-80° C interval in the cooling curve, approximately 10° C lower in the heating curve [41]. Actually the crystallization peak is stated to be really sensitive to both silica concentration (see paragraph 3.1) and chain architecture so that it can appear different (with respect to its position and height) according to these factors. In particular the quicker the cooling, the more the peak slides leftwards (its enthalpy increases as well). Also the melting peak presents a Tm compatible with values reported in literature which however generally reports two peaks (Tm_1 and Tm_2): values vary from -50° C to -30° C [30,42].

DSC is an analysis technique which requires small amount of material and furthermore the process is fully automated. However there is always a certain concern that few milligrams

of the inspected material may not be representative of the overall component. Indeed the small parallelepipedons may have received different exposure to Etox according to their position in the original bigger sample. Step transition analysis is furthermore reported to be more difficult in cured materials [54].

5.3 Wettability and Swelling Investigations

Results in **wettability** experiment reveal clear changes in surface hydrophobicity after Etox exposure. The treatment makes PDMS surface less hydrophobic (up to 6° difference between C1 and C10 mean values after 2 minutes) and rejection cases report SP $\geq$ 0,95. Only for C1 and C4 null hypothesis is not rejected: immediately after contact their surfaces answer similarly (PV = 0,278 ; SP = 0,21), whereas p value gets really close to the threshold (PV = 0,057 ; SP = 0,51) after 2 minutes.
Indeed Fig.62 shows the three material classes have common shape in contact angle variation and Etox exposure results in shifting them downwards (with C1 and C4 curves displaying small gaps in between). This outcome results compatible with the not appreciable difference in contact angles (after one cycle) registered by Zhang et al. [53].

PDMS **swelling** in water is extremely limited, indeed some studies [36,37] report a swelling ratio of 1,00 ÷ 1,02 for PDMS after immersion in water (thus unsterilized silicone rubber barely absorbs this solvent). This tiny swelling ratio is in accordance with experiment results (swelling ratio < 1,0005).
C1, C4 and C10 after one week do not result statistically different, even though mean values suggest swelling ratio may increase as the Etox exposure is enhanced. After two weeks ANOVA and Mann-Whitney tests including C1 dataset reject the null hypothesis, so that C1 is recognized to differ. However values related to the second week are lower than those reported for the first week, indicating unchained components are diffusing outside from the crosslinked structure in the meanwhile. Therefore the analysis of a single parameter influenced by two phenomena at the same time may be not completely straightforward. Finally 9 weeks values reveal an overlap in lines connecting these 2 values to 2 weeks ones. The obtained curves may appear strange and may therefore be ascribed to random errors (which could be reasonable considering the small values employed in the comparison). Thus from the reported results one could infer Ethylene Oxide treatment

makes the silicone samples absorb more water. However the extremely small SRs and the potential differences among sample faces do not allow a straightforward interpretation of the phenomena. Instead of using water other solvents are reported to work better (meaning they allow greater swelling ratios) with PDMS: toluene (SR=1,31) for instance is often employed. However the highest SR are listed for diisopropylamine (SR = 2,13) and triethylamine (SR = 1,58) [13,37]. These higher swelling ratios would allow to better detect and estimate eventual differences among the three groups. Furthermore the experiment should be carried out by employing samples whose faces are equally affected by Etox treatment.

5.4 Surface Spectrography and Cytotoxicity Investigations

Spectra obtained by **ATR-FTIR** result perfectly compatible with what was attended from the investigated material (with its chemical structure), with only CO_2 and H_2O small peaks or trembling parts as unexpected elements in the spectra. Apart from a certain gap among spectrum baselines, recognized peaks appear overlap well and the method explained previously (see paragraph 4.5) suggests the eventual changes (in surface molecular vibrations) to be lower than 1% among the different Etox exposures. Thus no particular alteration is assessed, since a relevant change generally appears already visible in the spectrum at full scale. ATR-FTIR inspection of E2A (polyurethane with only 20% of PDMS) and P80A by Simmons et al. [10] reveals only the latter results altered after 3 Etox cycles, suggesting a certain percentage of PDMS can supply resistance to surface attack. Therefore one may expect pure PDMS, even for 10 cycles instead of 3, to show great surface resistance.

In vitro **Cytotoxicity** qualitative tests reveals cells are compatible with serum cultured up to 72 hours with material sterilized by Etox. Similarly to the time of culture, the exposure level to this sterilant appears not to influence test outcomes. Cell density results compatible in all cases, the absence of dead cells is observed as well. However compatibility with cells should be further investigated by using a quantitative analysis (colorimetric assay for the quantification of cell viability) and directly investigating the answer to direct contact between the material and cells. As surface hydrophobicity and hardness vary due to Etox sterilization, cell interaction with altered substrates should be inspected as well. In fact cell

attachment, spreading and differentiation are phenomena strictly connected to substrate properties and may change therefore [55,56]. Also *in vivo* tests would enrich this work as certain sources reveal some differences (e.g. number of inflammatory cells, capsule thickness) are visible only after *in vivo* implantation [53]. Indeed silicone and other hydrophobic materials get quickly coated by proteins after implantation, with the formation of a scar-like capsule around them [3].

5.5 Summary of parameter changes

Tab.50 aims at summarizing all the investigated parameters and representing the effects of Etox on material properties all together.

Parameter (or Analysis)	Rejection	Outcast Cases	Effect
UTS (500 e 100 separated)	No		=/-
UTS (500 e 100 together)	No	C4-C10	-
UTS (500 e 100 separated + C0)	No* (only ANOVA)		-
Ult. El. (500 e 100 separated)	No*		-
E_lin	No		=
E_200	No		=
E'_0°C e 37°C (all frequencies)	No		+
E''_0°C e 37°C (all frequencies)	No		+
Hardness	Yes	C4-C10*	++
Tm_group1	No		=/-
Enthalpy_Tm_group1	No		=
Tg (group2)	No		=
Enthalpy_Tm_group2	No*°		**X**
Tm_group2	No°		**X**
Enthalpy_Tc (group2)	Yes	C1-C10*, C4-C10	**++ (+)**
Tc_group2 (group2)	Yes		**XX**
ATR-FTIR	No		=
Hydrophobicity	Yes	C1-C4_0s, C1-C4_120s*	--
Swelling Ratio_1week	No°*		+
Swelling Ratio_2weeks	Yes°	C4-C10	++
Swelling Ratio_9weeks	Yes°	C1-C4*, C1-C10	**XX**
Cytotoxicity	No		

Table 50. The second column indicates whether the null hypotheses are rejected in the statistical methods, the third one lists those cases whose results differ from what stated in the second column, the fourth one the type of change and its statistical relevance (meanings are described underneath in Tab.51).

Symbol	Meaning
-	decrease (lacking of statistical relevance)
--	decrease (statistically relevant)
+	increase (lacking of statistical relevance)
++	increase (statistically relevant)
=	no change
=/-	no change (eventual little decrease at the latest)
=/+	no change (eventual little increment at the latest)
X	not linear answer to Etox (change not detected)
XX	not linear answer to Etox (change detected)
*	some p values next to threshold
°	presence of potential or detected outliers

Table 51. The meanings of the symbols listed in Tab.50 are provided. These symbols want to report the type of change and suggest the statistical relevance related to that.

Such a purpose is difficult to achieve as parameter trends and their statistical relevance cannot be condensed easily together in a unique symbol. A comprehensive explanation is the only way to make the reader understand how the parameters are affected by Etox treatment but this table is beyond this purpose. For better comprehension the past pages should be taken into account.

5.6 Hypotheses about changes

As the only tests exhibiting a trustworthy change are wettability and hardness tests, a connection between them is expected. ATR-FTIR spectra suggest no alteration in surface molecular vibrations so that a possible explanation has to be researched elsewhere. Another property related to material surface consists in the roughness exhibited by the surface profile. This term is commonly used with a generic meaning as this feature is actually composed by two elements: waviness and roughness. Waviness consists in macro-type wavelength patterns whereas roughness mainly refers to shorter wavelength variations. The latter is generally ascribed to machining processes and their tool quality. When micro or nano indentations are performed, the waviness component is generally neglected since the indenter dimension is small with respect to that [57]. As the indenter employed in the present work has a tip of approximately 0,8 mm, the same assumption

would result quite labile. However this thesis lacks a microscopy surface inspection (e.g. SEM), therefore the relation between these two profile components (on the employed samples) cannot be assessed. Thus no distinctions between them will be made and hereafter the generic term "roughness" will be employed instead.

This parameter is known to affect both hardness and hydrophobicity measurements. Since the calculation of the hardness is based on the assumption that sample surface is flat, the rougher the surface the more distant from ideal results the outcomes will be. The penetration depth has been explained to be employed in hardness calculation, however surface roughness can have a significant impact on the measurement of this parameter. In fact hardness is reported to have a lower value if the indenter comes into contact with peaks. Indeed the registered penetration results larger than assuming a flat surface (a valley would result in the opposite behavior) [58]. These considerations are particularly significant for micro indenters but alterations for higher scale indenter are likely as well.

Similarly roughness affects wettability properties of a surface. Several phenomena operate synergically returning an overall wettability phenomenon (fluid answer to the substrate it gets in contact with). Young's law represents a simple equation describing the behavior of a droplet on rough surfaces. However one has to take into account that many cases can occur and many factors cooperate to determine drop behavior, therefore an interpretation of the observed reaction cannot be addressed to a single reason.

Young's equation referring to a specific liquid-solid system is described as:

$$\gamma_{lv} \cos\theta_Y = \gamma_{sv} - \gamma_{sl}$$

relating three thermodynamic parameters: liquid-vapor (γ_{lv}), solid-vapor (γ_{sv}) and solid-liquid (γ_{sl}) interfacial tensions. The combination of these three parameters should result in a well specific θ_Y (Young's contact angle). In practice this is not true since many metastable states of a droplet on a solid surface can occur: contact angle value this way exhibits a range between advancing and receding angles, instead of the calculated θ_Y (ideal case) [59,60]. Wenzel stated that increasing surface roughness results in an enhancement of the wettability condition determined by surface chemistry (the same treatment enhances or lowers contact angles depending on their values before roughness enhancement). In fact Wenzel's theory is expressed by the following equations:

$$\cos\theta_m = r \cdot \cos\theta_Y$$

With θ_m describing the measured contact angle and r the roughness ratio (r = 1 for perfect smoothness, r > 1 otherwise). The employment of this formula requires the assumption liquid penetrates into surface grooves, which actually is considered true when the droplet dimension is at least twice bigger than roughness scale [60]. According to this formula the sign of $\cos\theta_m$ depends on that of $\cos\theta_Y$ (with r as amplification factor), so that the effect on contact angles depends on this second term. PDMS is an hydrophobic material ($\theta_Y > 90°$) therefore when surface gets rougher, it gets more hydrophobic as well. On the contrary an hydrophilic material results even more hydrophilic when it gets rougher (Fig.75).

After these details about the role surface roughness plays on both hardness and wettability measurements, the following hypothesis is suggested to explain test outcomes. Samples employed in both tests have faces whose profile is determined by the injection molding procedure. In fact injection molded-samples show a roughness dependent on the condition of cavity surfaces in the mold and on the parameters of the injection process [61]. These faces are then directly exposed to sterilant action during Etox cycles so that one may suspect Etox sterilization affects surface roughness lowering it (altering surface properties as well). The mechanisms and reactions responsible for this suspected phenomenon would require however further investigation.

Fig.76 explains the hypothesized phenomena in the two cases (unsterilized and sterilized samples) by representing material surface as two connected layers. A first layer is sketched as a row of contiguous triangles (focusing on a 2D profile) representing surface roughness (assuming consistent roughness pattern). A second layer (thicker than the first layer but here shown as thick as the previous one) represents the "real" surface (that with a flat profile) which mainly contributes to the surface resistance to indenter penetration. The red line in these second elements ideally represents the depth reached by the indenter when the durometer is pressed against the surface.

Assuming Etox sterilization to result into a roughness decrease, the structure on the left may represent C1 surface (r_1) and that on the left C10 surface (r_2). In this case the decrease in roughness is sketched as a first layer with the same pattern but with lower peaks. Thus $r_1 > r_2$, resulting in higher hydrophobicity for C1 surface as the surface before treatment is

already hydrophobic. According to that, the decrease in roughness may explain the smaller contact angles (and therefore the obtained lower hydrophobicity).

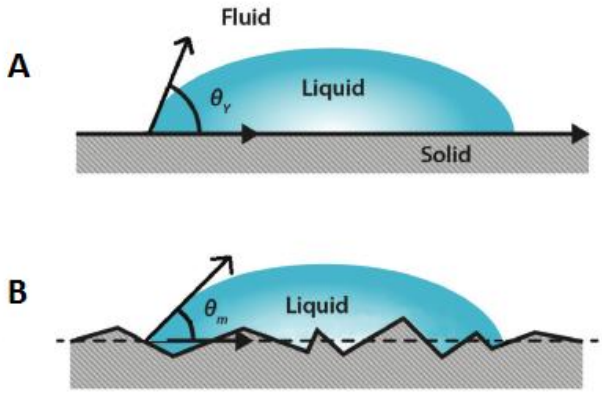

Figure 75. Difference in droplet contact angles between perfectly smooth surface A (r = 1) and rough one B (r > 1) of an hydrophilic material (θ_Y < 90°). Due to the locally slanted profile, the observed contact angle results lower for B. Thus when this hydrophilic material gets rougher by a certain surface treatment, its hydrophilicity is enhanced.

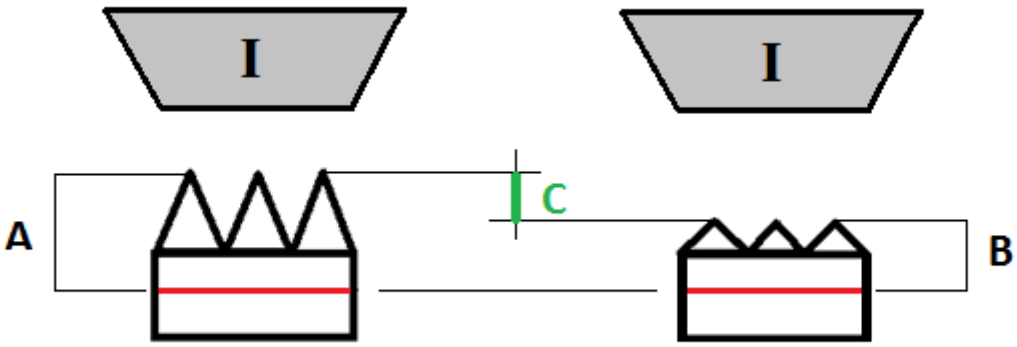

Figure 76. Indenter tip (I) is pulled against material surface which shows a different topography in the two cases (C1 on the left and C10 on the right); the lower peaks in the first layer of the second case want to suggest a lower roughness. The durometer starts registering the penetration depth at different heights but the depths in the second layer are assumed equal (as the first layer contributes secondly to surface answer against the indenter). Considering A and B the registered penetrations, C = A - B would justify the difference in hardness values returned by the instrument. Furthermore as surface is hydrophobic before Etox treatment a decrease in roughness would bring to an hydrophobicity drop.

Dealing with hardness test, the indenter is assumed to reach equal depth in the two cases as the first layer is composed by small elements which deform quite easily with respect to the stratum beneath. However in C1 case the height which the durometer starts to register the depth is higher than for the C10 case (since the surface peaks are higher). According to that, the durometer would register a greater penetration (A > B) and thus a lower hardness in C1 case. The difference in penetration depth (C) would be responsible for the difference in the hardness calculated by the durometer.

Roughness decrease is reported above as a simple lowering of peak tips in the first layer. Continuing to refer to roughness as peak height, another possible phenomenon may be that the peaks in the first layer locally merge each other at the level of the triangle bases, keeping the tips unaltered. This event is reported in case "b" of Fig.77. Both "a" and "b" evolutions display peaks lower than for the C1 case (structure on the left). These two possible interpretations might be confirmed by surface inspections, for instance AFM and SEM (more difficult) and may be employed for this purpose.

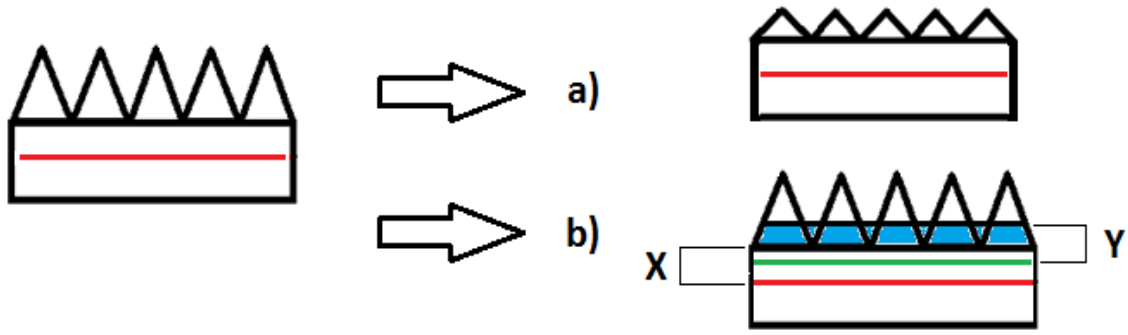

Figure 77. 2 possible schematizations and interpretations of the hypothesized drop in surface roughness. Case "a" represents the already discussed decrease in peak tips, case "b" hypothesizes the fusion between peak bases so that a new layer is created (the blue one). Now this new layer would participate in bearing the indenter load as the layer beneath does, thus the red line would shift upwards (at the level of the green one). If one assumes the second layer and the blue one to have similar properties, X and Y would result similar.

Test outcomes for swelling test have been reported not to be completely straightforward according to several factors in the experiment. Assuming now that these outcomes are trustworthy anyway, outcomes for the 9th week appear not clear: C10 mean SR is really close to C1 and smaller than C4. One may hypothesize this to be a wrong or imprecise

result, which actually could be reasonable considering the small values exhibited in the results. However apart from this interpretation, other reasons could be taken into account since swelling test deals with several phenomena. As already mentioned swelling and oligomer diffusion are processes happening at the same time. The gaps progressively left from oligomer species migration are gradually occupied by water molecules which have lower density (as reported by the Specific Gravity of 1,15 in Tab.3). In addition to that, PDMS degradation in water could be taken into account as well. Such a complex combination of factors has been widely investigated: the answers of diverse polymers to immersion in different types of solvents have been widely debated. Nevertheless definitive and accurate conclusions cannot be drawn quite easily so that authors often suggest their works to be the starting points for future analyses. Therefore an explanation for C10 values and the exact processes leading to them are beyond the purpose of the present work which marginally deals with this type of investigations. Nevertheless some considerations and hypotheses are reported in order to suggest some phenomena which may take place between PDMS and water.

Feng J et al. [62] report silicone rubber with higher hardness (samples differ up to 20 Shore A) show greater weight loss independently from the various aqueous solutions they are immersed in. Sample hardness however is affected also by the amount of fillers impregnated among the crosslinked structure. Thus they explain the higher weight loss for the materials with higher hardness as the leaching of more fillers with respect to low hardness samples (in case of aggressive solvents a contribution is given also by degradation products obviously). The idea behind this explanation might justify the value associated with C10 by hypothesizing a variation in the content of fillers for MED-4860P as well. A possible way they eventually could be generated and diffuse outside should be proposed however. Eventual chain scissions might represent a possible reason, even though Tg is demonstrated not to differ. However Tg is later explained to be affected by several parameters (so that small variations in chain structure may be balanced by other ones, promoting opposite Tg shifts complementary to each other). For instance chain scission has been reported commonly as a problem for plastic materials when they are exposed and sterilized by gamma radiations or electron-beam [10,17,63]. As described previously Etox sterilization mechanism resides in the alkylation reaction affecting sulfhydryl, hydroxyl, amino and carboxyl groups which Etox easily reacts with. However

the structure of the material under inspection (see paragraph 3.1) does not include any of these groups as the ATR-FTIR spectra reveal. Indeed examples of PDMS resistance to alkylation are reported for applications requiring media for alkylating agent diffusion [64]. Exposure to alkylating process is repeated for C4 and C10 so that one may wonder whether a massive exposure may affect partially the material instead. In this case if the creation of these extra fillers is assumed to take place already in the sterilization process, then they may contribute to hardness enhancement independently from the idea relating wettability and hardness tests (hypothesizing a roughness decrease). Nevertheless water, both in combination with Etox and separately, may be responsible for this proposed alteration. Indeed this second element either in liquid state or moisture may induces hydrolysis in the material.

In his experiments Hamilton R [65] reports silicone materials (mainly linear polydimethylsiloxanes are inspected) undergo hydrolysis degradation reacting with bases (NaOH), acids (HCl) and blood (pH = 7,4). Instead no changes are appreciated for water or neutral aqueous sorbitol up to 11 weeks. In the present thesis the water employed in swelling tests is demonstrated to have a pH between 6,25 and 7 so that the hydrolysis catalyzed by acids cannot happen. Hamilton R reports chain cyclization and its following scission can be caused by reactive chain ends folding back over their own chains. These reactive end groups allowing silicone hydrolysis are however stated to be less likely (with respect to other materials) for PDMS chains as they present methyl groups at the end which are not particularly reactive [65]. In the present case however, as the ATR-FTIR results reveal, also CH_2 terminations are present (in uncrosslinked C=C end chain groups). An eventual activation of some terminal groups may result in the reaction described in Fig.78 with the release of cyclic species. Considering such a process occurring at the pendant chains whose extremities are not linked to the rest of the reticulum, one may assume scarce impact on mechanical properties and increased release of filling elements.

Kennan JJ et al. [66] present a research on hydrolysis in peroxide and hydrosilylation cured silicone elastomers after filler purification leaching. Both materials are inspected after 45 hours immersion (up to 100° C) in saline solution, returning no significant evidence of hydrolysis (even if some changes are detected they cannot be univocally ascribed to hydrolysis process). Pt-cured silicone is generally considered even more resistant than peroxide-cured one, so that a similar or even better resistance could be attended. Indeed

differences in Swelling Ratios in the present thesis appear extremely small so that even if some changes had occurred in their experiment, it would have made sense that they catalogue them as not statistically relevant. The opposite classification would be impossible for them as they measure the potential hydrolysis not directly by leaching analysis but by contact angle (for the surface) and mechanically (for bulk properties). These methods in case of extremely low hydrolysis could not be considered sensitive enough.

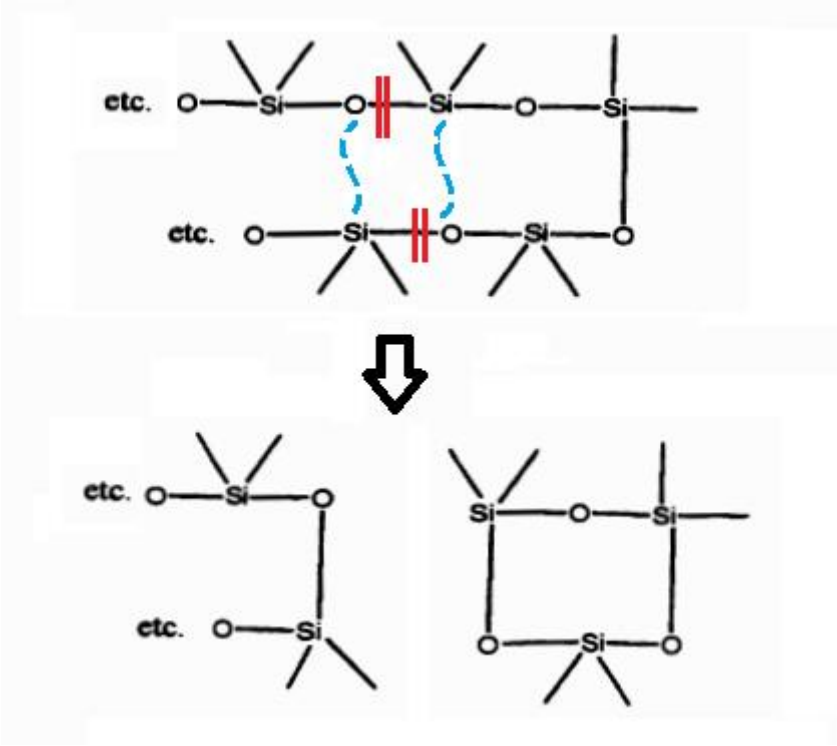

Figure 78. When the extremity group of a chain gets reactive, the extremity fold back and the illustrated reaction occurs. The original chain gets shorter and low molecular weight species are generated.

Finally a more simple explanation for the weight loss may consist in the removal of superficial layers when they are dried by absorbent paper so that small fragments of surface can be peeled off. The differences in surfaces of the three material types, together with the alternation between air and water (in order to scale the samples) may result in different surface erosion during these phases.

One should remember the presented considerations and comparisons aim at just supplying some possible interpretations of the registered values. Similarly to the previous

interpretation for hardness variation, only new specific tests (e.g. surface inspection, leaching analysis) may clarify whether the present hypotheses are reasonable or not.

Finally a reflection about the Tg values obtained by thermal analysis is proposed. According to DSC outcomes Tg does not report any alteration. Generally this fact suggests no chain scission or crosslinking occurred. However other mechanical parameters (e.g. E', E'', UTS and Ultimate Elongation) suggest variations whose reliability results questionable according to the obtained p values and statistical powers.

This final paragraph does not aim at demonstrating anything about the mentioned parameters, instead it wants to suggest how the lack of variation in Tg could not imply necessarily the absence of chain structure variations (in particular if those ones would be particularly small). Indeed in the previous paragraph the eventual chain scission in correspondence of free chain ends has been mentioned. Tg has already been described as a complex parameter which can be studied by different techniques according to different processes. Additionally crosslinking is not the only feature affecting Tg: its value actually has been experimentally observed to be influenced by many other variables (e.g. crystallinity, molecular weight, test rates, plasticizer content, aromaticity and tacticity) [67,68]. For instance higher crystallinity and heating/cooling rates induce greater Tg values, on the contrary a higher number of chain ends lowers this parameter. This suggests that the absence of substantial change in Tg might actually hide small alterations whose effects, when combined, result in a null impact on this parameter (increment factors and decrease ones balance each other).

A demonstration of how Tg is affected by variation in chain structure is here briefly reported by the Fox-Flory law. This formula can be found in the literature reported in different ways [67,68,69,70]. An interesting summary by Harrison IR (Pennsylvania State University) [68] reports an alternative version of the common formula [67,69,70], modified in order to reveal how the crosslinker agent contribute to Tg:

$$Tg = Tg_{\infty} - K/M + K_X \cdot (\#\ crosslinks/gm)$$

where Tg_{∞} is the glass transition temperature for an ideal chain of infinite length, K a characteristic parameter of the dependence between Tg and M, M the molecular weight and K_x an amplification factor related to crosslink density [68,70]. According to this

source, Tg grows linearly with crosslink density only when the crosslinker agent is similar to the polymer chains it is connecting to, otherwise the increment is less steep and not linear. (Fig.80). The second and the third terms are generally reported differently (aggregated as K/M_w) remarking aside the importance of crosslinker's nature [67].

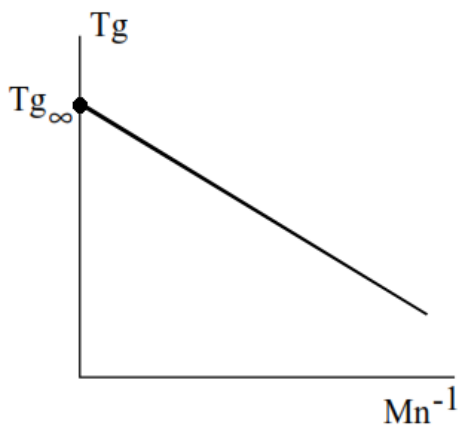

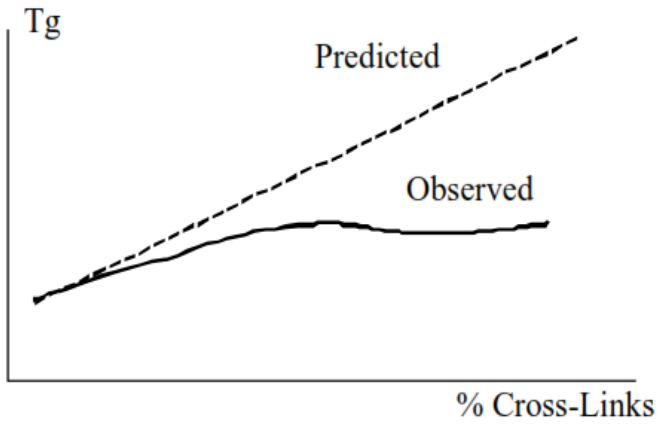

Figure 79 and Figure 80. Tg decreases for smaller Molecular Weight according to Fox-Flory's law. An increment in the crosslink density results in higher Tg, however the observed increase is comparable to the predicted one only when crosslinker agent does not differ too much from the polymer chains it connects to.

Similarly Wu L [67] reports this formula can be enriched with new terms including other factor contributions (e.g plasticizers and attended percentage of cured polymer). Therefore the last paragraph aims at showing that some tiny changes, faintly affecting other test outcomes, may not be recognized necessarily by Tg value in DSC. The analysis of other parameters related to glass transitions (e.g. transition length) in the same thermograms may add new elements of comparison for this purpose.

6 Conclusions

The reported tests have been chosen to investigate a great number of parameters in PDMS (MED-4860P) silicone rubber, aiming at determining whether they change after several sterilization cycles by Etox. Results have been shown to lack often statistical relevance, however the present work draws two important conclusions.

Firstly the properties which appear to be altered the most by Etox treatment are those related to surface. Hardness and wettability tests allow to distinguish samples treated by different Etox amounts since a slight increase in hardness and a surface hydrophobicity drop are observed as the number of sterilization cycles increases. Similarly swelling tests suggest differences among C1, C4 and C10 datasets, showing that after 1 and 2 weeks the more sterilizations a sample undergoes, the more water it can absorb. This outcome could be ascribed to the decrease in surface hydrophobicity, indeed the solvent faces lower resistance by material surface so that slightly higher absorption in the first layers may be reasonable. The decrease in Swelling Ratio should be linked to the diffusion of uncrosslinked low molecular weight species out from the crosslinked structure. Some considerations about C10 swelling ratios after 9 weeks (exhibiting a suspected weight loss) are proposed trying to justify them. A possible interpretation may consist in chain scission occurring at the pendant chains of the reticulum or the removal of first layers while drying the samples before scaling them.

On the other hand bulk properties seem to get less influenced by this sterilization procedure: elastic moduli E_lin and E_200 do not reveal any change at all, whereas UTS and Ultimate Elongation might slightly decrease (a higher sample number may confirm this hypothesis). Storage and Loss moduli may be suspected to increase even though this interpretation strongly lacks statistical significance in spite of 10 employed samples. The Tg results unaffected suggesting no chain scissions or variation in crosslink density, however certain reflections about the certainty of no changes at all due to that have been proposed. Other precise considerations about DSC outcomes cannot be inferred even if the enthalpy associated with the crystallization transition results enhanced by a higher number of sterilizations.

As surface behavior is observed to differ according to Etox treatment, a potential reason is expected to be found by surface investigation. The chosen method (ATR-FTIR) however

registers spectra which do not differ appreciably. Thus a possible explanation is submitted taking into consideration the impact of surface roughness on the outcomes of both experiments, hypothesizing Etox sterilization gradually lowers the roughness. New surface analyses (SEM or AFM) may confirm this hypothesis.

The second conclusion one can draw from test results deals with the reason why Cochlear industry is interested into the present investigation. Tests are performed aiming at demonstrating whether PDMS samples sterilized more than once by Etox can be assumed similar to those sterilized only once. Indeed C10 datasets are often demonstrated to differ (or at least can be suspected of that) so that employment of samples sterilized for several times (more than four cycles) should be dissuaded. In particular silicone encapsulation may result less effective similarly to its resistance to water drops. The risk would not be directly related to the amount of absorbed water but to an alteration in the overall shielding action against water (or moisture). Furthermore, even though C10 samples do not exhibit problems with cells in cytotoxicity tests, the changes in hardness, hydrophobicity and swelling can alter cell behavior on these substrates. Therefore direct instead of indirect contact of cells with the material should be investigated, checking cell attachment, spreading and differentiation phenomena. On the other hand C1 and C4 appear more compatible even though some differences are exhibited anyway. Hydrophobicity is slightly lower and hardness increases weakly for C4 with respect to C1. Similarly swelling test results are not statistically different apart from the 9^{th} week. For the comparisons among mechanical parameters the reader is exhorted to refer to previous pages. The only problem in employing C4 PDMS instead of C1 one may be therefore the same mentioned for C10 about a lower efficiency in encapsulation against water (even if water absorption is still extremely poor). These considerations suggest the material may be considered still safe up to four Etox cycles and actually further sterilizations appear quite unlikely to be required in practice. Indeed a device (before its use) may be estimated to require one or two extra sterilizations at maximum after the original one (in case some small changes or check inspections are carried out).

Apart from the already mentioned improvements in the performed experiments, some other tests may enrich the present work. Tear test analyzes Tear Strength whose variation would not have a negligible impact on the material considering its implantation next to the

connection between jawbone and mandible (surrounding tissues have to bear significant tear stresses). Other reasons for surface alteration may be sought by XPS, whereas the impact of shelf life on C1, C4 and C10 could be recommended considering that the material is not immediately implanted. Finally two parameters are commonly investigated in polymers and would broaden the knowledge in this process: abrasion resistance and fatigue crack growth resistance.

7 References

[1] LeVier RR, Harrison MC, Cook RR, Lane TH. (1995) What is silicone? *Journal of Clinical Epidemiology*, 48(4), p.513-517.

[2] Andriot M, DeGroot JV, Meeks R, Gerlach E, Jungk M et al. (2008) Silicones in Industrial Applications. *Silicon-Based Inorganic Polymers*, Nova Science, p.61-161.

[3] Ratner BD, Hoffman AS, Schoen FJ, Lemons JE. (1996) *Biomaterials Science: An introduction to materials in medicine*, 3rd edition, Elsevier, 2012.

[4] http://tarek.kakhia.org/periodic_table/english/Silicon_14.Tarek_Kakhia.pdf

[5] http://www.elveflow.com/microfluidic-reviews-and-tutorials/

[6] Donaldson PEK, Aylett BJ. (1995) Aspect of silicone rubber as encapsulant for neurological prostheses, Part 2: adhesion to binary oxides. *Medical & Biological Engineering & Computing*, 33, p.285-292.

[7] Donaldson PEK. (1997) Aspect of silicone rubber as encapsulant for neurological prostheses, Part 4: Two-part rubbers. *Medical & Biological Engineering & Computing*, 35, p.283-286.

[8] Lotters JC, Olthuis W, Veltink PH, Bergveld P. (1997) The mechanical properties of the rubber elastic polymer polydimethylsiloxane for sensor applications. *Journal of Micromechanics and Microengineering*, 7, p.145-147.

[9] http://americanurethane.com/polyurethane-properties.html

[10] Simmons A, Hyvarinen J, Poole-Warren L. (2006) The effect of sterilization on a poly(dimethylsiloxane)/poly(hexamethylene oxide) mixed macrodiol-based polyurethane elastomer, *Biomaterials*, 27, p.4484-4497.

[11] Urayama K, Kawamura T, Kohjiya S. (2009) Structure–mechanical property correlations of model siloxane elastomers with controlled network topology. *Polymer*, 50, p. 347–356.

[12] Tanzi MC. (2006)*Fondamenti di Bioingegneria Chimica: non solo biomateriali*. Pitagora, Bologna, p.35, 96-99, 117-119, 2006.

[13] Mahomed A. (2008) *Properties of elastomers for small-joint replacements*. PhD thesis, University of Birmingham.

[14] http://www.dowcorning.com/

[15] Campbell DJ, Beckman KJ, Calderon CE, Doolan PW, Moore RH et al. (1999) Replication and Compression of Bulk Surface Structures with Polydimethylsiloxane Elastomer. *Journal of Chemical Education*, 75(4), p.537-541.

[16] Heiner J, Stenberg B, Persson M. (2003) Crosslinking of siloxane elastomers. *Polymer Testing*, 22, p.253-257.

[17] Gautriaud E, Stafford KT, Adamchuk J et al. (2010) Effect of sterilization on the mechanical properties of silicone rubbers. *BioProcess International*, 8(4).

[18] Messier A, Schorsch G, Rouviere J, Tenebre L. (1989) On certain solved and unsolved problems with water/PDMS/surfactant systems. *Progress in Colloid & Polymer Science*, 79, p.249-256.

[19] http://www.fao.org/

[20] Jivani RR, Lakhtaria GJ, Patadiya DD, Patel LD, Jivani NP, Jhala BP. (2014) Biomedical microelectromechanical systems (BioMEMS): Revolution in drug delivery and analytical techniques. *Saudi Pharmaceutical Journal*. (article in press, http://dx.doi.org/10.1016/j.jsps.2013.12.003)

[21] http://www.medicinenet.com/simethicone/article.htm

[22] Burgess IF. (2009) The mode of action of dimeticone 4% lotion against head lice, Pediculus capitis. *BMC Pharmacology*, 9(1), p.3.
[23] http://ec.europa.eu/enterprise/policies/
[24] Donaldson N, Baviskar P, Cunningham J, Wilson D. (2012) The permeability of silicone rubber to metal compounds: Relevance to implanted devices. *Journal of Biomedical Materials Research. Part A*, 100(3), p.588-598.
[25] http://www.nidcd.nih.gov/
[26] Mendes GCC, Brandao TRS, Silva CLM. (2007) Ethylene oxide sterilization of medical devices: A review. *American Journal of Infection Control*, 35, p.574-581.
[27] Gunnigle MC, Renner JA, Romano SJ, Abodeely HA. (1975) Residual Ethylene Oxide: Levels in Medical Grade Tubing and Effects on an In Vitro Biologic System. *Journal of Biomedical Materials Research*, 9, p.273-283.
[28]http://www.guidechem.com/trade/pdetail2586982.html
[29] http://www.chemnet.com/cas/it/68037-59-2/
[30] Aranguren MI. (1998) Crystallization of polydimethylsiloxane: effect of silica filler and curing. *Polymer*, 39(20), p.4897-4903.
[31] ASTM D 412 – 06, 2008, Standard Test Methods for Vulcanized Rubber and Thermoplastic Elastomers-Tension, ASTM International, West Conshohocken, PA, www.astm.org
[32] Braden M, Siddiqui A, Patel M, Parker S. (2010) An experimental and theoretical study of the effect of sample thickness on the Shore hardness of elastomers. *Dental Materials*, 26(6), p.560–564.
[33] ASTM D 2240 – 00, 2002, Standard Test Methods for Rubber Property – Durometer Hardness, ASTM International, West Conshohocken, PA, www.astm.org
[34] http://www.tainstruments.com/
[35] http://www.colby.edu/chemistry/PChem/lab/DiffScanningCal.pdf
[36] Honda H, Miyazaki M, Nakamura H, Maeda H. (2006) Controllable polymerization of biopolymers in a microreaction system. *World Congress of Medical Physics and Biomedical Engineering, Vol I*, p.234.
[37] Lee JNG, Park C, Whitesides GM. (2003) Solvent Compatibility of Poly(dimethylsiloxane)-Based Microfluidic Devices. *Analytical Chemistry*, 75(23), p.6544-6554.
[38] Motulsky H. (1995) *Intuitive Biostatistics*. Oxford University Press, New York, p.341-355, 1995.
[39] Mumby PJ. (2002) Statistical power of non-parametric tests: A quick guide for designing sampling strategies. *Marine Pollution Bulletin*, 44, p.85–87.
[40] http://www.minitab.com/
[41] Dollase T, Wilhelm M, Spiess HW, Yagen Y, Yerushalmi-Rozen R, Gottlieb M. (2003) Effect of Interfaces on the Crystallization Behavior of PDMS. *Interface Science*, 11, p.199–209.
[42] Dollase T, Spiess HW, Yerushalmi-Rozen R, Gottlieb M. (2002) Crystallization of PDMS: The effect of physical and chemical crosslinks. *Europhysics Letters*, 60 (3), p.390–396.
[43] Duquesne S, Magniez C, Camino G. (2007) *Multifunctional Barriers for Flexible Structure: Textile, Leather and Paper*, Material Science (97),Springer, p.242, 2007.
[44] Silverstein RM, Webster FX, Kiemle DJ. (1962) *Spectrometric identification of organic compounds (seventh edition)*. Wiley, p.83, 2005.
[45] http://gelest.com/goods/pdf/Library/11Infra.pdf
[46] Stuart B. (2004) *Infrared Spectroscopy: Fundamentals and Applications*. Wiley, p.83-84, 2004.

[47] Regehr KJ, Domenech M, Koepsel JT, Carver KC, Ellison-Zelski SJ et al. (2009) Biological implications of polydimethylsiloxane-based microfluidic cell culture. *Lab Chip*, 9(15), p.2132–2139.
[48] Terheyden H, Lee U, Ludwig K, Kreusch T, Hedderich J. (2000) Sterilization of elastic ligatures for intraoperative mandibulomaxillary Immobilization. *British Journal of Oral and Maxillofacial Surgery*, 38, p.299-304.
[49] Manson JM, Kim SL, Sperling LH. (1976) *Influence of Crosslinking on the Mechanical Properties of High Tg Polymers.* Technical Report AFML-TR-76-124.
[50] Patil PN, Rath SK, Sharma SK, Sudarshan K, Maheshwari P et al. (2013) Free volumes and structural relaxations in diglycidyl ether of bisphenol-A based epoxy–polyether amine networks. *Soft Matter*, 9, p.3589–3599.
[51] http://www.ptli.com/testlopedia/tests/dma-d4440.asp
[52] http://www.perkinelmer.com/CMSResources/ ("DMA A Beginner's Guide")
[53] Zhang YZ, Bjursten LM, Freij-Lamson C, Kober M, Wesslén B. (1996) Tissue response to commercial silicone and polyurethane elastomers after different sterilization procedures. *Biomaterials*, 17, p.2265-2272.
[54] Sims GD, Gnaniah SJP. (2009) Improved procedures for the determination of Tg by Dynamic Mechanical Analysis, in: *17th International Conference on Composite Materials ICCM 17, 27-31 July*, Edinburgh, UK.
[55] Miksovskya J, Voss A, Kozarova R, Kocourek T, Pisarik P et al. (2014) Cell adhesion and growth on ultrananocrystalline diamond and diamond-like carbon films after different surface modifications. *Applied Surface Science*, 297, p.95-102.
[56] Habimana O, Semião AJC, Casey E. (2014) The role of cell-surface interactions in bacterial initial adhesion and consequent biofilm formation on nanofiltration/reverse osmosis membranes. *Journal of Membrane Science*, 454, p.82-96.
[57] Schuetz G. (2005) Hardness Testing And Surface Variation. *Modern Machine Shop*, 78(2), p.98.
[58] http://www.csm-instruments.com/it/webfm_send/47
[59] Yuan Y, Lee TR. (2013) Contact Angle and Wetting properties. *Surface Science Techniques*, 23, p.327.
[60] http://www.biolinscientific.com/attension/
[61] Bryce DM. (1998) *Plastic Injection Molding: Mold Design and Construction Fundamentals*. Society of Manufacturing, Dearborn, p.27.
[62] Feng J, Zhang Q, Tu Z, Tu W, Zhongmin W et al. (2014) Degradation of silicone rubbers with different hardness in various aqueous solutions. *Polymer Degradation and Stability*, 109, p.122-128.
[63] Simmons A. (2004) Sterilisation of Medical Devices. *Business briefing: medical device manufacturing & technology*, p.1-4.
[64] Koo HJ, Waynant KV, Zhang C, Haasch RT, Braun PV. (2014) General Method for Forming Micrometer-Scale Lateral Chemical Gradients in Polymer Brushes. *Chemistry of Materials*, 26(8), p.2678–2683.
[65] Hamilton R. (2001) *Hydrolysis of Silicone Polymers in Aqueous Systems.* MsC Thesis, Lakehead University.
[66] Kennan JJ, Peters YA, Swarthout DE, Owen MJ, Namkanisorn A et al. (1997) Effect of saline exposure on the surface and bulk properties of medical grade silicone elastomers. *Journal of Biomedical Materials Research*, 36(4), p.487-97.

[67] http://www.huntsman.com/ (Rheology Study in Polyurethane Rigid Foams)
[68] http://www.personal.psu.edu/users/i/r/irh1/PDF/
[69] http://scholar.lib.vt.edu/theses/available/etd-42198-113329/
[70] Montserrat S, Colomer P. (1984) The Effect of the Molecular Weight on the Glass Transition Temperature in Amorphous Poly(Ethylene Terephthalate). *Polymer Bulletin*, 12, p.173-180.